NUREG/CR-6913
ANL-06/41

Chemical Effects Head-Loss Research in Support of Generic Safety Issue 191

Argonne National Laboratory

U.S. Nuclear Regulatory Commission
Office of Nuclear Regulatory Research
Washington, DC 20555-0001

AVAILABILITY OF REFERENCE MATERIALS IN NRC PUBLICATIONS

NRC Reference Material

As of November 1999, you may electronically access NUREG-series publications and other NRC records at NRC's Public Electronic Reading Room at http://www.nrc.gov/reading-rm.html. Publicly released records include, to name a few, NUREG-series publications; *Federal Register* notices; applicant, licensee, and vendor documents and correspondence; NRC correspondence and internal memoranda; bulletins and information notices; inspection and investigative reports; licensee event reports; and Commission papers and their attachments.

NRC publications in the NUREG series, NRC regulations, and *Title 10, Energy*, in the Code of *Federal Regulations* may also be purchased from one of these two sources.

1. The Superintendent of Documents
   U.S. Government Printing Office
   Mail Stop SSOP
   Washington, DC 20402–0001
   Internet: bookstore.gpo.gov
   Telephone: 202-512-1800
   Fax: 202-512-2250
2. The National Technical Information Service
   Springfield, VA 22161–0002
   www.ntis.gov
   1–800–553–6847 or, locally, 703–605–6000

A single copy of each NRC draft report for comment is available free, to the extent of supply, upon written request as follows:

Address: U.S. Nuclear Regulatory Commission
Office of Administration
Mail, Distribution and Messenger Team
Washington, DC 20555-0001
E-mail: DISTRIBUTION@nrc.gov
Facsimile: 301–415–2289

Some publications in the NUREG series that are posted at NRC's Web site address http://www.nrc.gov/reading-rm/doc-collections/nuregs are updated periodically and may differ from the last printed version. Although references to material found on a Web site bear the date the material was accessed, the material available on the date cited may subsequently be removed from the site.

Non-NRC Reference Material

Documents available from public and special technical libraries include all open literature items, such as books, journal articles, and transactions, *Federal Register* notices, Federal and State legislation, and congressional reports. Such documents as theses, dissertations, foreign reports and translations, and non-NRC conference proceedings may be purchased from their sponsoring organization.

Copies of industry codes and standards used in a substantive manner in the NRC regulatory process are maintained at—

The NRC Technical Library
Two White Flint North
11545 Rockville Pike
Rockville, MD 20852–2738

These standards are available in the library for reference use by the public. Codes and standards are usually copyrighted and may be purchased from the originating organization or, if they are American National Standards, from—

American National Standards Institute
11 West 42nd Street
New York, NY 10036–8002
www.ansi.org
212–642–4900

Legally binding regulatory requirements are stated only in laws; NRC regulations; licenses, including technical specifications; or orders, not in NUREG-series publications. The views expressed in contractor-prepared publications in this series are not necessarily those of the NRC.

The NUREG series comprises (1) technical and administrative reports and books prepared by the staff (NUREG–XXXX) or agency contractors (NUREG/CR–XXXX), (2) proceedings of conferences (NUREG/CP–XXXX), (3) reports resulting from international agreements (NUREG/IA–XXXX), (4) brochures (NUREG/BR–XXXX), and (5) compilations of legal decisions and orders of the Commission and Atomic and Safety Licensing Boards and of Directors' decisions under Section 2.206 of NRC's regulations (NUREG–0750).

DISCLAIMER: This report was prepared as an account of work sponsored by an agency of the U.S. Government. Neither the U.S. Government nor any agency thereof, nor any employee, makes any warranty, expressed or implied, or assumes any legal liability or responsibility for any third party's use, or the results of such use, of any information, apparatus, product, or process disclosed in this publication, or represents that its use by such third party would not infringe privately owned rights.

NUREG/CR-6913
ANL-06/41

Chemical Effects Head-Loss Research in Support of Generic Safety Issue 191

Manuscript Completed: October 2006
Date Published: December 2006

Prepared by
J. H. Park, K. Kasza, B. Fisher, J. Oras
K. Natesan and W. J. Shack

Argonne National Laboratory
9700 South Cass Avenue
Argonne, IL 60439

P.A. Torres, NRC Project Manager

Prepared for
Division of Fuel, Engineering and Radiological Research
Office of Nuclear Regulatory Research
U.S. Nuclear Regulatory Commission
Washington, DC 20555-0001
NRC Job Code N6100

Abstract

This summary report describes studies conducted at Argonne National Laboratory on the potential for chemical effects on head loss across sump screens. Three different buffering solutions were used for these tests: trisodium phosphate (TSP), sodium hydroxide, and sodium tetraborate. These pH control agents used following a LOCA at a nuclear power plant show various degrees of interaction with the insulating materials Cal-Sil and NUKON. Results for Cal–Sil dissolution tests in TSP solutions, settling rate tests of calcium phosphate precipitates, and benchmark tests in chemically inactive environments are also presented. The dissolution tests were intended to identify important environmental variables governing both calcium dissolution and subsequent calcium phosphate formation over a range of simulated sump pool conditions. The results from the dissolution testing were used to inform both the head loss and settling test series. The objective of the head loss tests was to assess the head loss produced by debris beds created by Cal–Sil, fibrous debris, and calcium phosphate precipitates. The effects of both the relative arrival time of the precipitates and insulation debris and the calcium phosphate formation process were specifically evaluated. The debris loadings, test loop flow rates, and test temperature were chosen to be reasonably representative of those expected in plants with updated sump screen configurations, although the approach velocity of 0.1 ft/s used for most of the tests is 3–10 times that expected in plants with large screens . Other variables were selected with the intent to reasonably bound the head loss variability due to arrival time and calcium phosphate formation uncertainty. Settling tests were conducted to measure the settling rates of calcium phosphate precipitates (formed by adding dissolved Ca to boric acid and TSP solutions) in water columns having no bulk directional flow.

For PWRs where NaOH and sodium tetraborate are used to control sump pH and fiberglass insulation is prevalent, relatively high concentrations of soluble aluminum can be expected. Tests in which the dissolved aluminum (Al) resulted from aluminum nitrate additions were used to investigate potential chemical effects that may lead to high head loss. Dissolved Al concentrations of 100 ppm were shown to lead to large pressure drops for the screen area to sump volume ratio and fiber debris bed studied. No chemical effects on head loss were observed in sodium tetraborate buffered solutions even for environments with high ratios of submerged Al area to sump volume. However, in tests with much higher concentrations of dissolved Al than expected in plants, large pressure drops did occur. Interaction with NUKON/Cal–Sil debris mixtures produced much lower head losses than observed in corresponding tests with TSP, although tests were not performed over the full range of Cal–Sil that might be of interest.

FOREWORD

The U.S. Nuclear Regulatory Commission (NRC) is engaged in research activities related to resolving Generic Safety Issue (GSI) 191, "Assessment of Debris Accumulation on PWR Sump Performance." The integrated chemical effects testing (ICET) research program conducted at the University of New Mexico under the direction of Los Alamos National Laboratories (LANL) provided some insights into and initial understanding of the solution chemistry, as well as types and amounts of chemical reaction products that may form following a loss-of-coolant accident (LOCA) at a pressurized-water reactor (PWR). However, the ICET program was not intended to assess the head loss implications of chemical byproducts observed in the testing. As a result, the NRC's Office of Nuclear Regulatory Research (RES) initiated research at Argonne National Laboratories (ANL) to understand the head loss attributable to chemical effects in a simulated PWR sump pool environment.

The objectives of the chemical effects head loss testing program were to (1) evaluate the head loss associated with chemical byproducts observed in the ICET program and (2) understand how relevant changes within the sump pool environment affect the formation of chemical byproducts, their physical characteristics, and any associated head loss. Toward that end, the program investigated the head loss across a sump screen that results from the combination of containment debris and chemical byproducts formed in a post-LOCA sump pool. It also measured the head loss of the buffered trisodium phosphate, sodium hydroxide, and sodium tetraborate environments observed in the ICET program (the latter two of which contain dissolved aluminum). In addition, the program included dissolution tests to identify the dissolved calcium concentrations produced in simulated containment pool conditions, as well as tests to assess the settling rates of calcium phosphate precipitates.

This report documents the results of the chemical effects head loss testing program. In particular, those results indicate that (1) significant effects on head loss were observed as a result of chemical effects in environments buffered with trisodium phosphate or sodium hydroxide, as well as environments with significant dissolved aluminum; (2) no head loss attributable to chemical effects was observed in environments buffered with sodium tetraborate; (3) complete dissolution of calcium-silicate (Cal-Sil) insulation could take 1–4 days or more, depending on the dissolution rate of trisodium phosphate and the concentration of Cal–Sil insulation, and (4) precipitates can agglomerate at higher dissolved calcium concentrations.

This report provides some initial understanding and insights regarding the head loss attributable to chemical byproducts observed in the ICET program, as well as other sump pool environments not examined in that program. As such, this report is intended to assist the NRC staff in conducting safety reviews of licensees' responses to Generic Letter (GL) 2004-02, "Potential Impact of Debris Blockage on Emergency Recirculation During Design-Basis Accidents at Pressurized-Water Reactors." In addition, insights gained from this report will be helpful to both the NRC staff and the nuclear power industry, as it considers changes in plant design and operation that may help to resolve GSI-191.

Brian W. Sheron, Director
Office of Nuclear Regulatory Research
U.S. Nuclear Regulatory Commission

Contents

Figures

Tables

Executive Summary

The U.S. Nuclear Regulatory Commission (NRC) and the nuclear utility industry undertook a joint series of tests, the Integrated Chemical Effects Test (ICET) project, that would simulate the chemical environment present inside the sump after a LOCA. This joint effort was undertaken through a memorandum of understanding between the NRC and the Electric Power Research Institute (EPRI). The ICET tests were conducted by Los Alamos National Laboratory (LANL) at the University of New Mexico (UNM) and simulate the chemical environment present in the water of the containment sump after a loss-of-coolant-accident (LOCA). The chemical systems were monitored for an extended time to identify the presence, composition, and physical characteristics of any chemical products that form during the test. Five different environments were studied in the tests. Large amounts of chemical products were observed to form in the ICET–1 and ICET-3 tests. In ICET–1 with NaOH for pH control and NUKON fiberglass insulation, the product was due to dissolution of aluminum metal and subsequent formation of aluminum oxyhydroxides.. In ICET–3 with a trisodium phosphate (TSP) buffer and NUKON fiberglass and Cal–Sil insulation, the product was due to the formation of calcium phosphates due to the reaction of Ca leached from the Cal–Sil insulation . The ICET–3 environment appeared to have the most potential for significant head loss, because the product formed very early in the test, corresponding to a time when the need for cooling would be greatest in an accident situation.

A test loop was constructed at Argonne National Laboratory to study the effects of the chemical products observed in the ICET tests on head loss. Significant effects on head loss due to chemical products were observed in environments associated with the Integrated Chemical Effects Test–3 (ICET-3). Significant chemical effects are also observed in environments with significant dissolved aluminum and NaOH buffers which correspond to the ICET–1 test.

In ICET–3 environments, the effects are due to the formation of calcium phosphate precipitates. The head losses associated with pure physical debris beds of NUKON and Cal–Sil are generally much smaller than those that occur across debris beds in which some of the Cal–Sil has been replaced with a corresponding amount of calcium phosphate precipitates. For a screen loading corresponding to 0.71 kg/m^2 of Cal–Sil and an $\approx$ 12 mm thick NUKON bed (0.71 kg/m^2), the pressure drop across the physical debris bed in benchmark testing in chemically inactive environments is approximately 1.4 psi at an approach velocity of 0.1 ft/s. With TSP, and thus calcium phosphate precipitates present, the same debris loading caused the pressure drop across the bed to be greater than 5 psi for the same approach velocity. For a thin NUKON bed ($\approx$ 3 mm), very large pressure drops were observed for the lowest tested Cal–Sil loading, 0.47 kg/m^2. However, with thicker $\approx$ 12 mm NUKON beds, little chemical effect could be observed for Cal–Sil loadings $\leq$ 0.47 kg/m^2. These results show that the relation between head loss and fiber loading for a given particulate loading is highly nonlinear and not monotonic.

Beds in which no NUKON was present were also examined. In this case, a significant portion of the screen remains open for the highest screen loading of Cal–Sil tested, 1.2 kg/m^2. The pressure drops are very low with this open area.

It can take one to four or more days to reach the equilibrium concentration of calcium resulting from the leaching of Cal-Sil insulation depending on the TSP dissolution rate and the Cal–Sil concentration. Dissolution of 1.5 g/l Cal–Sil concentrations is retarded if all TSP is dissolved prior to the Cal–Sil addition (i.e., simulating a plant LOCA with instantaneous TSP dissolution). However, the Cal–Sil dissolution rate (for the concentrations studied) is not strongly dependent on the TSP dissolution rate for more realistic TSP dissolution rates. Even with instantaneous TSP dissolution, the equivalent dissolved Ca will exceed 75 mg/l in a few hours for Cal–Sil concentrations as low as 0.5 g/l. Such an equivalent dissolved Ca concentration was shown to produce pressure drops on the order of 5 psi at an approach velocity of 0.1 ft/s across a 0.71 kg/m^2 NUKON debris bed.

In the loop tests, essentially all the calcium phosphate that is formed is transported to the screen. Settling tests were performed to determine settling rates for calcium phosphate under conditions with no bulk directional flow. At higher dissolved calcium concentrations (300 ppm), the precipitates can agglomerate. The agglomerated precipitates settle more quickly, but approximately one half of the total precipitate settles more slowly than the agglomerated precipitate. At a lower dissolved calcium concentration (75 ppm), which is probably more representative of plant conditions, the estimated settling velocity is 0.8 cm/min.

The chemical products in the ICET–1 environment that can have significant effects on pressure drop are amorphous aluminum hydroxides. Pressure drops much larger than would be expected from corresponding debris beds in an inert environment have been observed in environments with NaOH buffer for dissolved Al levels of 375 and 100 ppm. These high pressure drops can occur with no visible precipitates. They occur in spite of the very small changes in bulk fluid properties like viscosity for these solutions.

To form the chemical products that can result in large pressure drops across sump screen debris beds, the dissolved Al concentration (which is controlled by the amount of Al in containment) must exceed the solubility limit. Literature data suggest that for a temperature of 4°C (40°F) and a pH of 9.2, this is ≈ 30 ppm. However, because of the complexity of the sump environment, it is difficult to justify the applicability of literature data to this situation. Current industry guidance recommends that all the dissolved Al be assumed to form a precipitation product.

Although a dissolved Al level of 100 ppm resulted in large pressure drops, the actual potential for increased head loss depends not only on this concentration, but also on the loop volume and screen size. For the ANL loop the volume is 119 liters, and the screen area with the PVC section is 0.016 m^2. In the ANL tests with 100 ppm dissolved Al, it appears that ≈ 50 ppm of the Al has been precipitated out as a product, this means that there is about 1 kg/m^2 of chemical product impinging on the screen and debris bed. With a NUKON loading of 0.7 kg/m^2, this is sufficient to produce a very high pressure drop. With a much larger ratio of screen area to sump volume or a different NUKON, different results may be obtained.

Subsequent tests with a surrogate precipitate produced externally and then added to the loop suggest that even much lower loadings of precipitation product (< 0.1 kg/m^2) are sufficient to produce high head losses in debris beds with a NUKON loading of 0.7 kg/m^2.

Sodium tetraborate buffers seem more benign than NaOH or TSP. A submerged Al area and sump volume that results in a 375 ppm dissolved Al concentration in a NaOH environment, results in a 50 ppm dissolved Al concentration with a sodium tetraborate buffer. The 375 ppm concentration resulted in high head loss in 0-2 h with a NaOH buffer; the corresponding 50 ppm concentration produced no significant head loss observed in ≈ 11 days with a STB buffer. Interaction with NUKON/Cal–Sil debris mixtures produced much lower head losses than observed in corresponding tests with TSP, although tests were not performed over the full range of Cal–Sil loadings that might be of interest.

Acknowledgments

The authors wish to acknowledge D. Engel and R. McDaniel for their assistance in the test program. They were primarily responsible for the building and operation of the test loop. They also provided valuable assistance in the design of the test loop and the associated systems and development of the head loss test procedures.

Acronyms and Abbreviations

ACRS	Advisory Committee for Reactor Safeguards
ANL	Argonne National Laboratory
BWR	Boiling water reactor
CNWRA	Center for Nuclear Waste Regulatory Analyses
CPVC	Chlorinated polyvinyl chloride
CSS	Containment Spray System
ECCS	Emergency core cooling system
EDS	Energy Dispersive X-ray Spectroscopy
GSI	Generic Safety Issue
ICET	Integrated Chemical Effects Test
ICP	Inductively Coupled Plasma
LANL	Los Alamos National Laboratory
LN	Liquid Nitrogen
LOCA	Loss of coolant accident
MHO	Reciprocal ohms (used as a measure of conductivity
NPSH	Net positive suction head
NRC	Nuclear Regulatory Commission
PNNL	Pacific Northwest National Laboratory
PVC	Polyvinyl chloride
PWR	Pressurized water reactor
RWST	Refueling water storage tank
SEM	Scanning Electron Microscope
STB	Sodium tetraborate
TEM	Transmission Electron Microscopy
TSP	Trisodium phosphate
UHP	Ultra High Purity
UNM	University of New Mexico

Symbols

Al	Aluminum
Al^{+3}	Aluminum Ion
$Al(OH)_3$	Aluminum Hydroxide
$Al(OH)_4^-$	Aluminate Ion
Al(NO3)3	Aluminum Nitrate
$Al(NO_3)_3 \cdot 9H_2O$	Aluminum Nitrate Nonahydrate
Al_2O_3	Aluminum Oxide or Alumina
Au	Gold
B	Boron
$B(OH)_3$	Boric Acid
Ca	Calcium

Symbols (continued)

$CaCl_2$	Calcium Chloride
$Ca_3(PO_4)_2$	Calcium Phosphate
$Ca_3(PO_4)_2 \cdot H2O$	Tricalcium Phosphate Hydrated
$Ca_9HPO_4(PO_4)_5OH$	Calcium Hydrogen Phosphate Hydroxide
$Ca_{10}(PO_4)_6(OH)_2$	Hydroxyapatite
Cu	Copper
Fe	Iron
Fe_3O_4	Magnetite or Iron Oxide
H^+	Hydrogen Ion
H_2O	Water
H_2O_2	Hydrogen Peroxide
HCl	Hydrochloric Acid
H_3BO_3	Boric Acid
HNO_3	Nitric Acid
K	Potassium
LiOH	Lithium Hydroxide
Mg	Magnesium
Na	Sodium
Na^+	Sodium Ion
NaOH	Sodium Hydroxide
$NaAlO_2$	Sodium Aluminate
Na_2SiO_3	Sodium Silicate
$Na_2B_4O_7$	Sodium Tetraborate
Na_3PO_4	Trisodium Phosphate
NO_3^-	Nitrate Ion
OH^-	Hydroxide
P	Phosphorous
PO_4^{3-}	Phosphate Ion
Si	Silicon
SiO_3^-	Silicate
Zn	Zinc

1 Introduction

The emergency core cooling system (ECCS) provides water to cool the core of the nuclear reactor in case of a loss of coolant accident (LOCA) that would result, for example, from a reactor coolant system pipe break. The water supplied by the ECCS comes from the refueling water storage tank (RWST) and safety injection tanks. The water supplied by the ECCS flows through the core and typically spills out the break and collects in the sump at the bottom of the containment. When the low level limit is reached in the RWST, the water that has accumulated in the containment sump will be recirculated through the reactor core using the ECCS system. This process provides long-term cooling for the core. Recirculation could start as soon as twenty minutes after the break for a large break LOCA.

The steam-water jet that issues from a break can dislodge thermal insulation and other materials in the vicinity of the rupture. Some fraction of this dislodged insulation and other materials, such as paint chips and concrete dust, will be transported to the containment floor by the steam–water flows from the break and the containment sprays and may accumulate on sump screens intended to prevent debris from entering the inlet of the ECCS and containment spray system (CSS) pumps.

This build up of debris will result in an increase in head loss across the sump screens and if the head loss across the screen becomes too large, the pumps will no longer have adequate net positive suction head (NPSH), which could result in cavitation and failure of the pumps to deliver the amount of water needed.

The U.S. Nuclear Regulatory Commission (NRC) first published regulatory guidance on the performance of pressurized-water reactor (PWR) containment sump screens and boiling-water reactor (BWR) suction strainers in 1974 in Regulatory Guide (RG) 1.82, "Water Sources for Long-Term Recirculation Cooling Following a Loss-of-Coolant Accident." (BWR suction strainers perform the same function as PWR containment sump screens.)

In the early 1990s, an event at the Barseback BWR in Sweden and several events at BWRs in the United States raised concern about potential blockage of sump screens. In 1996, the NRC asked BWRs to conduct plant-specific evaluations of their suction strainer performance and, if necessary, modify their plant design and/or operation.

A Generic Safety Issue (GSI) 191 was established to address the potential for debris accumulation on PWR sump screens to affect emergency core cooling system (ECCS) pump net positive suction head margin. On September 13, 2004, NRC issued Generic Letter 2004-02, which required PWR licensees to perform a mechanistic evaluation of the potential for debris blockage and operation with debris-laden fluids to impede or prevent the recirculation functions of the ECCS.

Until recently, these evaluations focused on physical debris — insulation, dust, paint chips, etc. However, the NRC Advisory Committee on Reactor Safeguards (ACRS) raised the possibility that chemical reactions in the sump could produce additional products that would increase the potential for sump blockage.

The U.S. Nuclear Regulatory Commission (NRC) and the nuclear utility industry undertook a joint series of tests, the Integrated Chemical Effects Test (ICET) project, that would simulate the chemical environment present inside the sump after a LOCA. This joint effort was undertaken through a memorandum of understanding between the NRC and the Electric Power Research Institute (EPRI). The ICET tests were conducted by Los Alamos National Laboratory (LANL) at the University of New Mexico (UNM) and simulate the chemical environment present in the water of the containment sump after a loss-of-coolant-accident (LOCA). The chemical systems were monitored for 30 days to identify the presence, composition, and physical characteristics of any chemical products that formed during the test.

The containment sump environments selected for study were based on input from the Westinghouse Electric Company, the NRC, and EPRI. The specific conditions, material types, and parameters in the ICET test series are intended to be broadly representative of all domestic PWRs. The Westinghouse Owners Group and the Babcock & Wilcox Owners Group aided in soliciting information. To obtain the necessary details of plant-specific conditions within containment (materials present, containment sump conditions, etc.), Westinghouse reviewed plant-specific documents, (such as Post-LOCA Hydrogen Generation Evaluations), other available plant documents (e.g., updated final safety analysis reports), and submitted survey questions to plant personnel. The plant survey responses formed the primary source of data for determining the parameters used to define the ICET test conditions.[1]

Five types of environments were considered in the ICET tests. They differed in the types of insulating materials that were present and the choice of pH buffering agent. A summary of the test conditions is given in Table 1.[1]

Table 1. Insulation materials and buffering agents used in the ICET tests

ICET test	Buffering agent	pH	Insulation
1	NaOH	10	100% fiberglass
2	TSP ($Na_3PO_4.12H_2O$)	7	100% fiberglass
3	TSP ($Na_3PO_4.12H_2O$)	7	80% Cal–Sil / 20% fiberglass
4	NaOH	10	80% Cal–Sil / 20% fiberglass
5	Sodium Tetraborate ($Na_2B_4O_7$)	8.0–8.5	100% fiberglass

The corrosion/dissolution/precipitation products observed in the tests have been described in a series of reports.[2–6] In these tests the precipitate products that appear to have the greatest potential for increasing head–loss are aluminum hydroxides, which were observed in ICET–1 and to a lesser extent in ICET–5, and calcium phosphates, which were observed in ICET–3. Measurement of the head loss associated with these chemical products was outside the scope of the ICET program.

The chemical effects head loss test program at Argonne National Laboratory (ANL) was intended to determine the potential for chemical products observed in ICET program to contribute to head loss. In addition to measuring head loss under ICET conditions, the tests at ANL examined a broader range of conditions than examined in ICET. In some cases the tests at ANL used surrogate chemical products in lieu of an integrated test in which the chemical products were formed by the dissolution and reaction of actual containment materials. Use of the surrogate forms was justified by comparisons with the chemistry of the products formed in the integral tests and other important physical characteristics such as the amorphous structure of the product. A summary description of the head loss tests run in the program is given in Table 2. More detailed descriptions of the tests and results are provided in the remainder of the report.

Table 2. Summary of the head loss tests performed at ANL

Test	Description	Test section	Screen	Date
ICET-3-1	NUKON 15 g; Cal–Sil 15 g; 200 ppm Ca	A	1	8/26/05
ICET-3-2	NUKON 15 g; Cal–Sil 15 g; 10, 25, 50 ppm Ca	A	1	9/1/05
ICET-1-3	NUKON 15 g; Cal–Sil 15 g;NaOH, 375 ppm Al	A	1	10/7/05
ICET-3-4	NUKON 7 g; Cal–Sil 25 g; TSP	A	1	11/15/05
ICET-3-5	NUKON 7 g; Cal–Sil 25 g; NoTSP	A	1	11/18/05
ICET-3-6	NUKON 15 g; Cal–Sil 15 g; TSP 1/8, 7/8	A	1	11/29/05
ICET-3-7	NUKON 15 g; Cal–Sil 15 g; No TSP	A	1	12/1/05
ICET-3-8	NUKON 15 g; $CaCl_2$ mixed together	A	1	12/7/05
ICET-3-9	NUKON 15 g; $CaCl_2$ added after bed stabilized	A	1	12/9/05
ICET-3-10	NUKON 15 g; Cal–Sil 15 g; TSP: 190g premix/190g loop	A	1	12/13/05
ICET-3-11	NUKON 15 g; Cal–Sil 15 g; No TSP	A	1	12/15/05
ICET-3-12	NUKON 15 g; Cal–Sil 5 g; TSP: 190g premix/190g loop	A	1	1/6/06
ICET-3-13	NUKON 15 g; Cal–Sil 5 g; NoTSP	A	1	1/11/06
ICET-3-14	NUKON 15 g; Cal–Sil 15 g; NoTSP	A	1	1/13/06
ICET-3-15	NUKON 15 g; Cal–Sil 10 g; No TSP	A	1	1/17/06
ICET-3-16-A1	NUKON 15 g; Cal–Sil 10 g; TSP: 190g premix/190g loop	A	1	1/19/06
ICET-3-17-A1	NUKON 15 g; Cal–Sil 15 g; TSP: 190g premix/190g loop	A	1	1/25/06
ICET-3-18-A1	NUKON 5 g; Cal–Sil 10 g; TSP: 190g premix/190g loop	A	1	1/31/06
ICET-3-19-A2	Cal–Sil 25 g; TSP: 190g premix/190g loop	A	2	2/2/06
BM-2-A2-N15.5	NUKON 15.494 g	A	2	2/8/06
BM-1-A2-N4.6	NUKON 4.593 g	A	2	2/10/06
BM-3-A2-N15.5-C3.1	NUKON 15.5 g; Cal–Sil 3.108 g	A	2	2/14/06
BM-2-A2-N15.5 repeat	NUKON 15.494 g	A	2	2/22/06
BM-1-A2-N4.4 repeat	NUKON 4.4 g; *invalid test*	A	2	2/24/06
BM-1-A2-N4.4 repeat2	NUKON 4.4 g	A	2	2/28/06
BM-3-A2-N15.5-C3.1 repeat	NUKON 15.5 g; Cal–Sil 3.1 g	A	2	3/2/06
ICET-1-1-B2_100ppm	NUKON 15.015g; Al Nitrate 164.06 g; 100 ppm Al	B	2	3/9/06
ICET-1-2-B2_200ppm	NUKON 11.57g; Al Nitrate 328.12 g; 200 ppm Al	B	2	3/14/06
ICET-1-3-B2_375ppm	NUKON 11.57g; Al Nitrate 615 g; 375 ppm Al	B	2	3/16/06

Table 2. Summary of the head loss tests performed at ANL (continued)

Test	Description	Test section	Screen	Date
ICET-1-1-B2_100ppm repeat	NUKON 11.5g; Al Nitrate 164 g; 100 ppm Al	B	2	3/23/06
ICET-1-1-B2_100ppm repeat2	NUKON 11.5g; Al Nitrate 164 g; 100 ppm Al	B	2	4/13/06
ICET-5-1-B2_042606	NUKON 11.5g; STB 1248g; LiOH 0.247g	B	2	4/26/06
ICET-3-STB1-A2	NUKON 15g; Cal–Sil 15g; STB 1248g; LiOH 0.287g	A	2	5/16/06

A LEXAN test section

B PVC test section

1 Perforated plate with 51% flow area and 3/16 in. holes with 1/4 in. staggered centers

2 Perforated plate with 40% flow area and 1/8 in. holes with 3/16 in. staggered centers

2 Head loss tests in ICET–3 environments

2.1 ANL test facility

A schematic of the ANL test loop is shown in Fig. 1. The piping in most of the loop is CPVC; the clear test section containing the test screen was either LEXAN or clear PVC. LEXAN has better high temperature strength; PVC is more resistant to NaOH solutions. The heater and cooler sections are stainless steel. The stainless steel pipe in the heater section is wrapped with heater tapes. In the cooler section, the pipe is surrounded by an outer shell which is filled with cooling water from the building water supply. Temperatures around the loop during operation are typically ±0.6°C (1°F). Loop velocities can be controlled over the range from 0.02 to 2 ft/s. Compatibility tests for the LEXAN and CPVC in the environments of interest are described in Appendix A.

The inner diameter of the LEXAN section is 6.5 in.; the inner diameter of the PVC section is 5.625 inches. Because of the mounting ring, the test screen has an effective flow diameter of 6 in with the LEXAN test section and an effective flow diameter of 5.125 in with the PVC test section. The fluid volume in the loop is 119 liters (4.2 ft^3). At 0.1 ft/s, the transit time around the loop is about 4 minutes. The sump screen in these tests is a flat perforated plate. Two different perforated plates have been used. One has a 51% flow area and 3/16 in. holes with 1/4 in. staggered centers; the other has a 40% flow area and 1/8 in. holes with 3/16 in. staggered centers. A test screen is shown in Fig. 2. Two pairs of pressure taps are installed. One pair is 2.5 in above and below the screen and the other is 12 in. above and below the screen. Differential pressure transducers measure the differential pressures across these pairs of taps.

In scaling results from the ANL test facility, the mass of chemical product and physical debris per unit area of screen must be considered. The amount of chemical product produced scales with fluid volume while the screen area per fluid volume determines the product mass per unit screen area. A 15 g loading of debris in the LEXAN section corresponds to a loading of 0.7 kg/m^2. To maintain the same loading per unit area in the PVC section requires 11.5 g of debris.

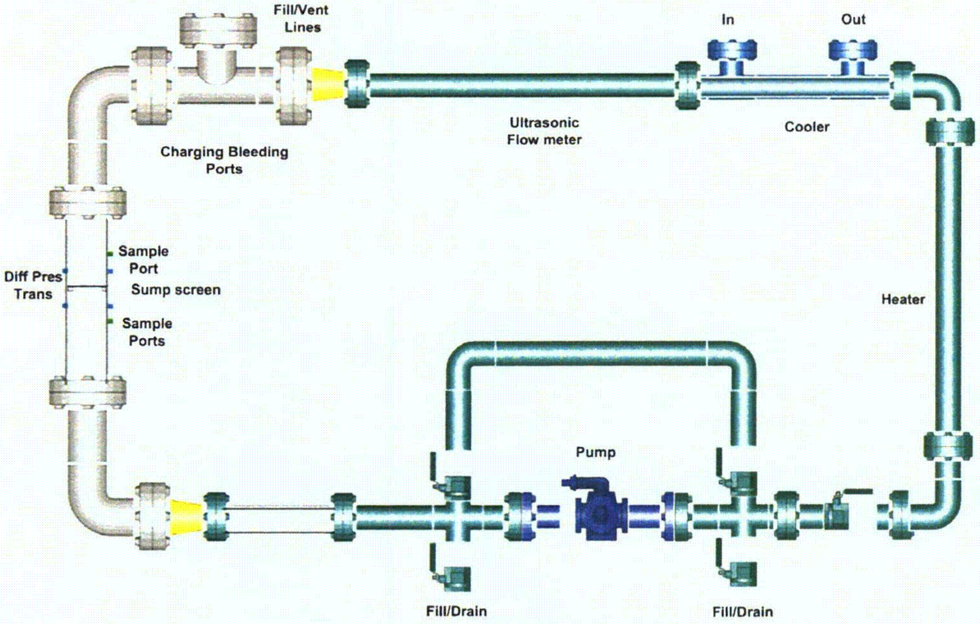

Figure 1. Schematic of the test loop

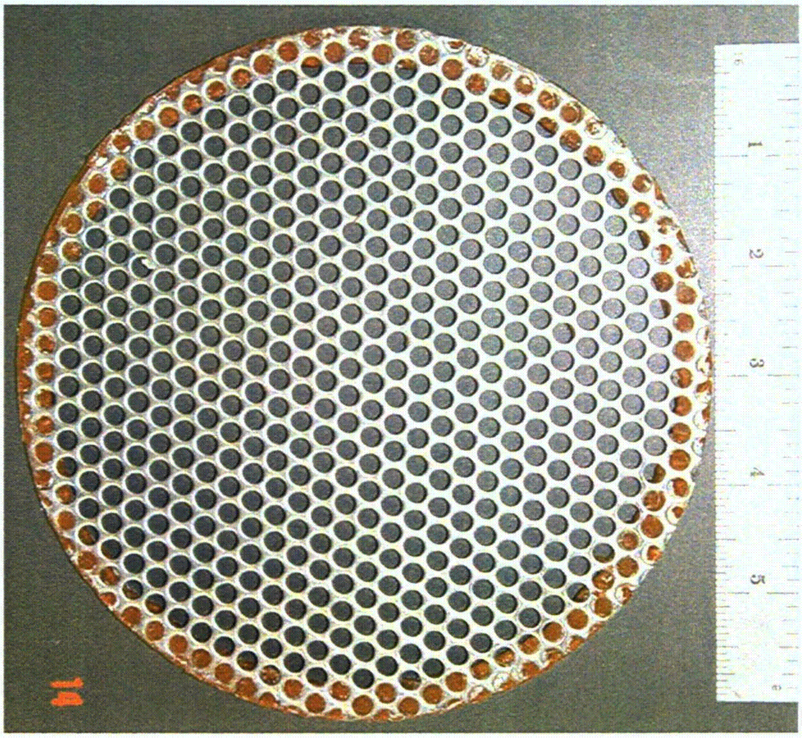

Figure 2. Perforated plate test screen with 51% flow area and 3/16 in. holes with 1/4 in. staggered centers.

Physical debris and chemicals are introduced to the loop through a charging port at the top of the loop. The horizontal configuration of the screen is not intended to reflect, but rather to permit the development of uniform beds with well–defined characteristics. The head loss behavior for such beds would characterize the local head loss behavior of more complex nonuniform beds that might form on more complex screen geometries.

2.2 Background

Initial investigation focused on the chemical precipitate formed from the combination of calcium silicate and TSP buffer since this precipitate formed very early in ICET 3, during a time when plant pump NPSH margins are lowest. Once testing was completed in the ICET 3 type environment, subsequent tests were performed with other buffers (e.g., sodium hydroxide and sodium tetraborate) where precipitation was observed when test solution was removed from the ICET tank and allowed to cool.

After a LOCA, physical debris will reside in the containment pool for some period of time before the initiation of emergency core cooling system recirculation. During this time, for plants using TSP for pH control, the containment pool environment will be changing as the TSP dissolves. After recirculation starts, debris will begin arriving at the sump screen to form a debris bed. If both NUKON and Cal–Sil debris are present, the sump screen debris bed will consist of some mix of plant debris, including Cal–Sil, NUKON, and calcium phosphate precipitates. The relative amounts of Cal–Sil and calcium phosphate precipitates in the debris bed as it initially forms will vary depending on the residence time in the containment sump prior to the onset of recirculation, the transport time to the sump screen, the initial containment sump pH, the containment sump temperature, and the TSP dissolution rate.

For some conditions, e.g., long residence times, a large fraction of the soluble constituents of Cal–Sil (primarily $CaSiO_3$ with some Na_2SiO_3) may have dissolved before the debris actually reaches the sump screen. In such cases, the debris bed will primarily contain a mix of NUKON fibers and calcium phosphate precipitates. In other cases, e.g., short residence times, little Cal–Sil dissolution may have occurred before the debris reaches the sump screen, and the bed that is initially formed will consist predominantly of a mix of NUKON fibers and Cal–Sil particulates. In this case, with time, the Cal–Sil within the bed can continue to dissolve, and any dissolved calcium (Ca) that is released will react with the available phosphate to form additional calcium phosphate precipitates, since the precipitation reaction will be Ca limited, i.e., there is typically much more phosphate available than is stoichiometrically required for all the Ca to precipitate.

2.3 Approach

Following the initial two tests to evaluate head loss in an ICET 3 environment, ANL performed a series of follow-up tests (ICET-3-4 to ICET-3-11) that evaluated the potential for head loss due to chemical effects in a TSP-buffered environment. The tests were designed to explore conditions corresponding to a range of debris amounts, containment sump residence times, and TSP dissolution times. The two basic physical parameters that are affected by these variables are the degree of Cal–Sil dissolution that will occur prior to the formation of the debris bed and the interaction between the chemical products and the physical debris during bed formation. For instance, some fraction of chemical precipitates and the debris will arrive at the sump screen together and some fraction of precipitates will form due to Cal–Sil dissolution within the debris bed after the bed has initially formed.

The NUKON and Cal–Sil mass loading per unit screen area utilized in these tests are reasonably representative of those plants that currently have, or will have after sump screen modifications, relatively low debris mass loading (i.e., less than 2 kg/m^2). Because the Argonne test loop has a fixed ratio of screen area to fluid volume ratio, it is impossible in most cases to simultaneously match both the debris loading per unit screen area and the debris loading per unit volume of fluid that would be encountered in an actual sump configuration. In assessing the head loss, the screen loading per unit area is the critical scaling parameter. The Cal–Sil dissolution rate, however, can be a function of the debris loading per unit volume. The current plant estimates of the Cal–Sil loading per unit volume of the containment sump are less than 1.5 g/l, for plants with both Cal–Sil insulation and TSP buffer. The small-scale dissolution test data presented later in this report show that the Cal–Sil dissolution rate at these low concentrations is not too strongly dependent on the concentration. Therefore, it is not too important to match the plant debris loading per unit volume within the test loop.

The NUKON fiberglass insulation and the Cal–Sil insulation used in the tests were prepared from materials obtained from Performance Contracting Inc. (PCI), Lenexa, Kansas. The NUKON was originally produced in the form of insulating blankets. The blankets were rough shredded to get a collection of loose fibers and clumps of fibers ranging in size from 1–2 cm in diameter. The shredded fiberglass is then mixed with water (≈ 1 g/65 ml water) in a blender for a short time (≈10 s) to produce a relatively smooth slurry. The Cal–Sil was originally produced in the form of molded blocks. The material is friable and was first broken up by hand–crushing with a mortar and pestle. The crushed material was mixed with water (≈ 1 g/65 ml water) in a blender for about a minute to produce a smooth slurry. In the present tests, the two slurries were then mixed together. The preparation of the slurry is done just prior to the performance of the head loss tests.

To simulate the dissolution of the Cal–Sil that occurs during the residence time in the containment sump prior to the onset of recirculation, the Cal–Sil and NUKON slurry was presoaked at temperature (60°C) in the baseline boric acid, lithium hydroxide (LiOH) solution for 30 minutes, and then added as a slurry to the loop. Since only 2.5 liters of solution were used for the presoak, the Cal–Sil concentration is much higher than it would be in the loop or in an actual sump. At high Cal–Sil concentrations (≥ 6 g/l), the total amount of Cal–Sil dissolution is limited by the solubility of calcium silicate ($CaSiO_3$).[7] Regardless of the initial pH or the rate of addition of TSP, the pH of solution rises to about 7, primarily because Cal–Sil contains sodium silicate (Na_2SiO_3) as an impurity. The sodium silicate is very soluble, and as it dissolves, the dissolved sodium (Na) causes the pH of the initial boric acid/LiOH solution to increase. At these high concentrations, the dissolved Ca level rises quickly to a saturation value of ≈200 ppm.[7] In highly concentrated solutions, addition of TSP increases the amount of Cal–Sil that will eventually dissolve, because the phosphate combines with the dissolved Ca and forms calcium phosphate precipitates, lowering the dissolved Ca level, and permitting further dissolution of the Cal–Sil. Thus, the highly concentrated presoak slurry is expected to form lower initial dissolved Ca concentrations than are realistically expected. In contrast, as subsequent dissolution data presented in this report show, at lower Cal–Sil concentrations, the increase in pH due to the dissolution of the sodium silicate impurity is much smaller, and rapid addition of TSP can decrease the Cal–Sil dissolution rate. Thus, because of the increase in pH, the highly concentrated presoak slurry, even with TSP additions to prevent the dissolved Ca from reaching saturation levels, is expected to have less leaching of Ca from the Cal–Sil than would occur under prototypical conditions.

The head loss tests were performed under isothermal conditions at 60°C (140°F). The debris in all the tests was introduced into the loop with the flow velocity in the loop at 0.1 ft/s. The intent in these tests was to maintain a constant velocity through the test until a stable bed configuration steady-state head loss was reached and then to cycle the velocity to examine the effect on head loss. In most the tests, the head losses were too large to maintain a constant flow of 0.1 ft/s. [The maximum head loss that currently can be maintained in the loop is about 6 psi (≈13.8 ft of water).] Because a flow velocity of 0.1 ft/s is higher than expected at the sump screen in most planned modified sump configuration, the head loss measurements are conservative with respect to this variable. However, although the measured head loss is conservative with respect to velocity, as noted previously, the maximum reported head loss in many cases was a function of the test loop capacity.

The test conditions used in this series of tests are summarized in Table 3. The judgments expressed in the Table 3 comment section that the test conditions represent "minimal", "maximum", or "typical" test values for the amount of Cal–Sil dissolution during the initial debris bed formation is based on the results of the Cal–Sil dissolution tests reported in the previous Quick Look Report[7], the new dissolution tests described in this report, and expected plant TSP dissolution times.[8]

Each head loss test utilized a slightly different procedure for simulating specific chemical product formation rates and debris arrival sequences depending on the test objective. While the general test procedures are similar to those described in Ref.(7), the unique procedures associated with each test were varied to obtain the conditions described in Table 3. Descriptions of the unique procedures associated with each test are subsequently presented along with a summary of the results.

Table 3. ICET-3 Environment head loss tests

Test No.	NUKON (g)[a]	Cal–Sil (g)	30 min Presoak	TSP[b]	Additional dissolved Ca (ppm)	Comment
ICET-3-1	15	15	No	Initially in loop	200	Simulates initial conditions in ICET-3; precipitates arrive after bed forms
ICET-3-2	15	15	No	Initially in loop	10, 25, 50 ppm Ca[d]	Parametric test starting with 1/20th dissolved Ca of ICET-3: precipitates arrive after bed forms
ICET-3-4	7	25	Yes	1/8th initially in loop; 7/8th metered in	None	Minimal Cal–Sil dissolution prior to initial bed formation; continued dissolution as test continues
ICET-3-5	7	25	Yes	None	None	Baseline physical debris only
ICET-3-6	15	15	Yes	1/8th initially in loop; 7/8th metered in	None	Minimal Cal–Sil dissolution prior to initial bed formation
ICET-3-7	15	15	Yes	None	None	Baseline physical debris only
ICET-3-8	15	0	No	Initially in loop	43.5[c]	$CaCl_2$ & NUKON added simultaneously; Maximum Cal–Sil dissolution prior to bed formation
ICET-3-9	15	0	No	Initially in loop	9, 18, 27 ppm Ca[d]	$CaCl_2$ added after NUKON bed stabilizes maximizes arrival time of precipitates to bed; Maximum Cal–Sil dissolution prior to arrival at the bed
ICET-3-10	15	15	Yes	1/2 metered presoak; 1/2 metered	None	Intended to represent a "typical" degree of Cal–Sil dissolution prior to bed formation
ICET-3-11	Replicates ICET-3-7					
ICET-3-12	15	5		1/2 metered presoak; 1/2 metered	None	Lower Cal–Sil loading
ICET-3-13	15	5	Yes	None	None	Baseline for ICET-3-12
ICET-3-14	Replicates ICET-3-7 & 11					
ICET-3-15	15	10	Yes	None	None	Baseline physical debris only
ICET-3-16-A1	15	10	Yes	1/2 metered presoak; 1/2 metered	None	Lower Cal–Sil loading
ICET-3-17-A1	Replicates ICET-3-10					
ICET-3-18-A1	5	10	Yes	1/2 metered presoak; 1/2 metered	None	Thinner NUKON bed
ICET-3-19-A2	–	25	Yes	1/2 metered presoak; 1/2 metered	None	Cal–Sil/calcium phosphate precipitate only debris

[a] 1 g of debris corresponds to a screen loading of 47.6 g/m^2

[b] The total amount of TSP in each test where TSP was added was always 3.4 g/l. Some fraction was either dissolved initially in the test loop or metered in during the presoak period. The remaining fraction was metered in during a 30-60 minute period after the debris was added to the loop.

[c] Ca equivalent to full dissolution of 15 g Cal–Sil.

[d] Ca additions added incrementally to sequentially reach values of dissolved Ca listed.

2.4 Individual ICET–3 test procedures and results

2.4.1 ICET-3-1 Test procedure and results

ICET-3-1 test procedure

The initial tests in the Argonne National Laboratory (ANL) chemical effects/head–loss testing program were intended to investigate the potential head loss associated with the chemical products observed in the third Integrated Chemical Effects Test (ICET–3).

In the ICET–3 tests, the TSP was added to the Cal–Sil solution through the sprays. In the ANL tests, the loop is filled with a solution containing boric acid, LiOH, and TSP. The concentration of TSP corresponds to that metered into the test solution over 4 hours in ICET–3 (about 4 g/l). Calcium chloride ($CaCl_2$) solution is then added to supply the desired inventory of dissolved Ca. In the first head loss test, the Ca inventory was taken to be that corresponding to the estimated Ca concentration in the ICET solution at the start of the TSP spray, which, as discussed previously, has been estimated to be about 200 ppm. As noted previously, this will result in the formation of an amount of calcium phosphate ($Ca_3(PO_4)_2$) per volume of solution comparable to that observed in the initial stages of ICET–3.

The loop was filled with deionized water and heated to 130°F. Boric acid in powder form was slowly added to the loop and circulated until it was dissolved. The LiOH and TSP were added as solutions. The concentrations of these chemicals in the loop were also chosen to match those in ICET–3. The test temperature was lower than that in ICET–3 (140°F), because the test loop was not fully insulated. Because of the retrograde solubility of $Ca_3(PO_4)_2$, the lower temperature results in the formation of slightly less precipitate.

After the chemical solution was prepared, the physical debris bed was built by adding a slurry containing 15 g NUKON/15 g Cal–Sil to the loop with the loop flow at 0.1 ft/s. This corresponds to a debris loading of 0.7 kg/m^2. The bed was about 3/4 in thick. The NUKON bed formed essentially in the first pass of the debris past the test screen.

ICET-3-1 test results

The pressure drop across the bed slowly increased as the test loop solution recirculated, presumably due to increasingly effective filtration of fine Cal–Sil particles. After recirculating for about 45 minutes, the flow rate was then increased to 0.2 ft/s. At this flow rate, the bed compressed to about 5/8 in thick. The flow rate was then reduced back to 0.1 ft/s. The pressure drop and flow velocity at each stage of the debris bed formation is shown in Fig. 3. The physical debris bed at this point in the test is shown in Fig. 4.

The $CaCl_2$ was then added to the vertical part of the test loop just above the clear test section. A total of 400 ml of $CaCl_2$ solution was added over a 4 minute period (the transit time around the loop at 0.1 ft/s) to obtain the 200 ppm dissolved Ca inventory. A fine, milky precipitate was observed as shown in Figure 5 just after the introduction of the $CaCl_2$. The pressure drop across the bed increased from 1.7 psi to greater than 7.0 psi within 10 minutes of introducing the $CaCl_2$. An accurate pressure drop measurement could not be obtained beyond this point, because the loop was running unpressurized, and the pump started to cavitate as the precipitate continued to accumulate on the bed. The flow rate and pressure drop as a function of time after $CaCl_2$ addition are also shown in Fig. 3. As discussed previously, the 200 ppm Ca inventory is likely not sufficient to produce the full amount of $Ca_3(PO_4)_2$ formed during ICET–3. However, no additional Ca was added to simulate the depletion of all the available phosphate as in ICET–3, since the pressure drop across the bed had already caused the pump to cavitate. Figure 6 shows the accumulation of the precipitate on the debris bed just before the pump was shut off.

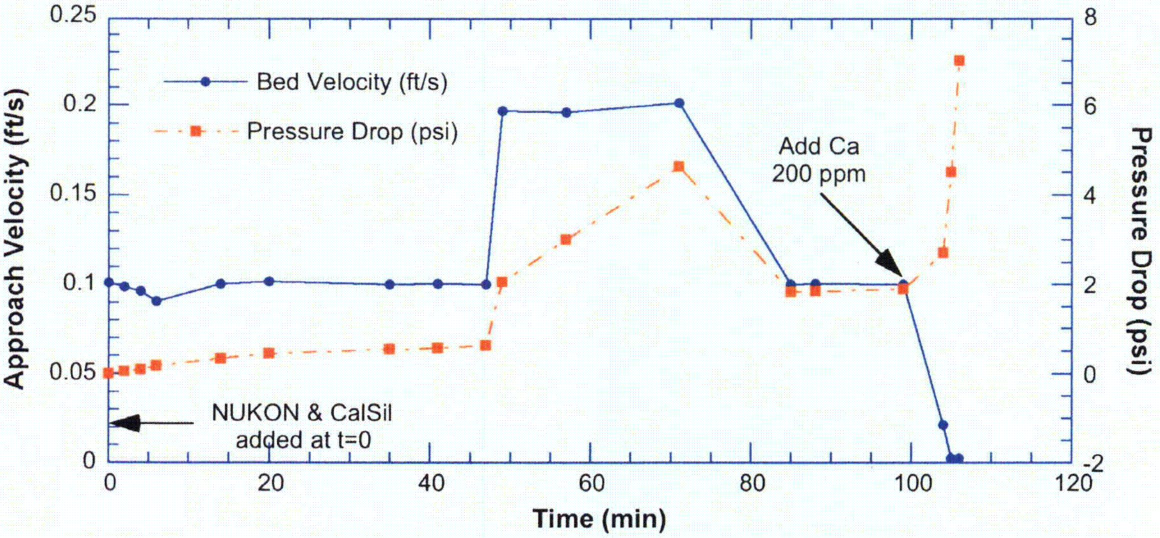

Figure 3. Flow rate and pressure drop as a function of time in ICET–3–1.

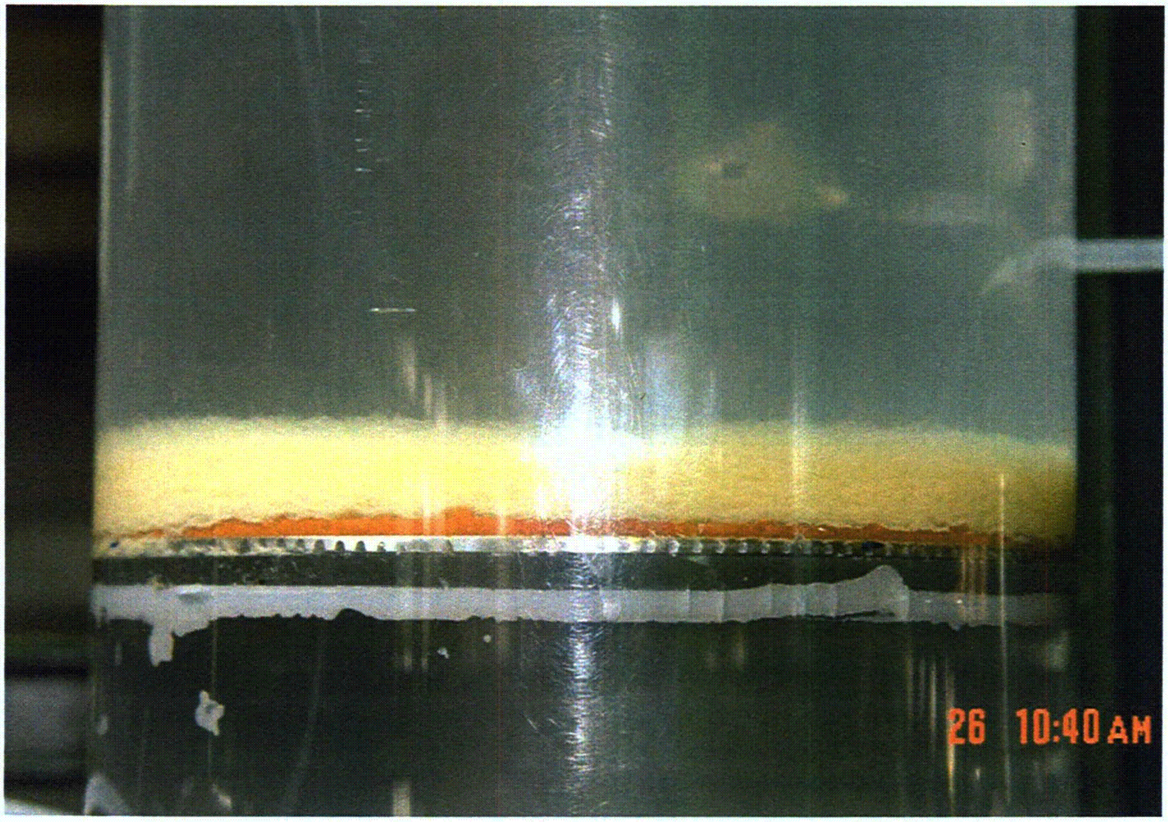

Figure 4. NUKON/Cal–Sil bed before formation of the $Ca_3(PO_4)_2$ precipitate

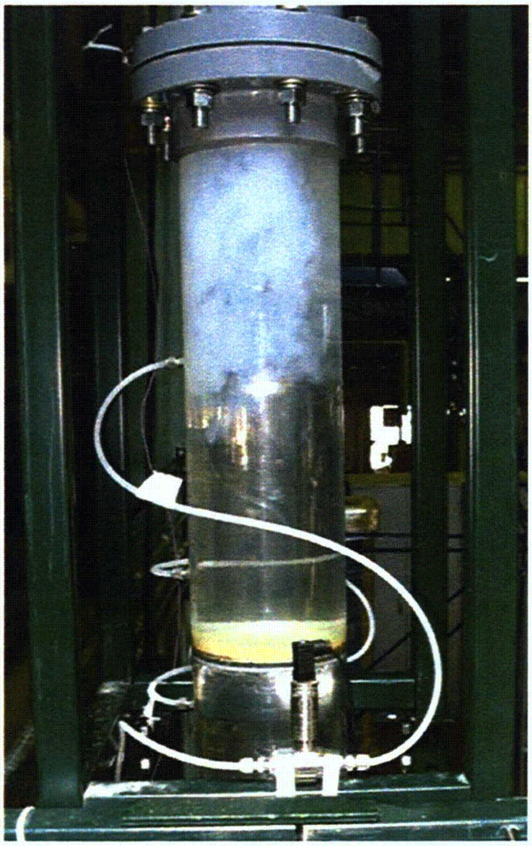

Figure 5.
$Ca_3(PO_4)_2$ forming after addition of $CaCl_2$ and approaching the debris bed.

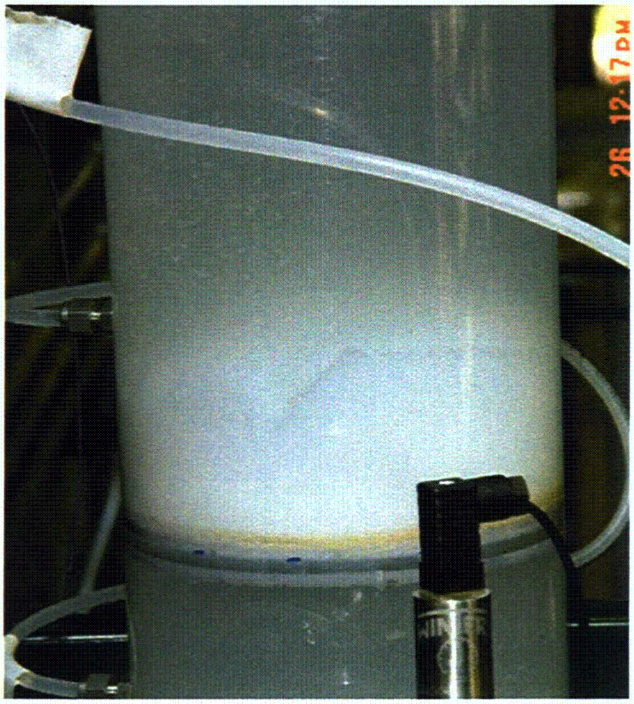

Figure 6.
Precipitate buildup on the fiber debris bed just after the pump was turned off.

2. 4.2 ICET-3-2 test procedure and results

The initial procedure for the second test was similar to the first test. The loop was filled with deionized water and heated to 130°F. Boric acid in powder form was slowly added to the loop and circulated until it was dissolved. The LiOH and TSP were added as solutions.

The physical debris bed was again built from 15 g of NUKON and 15 g of Cal–Sil. The bed was built at 0.1 ft/s and the flow rate was not increased above this value in contrast to the previous test. The debris bed was somewhat thinner than the initial debris bed for ICET–3-1 at 0.1 ft/s (5/8 in for ICET–3–2 and 3/4 in for ICET–3–1). The pressure drop across the bed was also slightly smaller at this flow rate (0.4 psi in ICET–3–2 and about 0.6 psi for ICET–3–1).

For this test, the $CaCl_2$ additions were made in stepwise fashion starting with an initial addition equivalent to 10 ppm (one-twentieth of the simulated ICET-3 inventory) of dissolved Ca. Then amounts were added incrementally corresponding to total dissolved Ca inventories of 25 ppm, and 50 ppm. Each addition was metered in over a 4 minute period as in the first test.

When $CaCl_2$ equivalent to an inventory of 10 ppm dissolved Ca in the loop volume was added, the pressure drop at a flow rate of 0.1 ft/s increased from 0.4 psi to 1.4 psi. The $Ca_3(PO_4)_2$ precipitate was again visible, but the cloud was much fainter than the previous test which had a 200 ppm Ca inventory. Additional $CaCl_2$ was then added to simulate a 25 ppm inventory. The pressure drop increased from 1.4 psi to 6.4 psi and the pump again started to cavitate, since the test loop was unpressurized. The velocity was then decreased to 0.01 ft/s at which point the pressure drop decreased to 0.5 psi. A final increment of $CaCl_2$ was added to simulate a 50 ppm inventory of total dissolved Ca. At a flow rate of 0.01 ft/s, the pressure drop increased from 0.5 psi to 1.0 psi within 4 minutes. Under continuing operation for another 12 minutes, the pressure drop increased to 5.2 psi, but the velocity could not be maintained as the suction pressure on the pump dropped. The flow rate and pressure drop as a function of time in ICET–3–2 are shown in Fig. 7.

An interesting qualitative difference was noted between the $CaCl_2$ additions at flow rates of 0.1 ft/s and those at 0.01 ft/s. At 0.1 ft/s, the precipitate was a finely dispersed milky cloud. At 0.01 ft/s, these particles seemed to agglomerate into light, flocculent assemblies up to perhaps 0.25 in. in diameter as shown in Fig. 8. These larger assemblies appear similar to the material observed in the ICET–3 tank where velocities are likely lower than 0.1 ft/s.

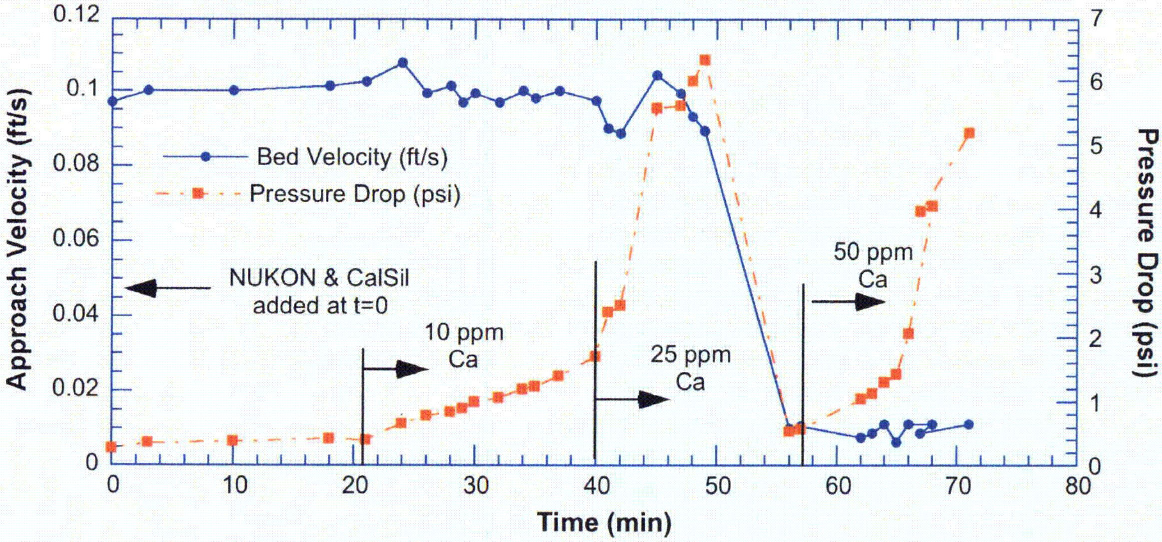

Figure 7. Flow rate and pressure drop as a function of time in ICET–3–2.

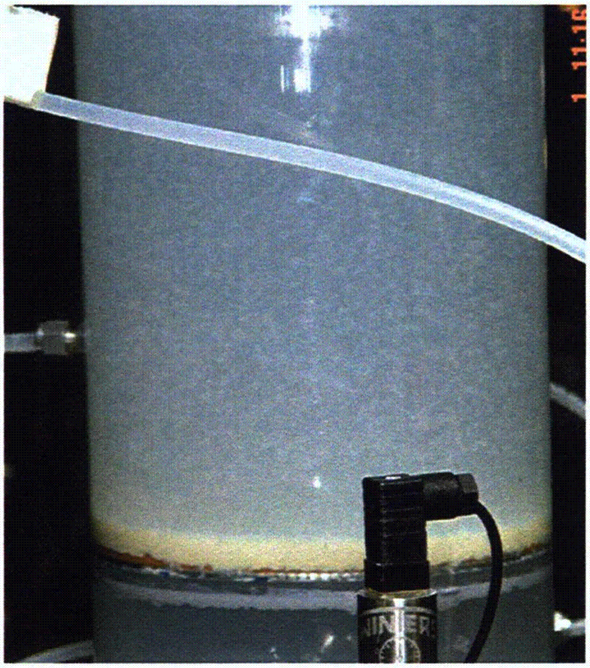

Figure 8.
Flocculent precipitates observed at 0.01 ft/s in ICET–3–2

2. 4.3 ICET-3-4 test procedure and results

ICET-3-4 test procedure:

The physical debris in ICET-3-4 consisted of 25 g (1.19 kg/m^2; 0.2 g/l) of Cal–Sil and 7 g of NUKON (0.33 kg/m^2; 0.06 g/l). The amount of Cal–Sil per unit area of the screen in this test was intended to bound the values expected after plants have installed their modified screen designs.[8] The Cal–Sil and NUKON were heated outside the test loop for 30 minutes at 60°C (140°F) in borated water (2800 ppm B and 0.7 ppm Li) to simulate the Cal–Sil/NUKON dissolution that occurs in the period between the LOCA and the onset of recirculation. Because no TSP was added during the presoak phase, the dissolution testing results for high concentrations of Cal–Sil (> 6 g/l)[7] show the concentration of dissolved Ca in the 2.5 L of presoak solution will saturate at ≈200 ppm. This gives an effective inventory of dissolved Ca in the loop of ≈ 4 ppm when the 2.5 L of presoak solution is added to the loop, which has a volume of ≈120 L. One eighth of the desired TSP concentration was premixed in the loop before the addition of the debris to simulate the TSP dissolution that occurs prior to the start for recirculation. The remaining TSP was to be metered into the loop over an hour to simulate the dissolution of the remaining TSP after the start of recirculation. Although there is uncertainty in how long it will take for the TSP to dissolve, even one eighth of the TSP inventory is sufficient, on a stoichiometric basis, to convert to calcium phosphates the dissolved Ca level equivalent to full dissolution of 0.2 g/l of Cal–Sil. Thus, the amount of precipitate that is formed as the debris slurry is added to the loop is limited by the amount of dissolved Ca available.

This test was intended to be a lower bound (for this Cal–Sil loading) for the amount of calcium phosphate precipitate arriving at the screen as the initial debris bed is formed. However, additional Cal–Sil dissolution and calcium phosphate formation was expected to occur after the initial formation of the bed. Therefore, it was planned that the test would proceed until either all the calcium phosphate had formed (based on stabilized dissolved phosphorus levels in the loop mixture), or the head loss reached steady state. It was anticipated that the test could last up to three days.

ICET-3-4 test results:

The test started at 7:45 am and terminated at 12:07 pm on November 15, 2005. Figure 2 shows the bed approach velocity and differential pressure across the screen, as a function of time during the test. Figure 10 shows an expanded view of the velocity and pressure during the first 15 minutes of the test. After the introduction of the debris, the pressure drop across the bed increased very rapidly to 6.5 psi, before any additional TSP could be metered into the loop. The pump started to ingest air so the flow velocity was reduced to 0.03 ft/s. However, after operating for several minutes at that velocity it became apparent that large amounts of air had accumulated under the test screen and the test was terminated.

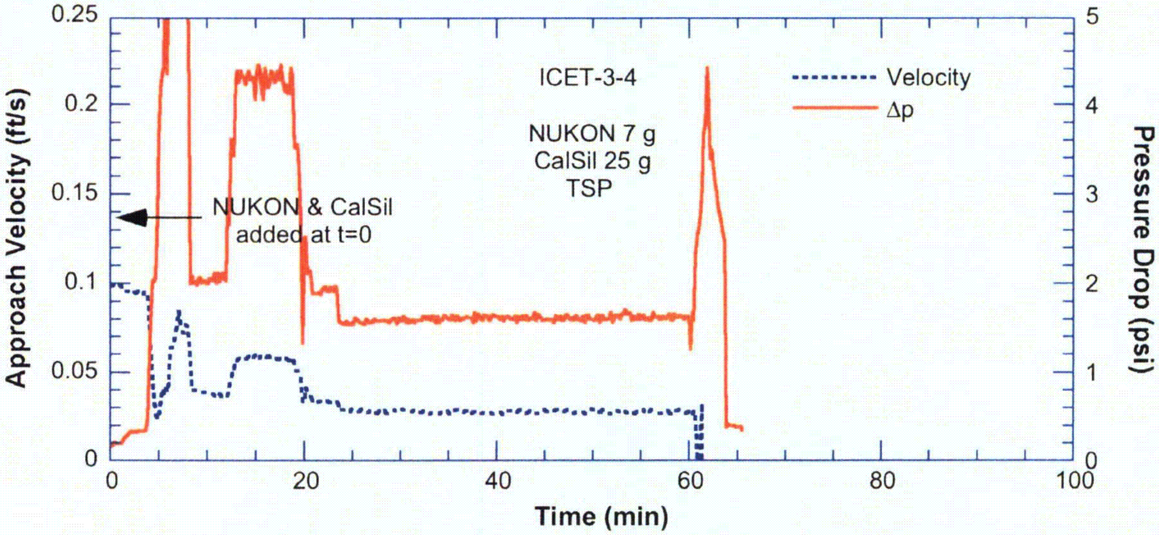

Figure 9. Bed approach velocity and differential pressure across the screen as a function of time for test ICET-3-4.

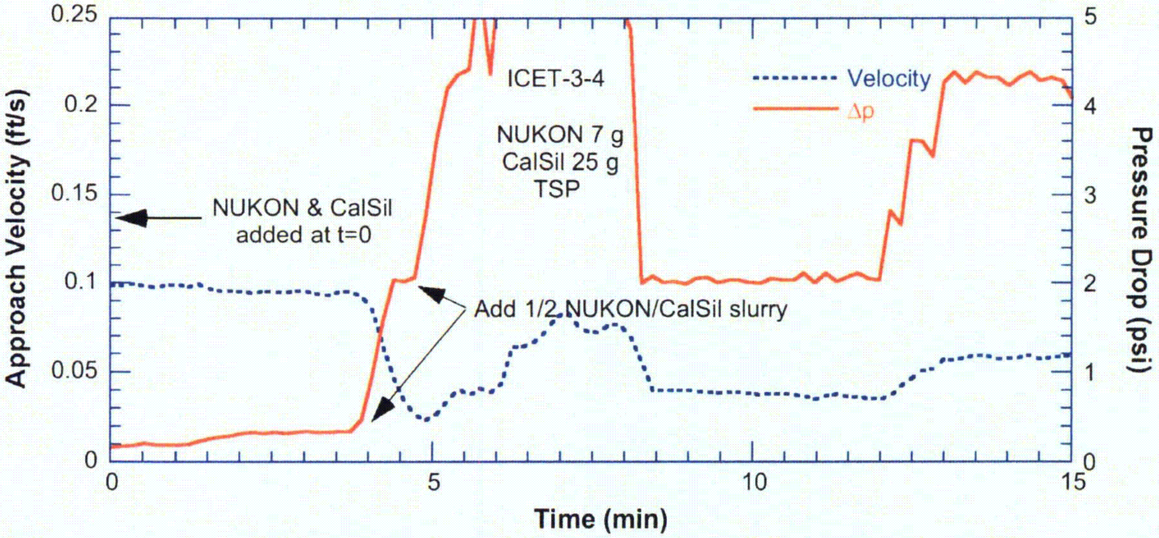

Figure 10. Expanded view of bed approach velocity and differential pressure across the screen during the initial 15 minutes of test ICET-3-4.

2. 4.4 ICET-3-5 test procedure and results

ICET-3-5 test procedure

The type and amount of physical debris for this test was identical to that for test ICET-3-4. This was a baseline test to determine the effects of the debris alone with no calcium phosphate precipitates. The Cal–Sil and NUKON were again heated outside the test loop for 30 minutes at 60° (140°F) in borated water (2800 ppm B and 0.7 ppm Li), but no TSP was added either to the presoak or to the loop during this test.

ICET-3-5 Results

This test again resulted in high head loss. Figure 11 shows the bed approach velocity and differential pressure across the screen, as a function of time during the test. After the debris was added to the loop, the pressure drop increased very rapidly. When the pressure drop across the bed increased to about 3 psi, jetting through the debris bed was observed at 25 minutes and the test was terminated at 35 minutes. It is not clear whether the difference in the peak values of Δp attained between this test (3 psi) and ICET-3-4 (6 psi) reflects simple scatter in when jetting can occur or whether the presence of the chemical product helps prevent jetting by more effectively plugging weak spots in the bed. Figure 12 shows an expanded view of the velocity and pressure during the first 10 minutes of tests ICET-3-4 & 5. Head loss for the debris loading in these tests was substantial and occurred within the first six minutes (or after approximately one test loop recirculation) after introducing debris. Other than the maximum pressure reached during the test, the presence of calcium phosphate did not clearly alter the observed accumulation of head loss during these tests.

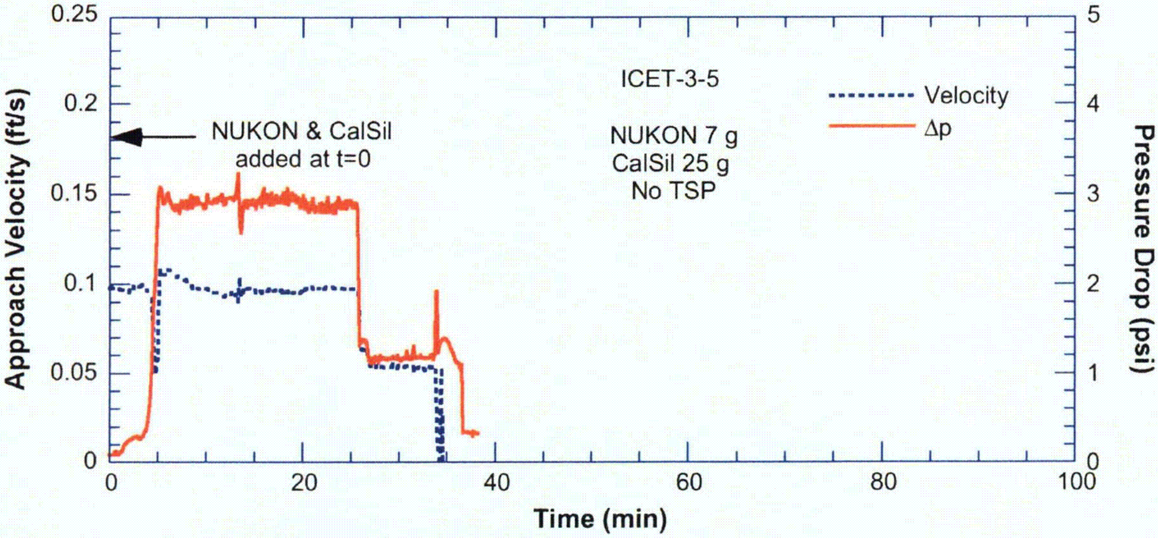

Figure 11. Bed approach velocity and differential pressure across the screen as a function of time for test ICET-3-5.

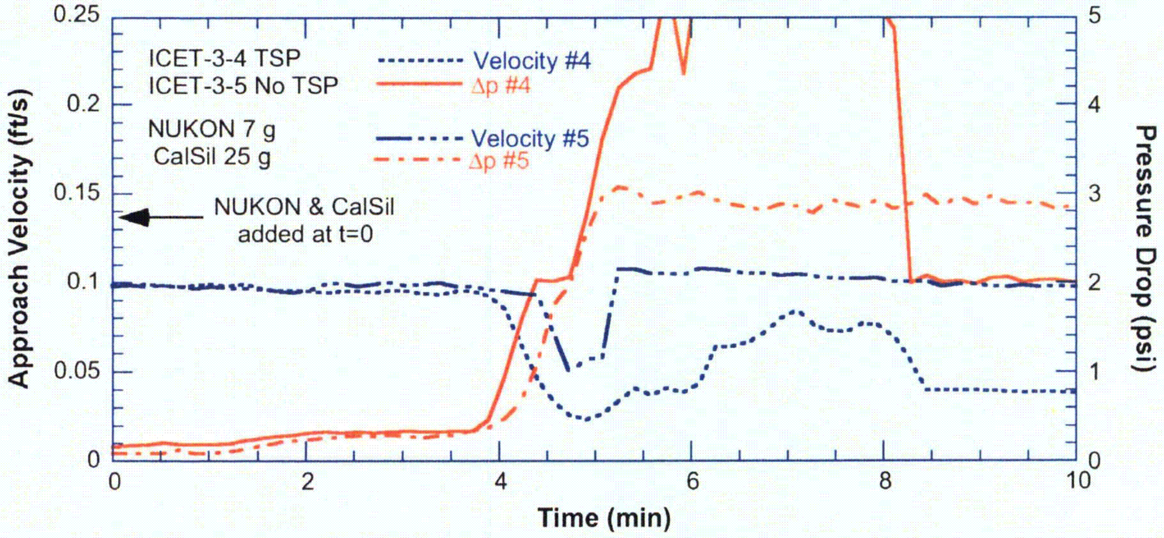

Figure 12. Expanded view of bed approach velocity and differential pressure across the screen during the initial 10 minutes of tests ICET-3-4 & 5.

2. 4.5 ICET-3-6 test procedure and results

ICET-3-6 test procedure

Due to the high head losses observed with the debris bed loading used in the previous tests, the debris loading in ICET-3-6 was changed to 15 g of Cal–Sil and 15 g of NUKON. The intent of this test was identical to that of test ICET-3-4, i.e., to minimize the amount of initial calcium phosphate precipitate arriving at the screen as the debris bed is formed for a given Cal–Sil loading. The motivation for decreasing the loading was to attempt to more clearly understand the head loss contribution that could be attributed to calcium phosphate formation. This debris loading had been previously used in ICET-3-1 & 2 and exhibited only modest increases in head loss in the portions of those tests in which chemical effects were absent. The 15 g Cal–Sil loading (0.13 g/l) is also representative for some plants containing TSP and Cal–Sil.[8]

ICET-3-6 test results

Figure 13 shows the bed approach velocity and differential pressure across the screen, as a function of time during the test. Figure 14 compares the head loss in this test during the first 45 minutes after introducing NUKON and Cal–Sil to the test loop with the earlier ICET 3-1 & 2 tests. Tests ICET-3-1 & 2 had similar amounts of debris loading as ICET-3-6, although the NUKON and Cal–Sil in ICET-3-6 came from different batches of materials. Additionally, the debris materials were not presoaked in ICET-3-1 & 2 to create an initial dissolved Ca inventory, thus less calcium phosphate would be expected initially in tests ICET-3-1 & 2. However, the initial amount of dissolved Ca in ICET-3-6 is minimized because no TSP was added during the 30 minute presoak. It is therefore not surprising that the difference in head loss between test ICET-3-6 and tests ICET-1 & 2 within the first 30 minutes is not too large. However, compared with ICET-1 & 2, the head loss in ICET-3-6 continues to increase as the test proceeds, more Cal–Sil dissolves, and more calcium phosphate is subsequently formed.

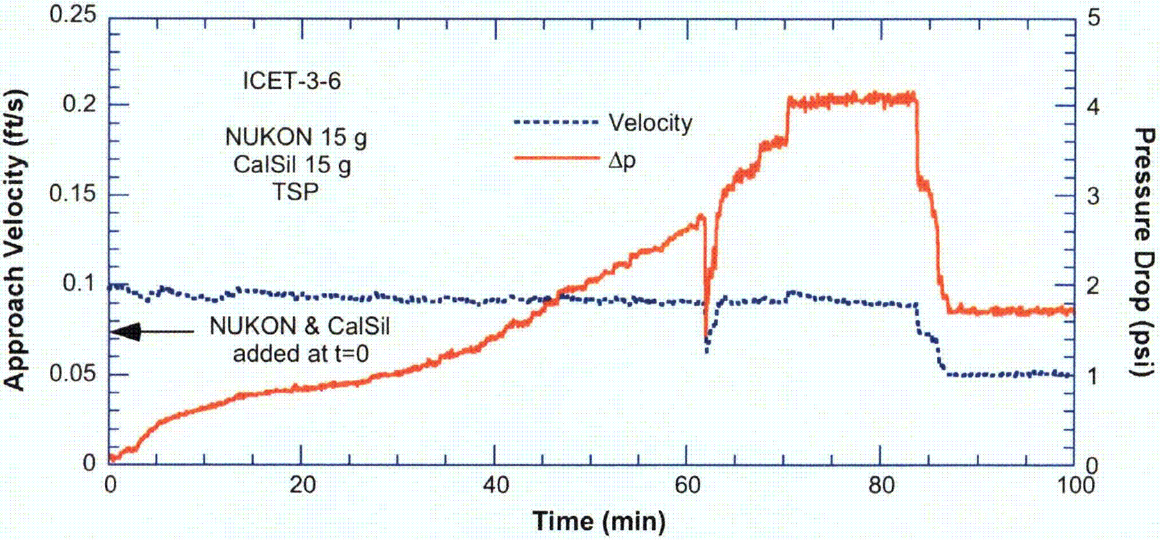

Figure 13. Bed approach velocity and differential pressure across the screen as a function of time for test ICET-3-6.

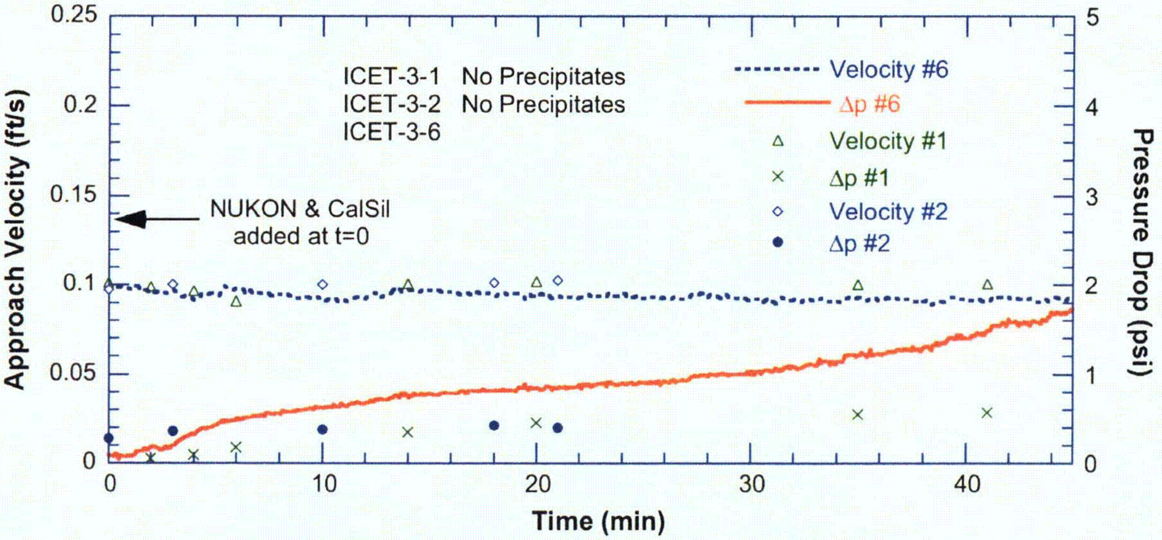

Figure 14. Expanded view of bed approach velocity and differential pressure across the screen during the initial 45 minutes of tests ICET-3-1, 2 & 6.

2. 4.6 ICET-3-7 test procedure and results

ICET-3-7 test procedure:

Test ICET-3-7 was a baseline test with a debris loading of 15 g of Cal–Sil and 15 g of NUKON and no TSP in the loop or in the presoak at any time. Therefore, no calcium phosphate precipitate is present to contribute to head loss. The Cal–Sil and NUKON were again heated outside the test loop for 30 minutes at 60°C (140°) in borated water (2800 ppm B and 0.7 ppm Li) and then added to the loop.

ICET-3-7 test results:

Figure 15 shows the bed approach velocity and differential pressure across the screen, as a function of time during the test. The pressure drop across the bed increased rapidly (within 25 minutes) to about 2.8 psi and then stabilized. It was suspected that, at this point, the bed had perforated and jetting was occurring even though the bed appeared smooth and uniform. However, a considerable layer of air had developed underneath the bed and this precluded the actual identification of any jet. To determine if jetting was occurring, the inlet tee, which is normally left open, was filled to the top with about one liter of demineralized water and sealed with a closure flange. The loop was then pressurized to 13 psi using demineralized water 46 minutes after the debris was added. Under pressure, the air layer under the bed was greatly reduced and it became possible to confirm that jetting was occurring and to identify jet locations in the bed, although the bed still exhibited no observable defects.

The pressure drop across the debris bed increased very rapidly compared to the corresponding pressure drops observed in ICET-3-1, 2, & 6 which had similar debris loadings. Because no TSP was introduced at any time during the test, no calcium phosphate precipitates were expected to form. Chemical analysis of grab samples taken periodically through the test confirmed that P levels were very low, as expected. Because the magnitude and rapidity of the pressure drop increase in this test are much greater than observed in both earlier tests with similar debris loading and in subsequent replicate tests under the same nominal conditions, the results of this test are believed to be anomalous. Two replicate tests (ICET–1-11 and 14) were performed to substantiate this conclusion.

During this test, some release of noncondensible gases was observed as the pressure drop across the bed increased to about 1.4 psi. This led to a re-evaluation of the procedure for deaerating the loop. In this test and in previous tests, the loop had been deaerated on the day prior to the test day by heating the water to 71°C (160°F) and circulating the test loop fluid at fairly high speeds (2 ft/s) for several hours. The loop was then allowed to cool overnight. This procedure had been chosen to avoid running the pump overnight unattended. However, as the test loop fluid cooled, additional gases were re-entrained in the fluid and thus, were available to be released at relatively low pressures. Exploratory tests had shown that heating of the water induced sufficient natural circulation to maintain a uniform temperature in the loop without the pump. The deaeration procedure for subsequent tests was modified to never let the loop cool down after the initial heat–up in order to minimize the noncondensible gases in the fluid. Natural circulation was used to maintain a uniform temperature without the need to run the pump unattended overnight.

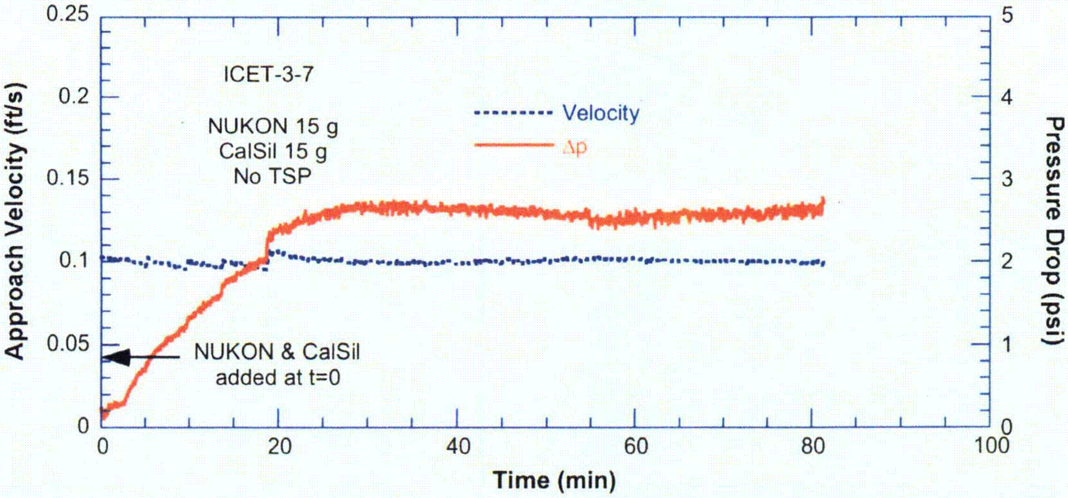

Figure 15. Bed approach velocity and differential pressure across the screen as a function of time for test ICET-3-7.

2. 4.7 ICET-3-8 test procedure and results

ICET-3-8 test procedure:

ICET-3-8 was intended to represent the limiting case when the Ca is almost completely leached from the Cal–Sil debris prior to the formation of the debris bed. In this test, the boric acid, lithium hydroxide and all of the TSP were added to the loop water and heated to 60°C prior to adding the physical debris. The physical debris consisted of 15 g NUKON which has been presoaked for ½ hour at 60°C. The NUKON slurry was then combined with 14.3 g of $CaCl_2$, which gives an amount of dissolved Ca level equivalent to complete stoichiometric dissolution of 15 g Cal–Sil. The NUKON/$CaCl_2$ mixture (about 2.5 L) was then added to the loop. The addition was done in about 30 seconds. Because the reaction of the dissolved Ca with the phosphate is very rapid, the test screen debris bed was formed with a simultaneous mix of NUKON and calcium phosphate precipitates.

ICET-3-8 test results:

Figure 16 shows the bed approach velocity and differential pressure across the screen as a function of time. After adding the NUKON and $CaCl_2$ mixture, the pressure drop across the bed increased very rapidly and it was not possible to maintain the loop flow velocity at 0.1 ft/s through the pump. After ≈8 minutes, the flow rate was decreased to 0.03 ft/s, and the pressure drop stabilized at ≈5 psi. The debris bed appeared to be uniform with a thickness between 8 – 10 mm early in the test before the pressure drop got too large. The bed compressed to a thickness of approximately 6 mm at the end of the test. The loop water quickly cleared indicating rapid debris bed filtration. No jetting through the bed was observed.

Figure 17 shows the photographs of the debris bed from this test after removal from the loop and at the end of the test with the loop almost drained. The debris bed height (see Figure 17b) has increased slightly compared with thickness at the end of the test. Additionally, the debris bed is comprised of two distinct layers (Figure 17b). The bottom layer is mixed NUKON and calcium phosphate precipitate while the top layer is predominantly calcium phosphate precipitate.

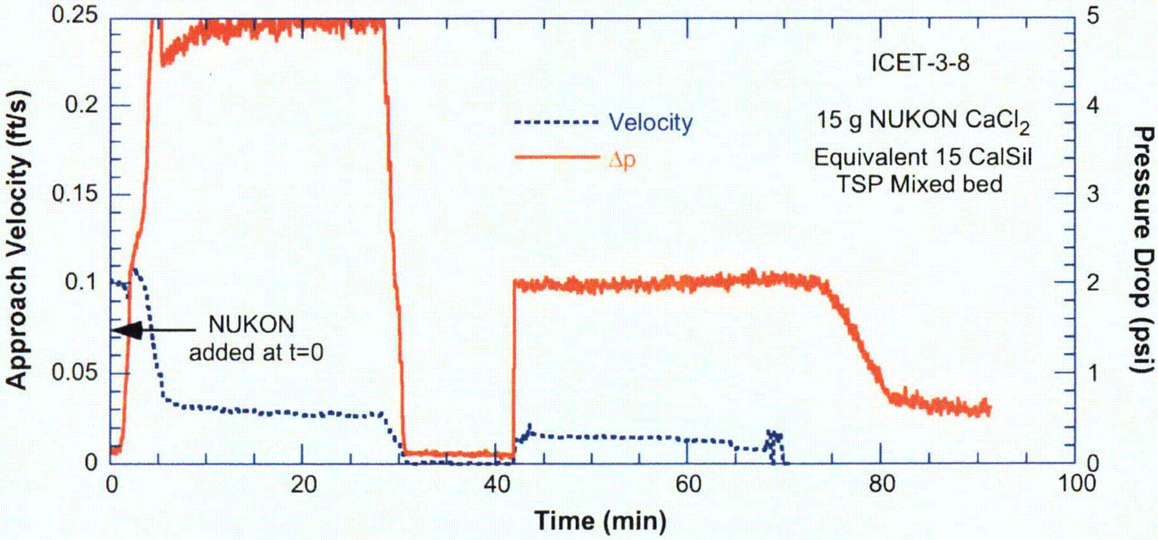

Figure 16. Bed approach velocity and differential pressure across the screen as a function of time for test ICET-3-8.

(a) (b)

Figure 17. (a) Debris bed from ICET-3-8 after removal from the loop: (b) Debris bed in the loop at the end of the test with the loop almost drained. The bed has two distinct layers. (Readers of the electronic version may wish to zoom to 500% to see the layers more distinctly.)

2. 4.8 ICET-3-9 test procedure and results

ICET-3-9 test procedure:

ICET-3-9 was intended to evaluate the head loss from chemical phosphate precipitate arriving at the test screen after the NUKON bed had formed. This test objective and procedure is similar to previous ICET-3-1 & 2 tests. The physical debris bed consisted of 15 g of NUKON and was formed before the addition of any $CaCl_2$, i.e., before the formation of any calcium phosphate precipitate. The loop initially contained a base solution with 2800 ppm B, 0.7 ppm Li, and TSP (3.4 g/l). A total of 14.3 g of $CaCl_2$ was chosen to give a dissolved Ca inventory equivalent to a complete stoichiometric dissolution of 15 g Cal–Sil. The $CaCl_2$ solution was planned to be added in 5 steps (1/5 of the total amount at each step) with the pressure drop allowed to reach steady state between each step. Only 3 of the 5 $CaCl_2$ additions were completed before the test was terminated.

ICET-3-9 test results:

The pressure drop across the screen prior to the addition of the NUKON was 0.07±0.02 psi at an approach velocity of 0.1 ft/s. [The pressures are recorded approximately every 5 sec by the data acquisition system. When the pressure data are presented as a running average over a minute, the standard deviation of the running average is much smaller, ±0.005.] The pressure drop across the NUKON bed before the addition of any $CaCl_2$ is shown in Fig. 18. The steady state drop across the bed at this stage of the test was 0.14±0.02 psi and the debris bed was about 14 mm thick. A relatively stable value of the pressure drop was reached after one pass around the loop (≈4 min).

Eighteen minutes after the NUKON was introduced, 200 ml of $CaCl_2$ solution was added. This addition represents the stoichiometric dissolved Ca equivalent (≈9 ppm) of 3 g of Cal–Sil. The pressure drop increased to 0.242 psi (Fig. 19) and the bed compressed to 12 mm. Twenty–eight minutes after the NUKON was introduced, a second 200 ml $CaCl_2$ addition was made. The pressure drop increased to 1.2 psi and the bed compressed to 9 mm. It appears from the data (Figure 19) that this value may not quite represent the steady state head loss for this condition. Forty–one minutes after the NUKON was introduced, the third 200 ml $CaCl_2$ addition was made. After this addition, the pressure drop increased dramatically and the approach velocity could not be maintained at 0.1 ft/s. The flow rate decreased to 0.02 ft/s 43 minutes after the initial NUKON addition, and could no longer be controlled because the pump inlet pressure was at 0 psi. The flow rate continued to slowly decrease while the pressure drop continued to rise gradually during the remainder of

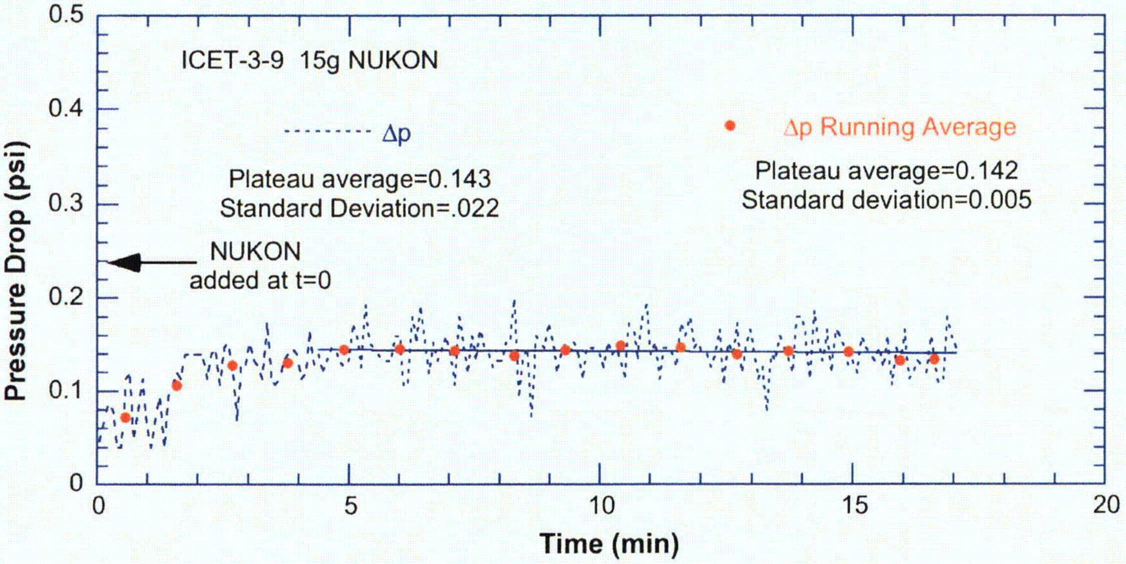

Figure 18. Pressure drop across the NUKON bed in test ICET-3-9 at an approach velocity of 0.1 ft/sec.

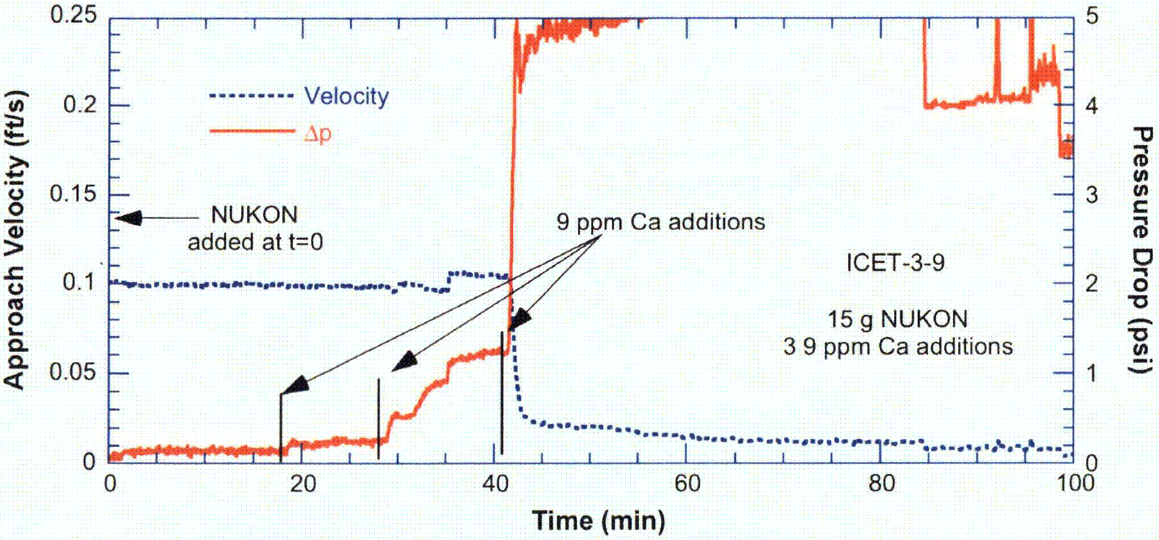

Figure 19. Bed approach velocity and differential pressure across the screen as a function of time for test ICET-3-9.

the test. The pressure drop asymptotically increased to ≈5.2 psi, as the velocity decreased. The bed thickness decreased to 7 mm at the highest pressure. Figure 19 shows the bed approach velocity and differential pressure across the screen as a function of time for entire duration of the test.

2. 4.9 ICET-3-10 test procedure and results

ICET-3-10 test procedure:

ICET-3-10 also used a debris loading of 15 g NUKON and 15 g Cal–Sil. The debris was presoaked for 30 minutes at 60°C, prior to introduction into the loop. One half of the total TSP addition was added to the debris slurry during the 30 minute presoak period, starting five minutes after the introduction of the debris and then continuing at a nominally uniform rate over the remaining 25 minutes. The remaining half of the TSP was metered directly into the loop over 30 minutes at a nominally uniform rate after the introduction of the debris. This TSP addition sequence was intended to represent a plant where TSP begins to dissolve 5 minutes after the start of a LOCA, and complete dissolution has occurred one hour after a LOCA. The conditions in this test were intended to represent a "typical" degree of leaching of the Cal–Sil prior to formation of the bed. However, because of the rapid rise in pH in the presoaking solution due to the high concentration of Cal–Sil, the presoaking probably leads to somewhat less Cal–Sil dissolution than would occur at more realistic concentrations for the same TSP history.

ICET-3-10 test results:

The bed approach velocity and differential pressure across the screen as a function of time for test ICET-3-10 is shown in Fig. 20. This test resulted in a rapid buildup of head loss. After 10 minutes, the flow velocity could not be maintained at 0.1 ft/s and the flow velocity gradually decreased. At the end of test, the pressure drop across the bed was 4.7 psi (±0.9%) at a bed approach velocity of 0.06 ft/s (±0.8%).

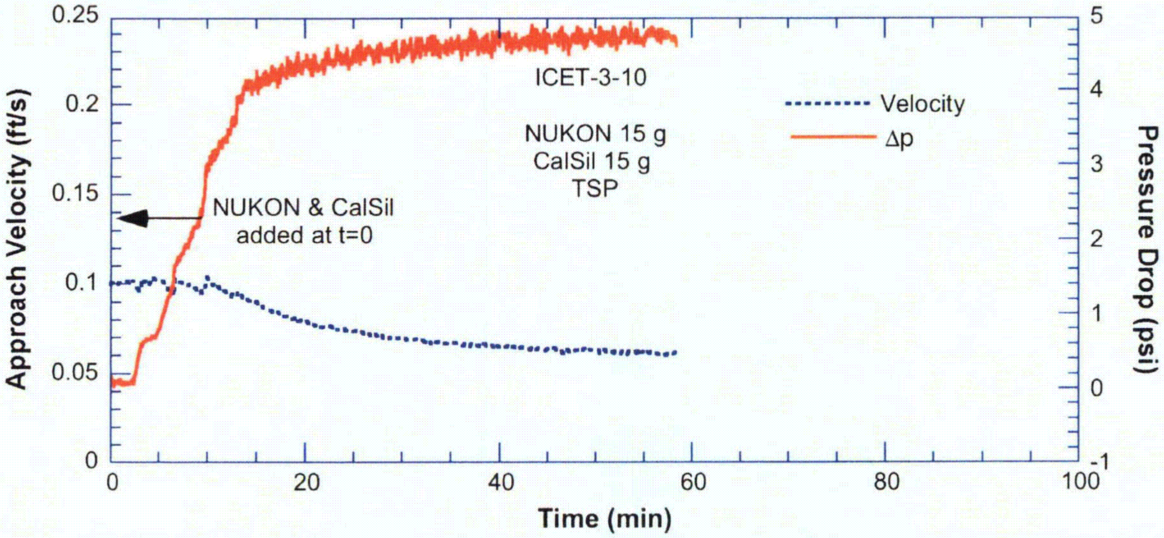

Figure 20. Bed approach velocity and differential pressure across the screen as a function of time for test ICET-3-10.

2. 4.10 ICET-3-11 test procedure and results

ICET-3-11 test procedure:

ICET-3-11 was a repeat of the baseline test, ICET-3-7, with a debris loading of 15 g NUKON and 15 g Cal–Sil. No TSP was introduced in the test during either the presoak or in the loop.

ICET-3-11 test results:

The bed approach velocity and differential pressure across the screen as a function of time for test ICET-3-11 is shown in Fig. 21. At 0.1 ft/s, the pressure drop stabilized at around 1.4±0.03 psi. After 210 minutes (≈52 recirculations) at a loop velocity of 0.1 ft/s, the loop velocity was cycled from 0.1 ft/s to 0.01 ft/s to 0.14 ft/s and back to 0.1 ft/s. Figure 22 shows the variation of the pressure drop across the bed as the velocity is cycled. Comparison with Fig. 18 shows that it takes much longer for a NUKON/Cal–Sil bed to reach a stable pressure drop than it does for a pure NUKON bed.

Test ICET-3-11 was a repeat of ICET-3-7. However, the pressure drop across the bed is very different for the two tests as shown in Fig. 23. No reason for this difference in behavior has been determined. The behavior illustrated in ICET-3-11 is consistent with the behavior observed in other tests without TSP while the ICET-3-7 results are substantially different and appear to be subject to an unidentified experimental interference. This point is illustrated in Fig. 24, which shows a comparison of bed approach velocities and differential pressures across the screen as a function of time for tests ICET-3-1, 2, & 11. The results of the ICET 3-7 tests are considered anomalous and have not been used in the evaluation of chemical effects in this report. An additional replicate test ICET 3–13, which will be discussed later in this report, was performed and was consistent with the results of ICET 3–11. Therefore, the ICET-3-11 results have been used as the baseline for comparisons with tests in which precipitates are present.

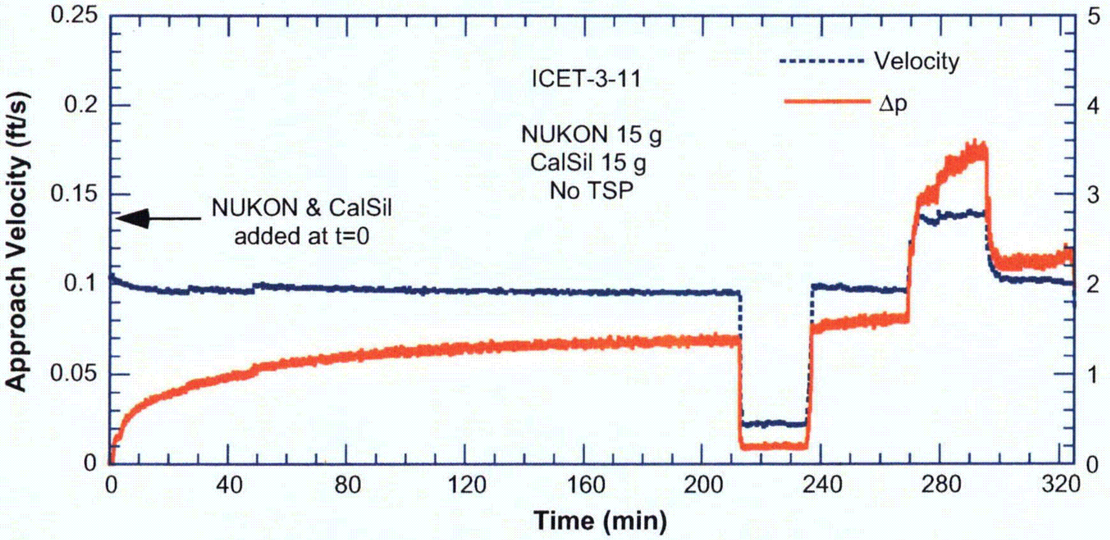

Figure 21. Bed approach velocity and differential pressure across the screen as a function of time for test ICET-3-11.

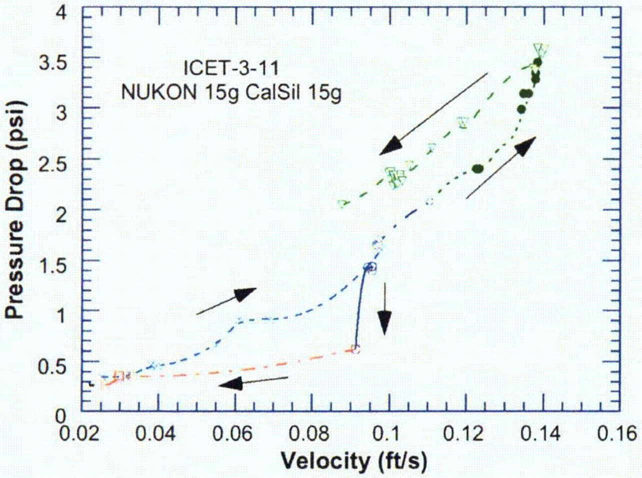

Figure 22.
Change in pressure drop across the bed as the velocity is cycled from 0.1 ft/s to 0.01 ft/s to 0.14 ft/s and back to 0.1 ft/s.

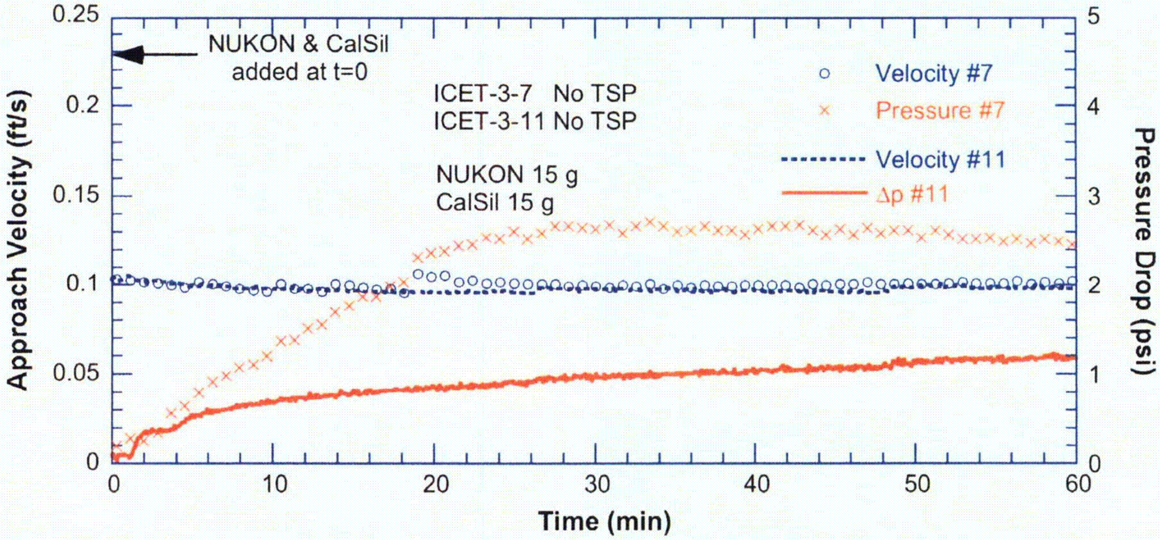

Figure 23. Bed approach velocities and differential pressures across the screen as a function of time for tests ICET-3-7 & 11.

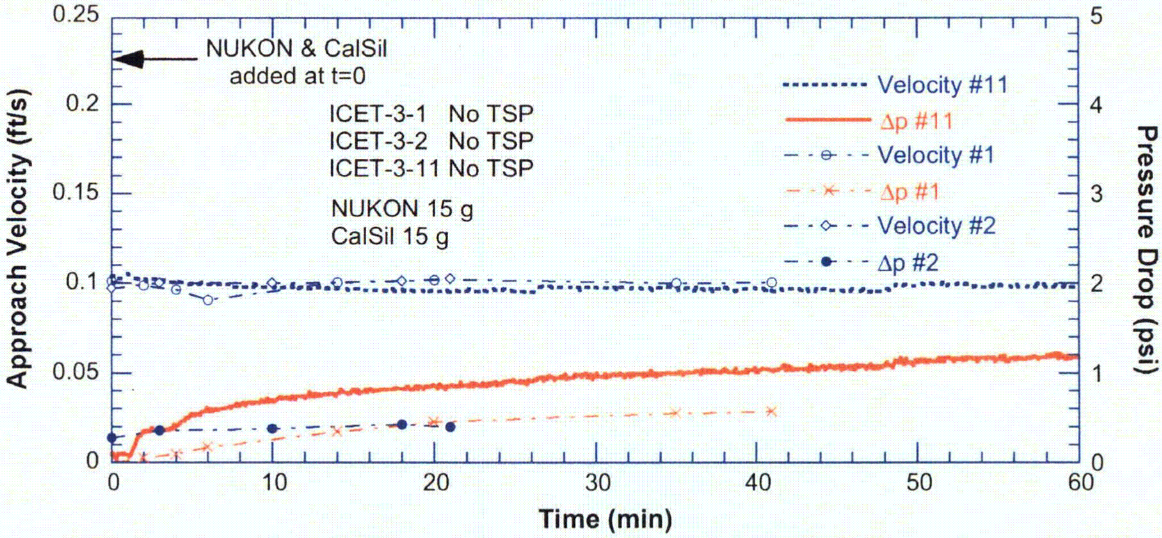

Figure 24. Bed approach velocities and differential pressures across the screen as a function of time for test ICET-3-1, 2, & 11.

2.4.11 ICET-3-12 test procedure and results

ICET-3-12 test procedure:

ICET-3-12 used a debris loading of 15 g NUKON and 5 g Cal–Sil. The debris was presoaked for 30 minutes at 60°C, prior to introduction into the loop. One half of the total TSP addition was added to the debris slurry during the 30 minute presoak period, starting five minutes after the introduction of the debris and then continuing at a nominally uniform rate over the remaining 25 minutes. The bed was about 1/2 in thick. The remaining half of the TSP was metered directly into the loop over 30 minutes at a nominally uniform rate after the introduction of the debris.

ICET-3-12 test results:

The bed approach velocity and differential pressure across the screen as a function of time for test ICET-3-12 is shown in Fig. 25. The head loss is not much greater than would be expected for a NUKON bed alone. There was a measurable change in the thickness of the bed as velocity was cycled between 0.1 ft/s and zero. Figure 26 shows the bed after removal from the loop. The smooth appearance is typical of the beds in the tests.

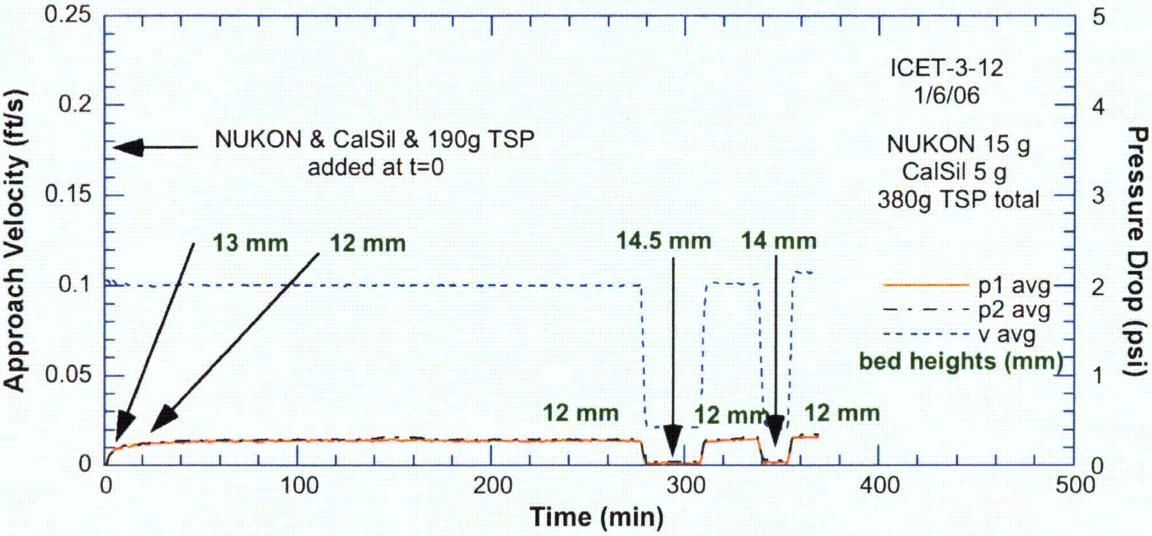

Figure 25. Bed approach velocity and differential pressure across the screen as a function of time for test ICET-3-12.

2.4.12 ICET-3-13 test procedure and results

ICET-3-13 test procedure:

ICET-3-13 also used a debris loading of 15 g NUKON and 5 g Cal–Sil. The debris was presoaked for 30 minutes at 60°C, prior to introduction into the loop. No TSP was added either to the slurry during the presoak or to the loop during the test. This is a baseline test in a chemically inactive environment for comparison with ICET–3–12.

ICET-3-13 test results:

The bed approach velocity and differential pressure across the screen as a function of time for test ICET-3-13 is shown in Fig. 27 along with the corresponding results from ICET–3–12. The head loss is virtually identical in the two tests, although TSP was present in ICET–3–12 and there was the potential for $Ca_3(PO_4)_2$ precipitation.

Figure 26. ICET–3–12 bed after removal from the loop. The smooth appearance is typical of the beds in the tests.

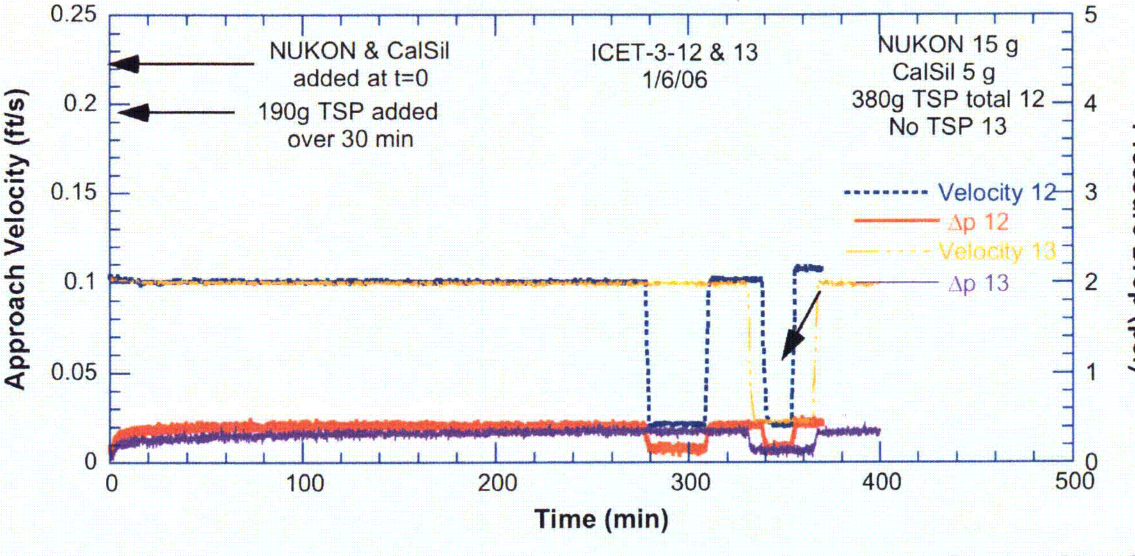

Figure 27. Bed approach velocities and differential pressures across the screen as a function of time for tests ICET-3-12 and 3–13.

2.4.13 ICET–3–14 test procedure and results

ICET-3-14 test procedure:

ICET-3-14 used a debris loading of 15 g NUKON and 15 g Cal–Sil. The debris was presoaked for 30 minutes at 60°C, prior to introduction into the loop. No TSP was added either to the slurry during the presoak or to the loop during the test. This is a baseline test in a chemically inactive environment for comparison with ICET–3–10. It replicates the conditions of ICET–3-7 and ICET–3–11.

ICET-3-14 test results:

The bed approach velocity and differential pressure across the screen as a function of time for test ICET-3-14 is shown in Fig. 28 along with the corresponding results from ICET–3–11.

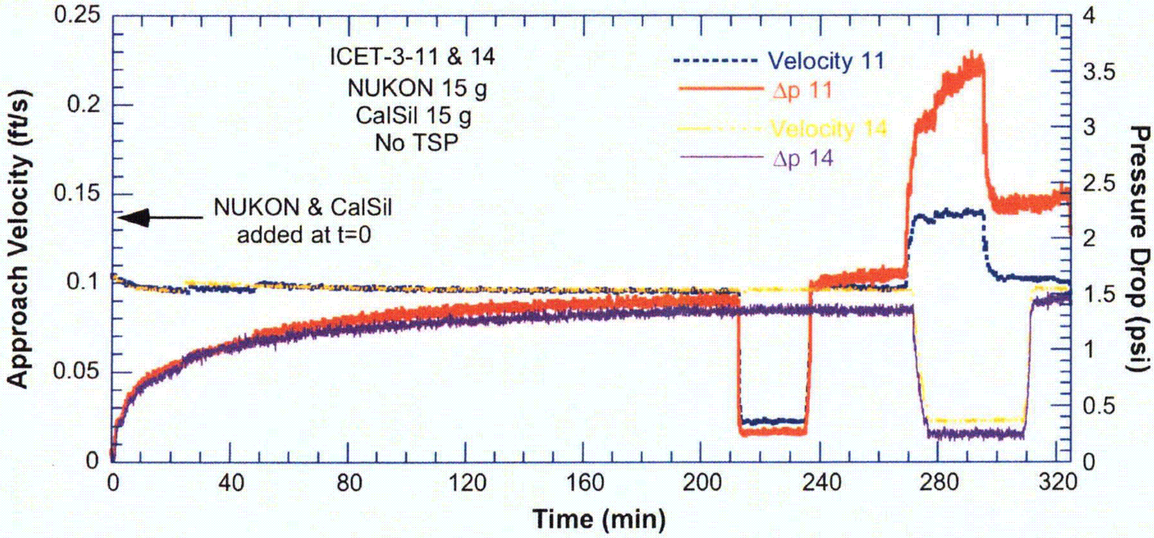

Figure 28. Bed approach velocities and differential pressures across the screen as a function of time for tests ICET-3-11 and 3–14.

2.4.14 ICET-15 test procedure and results

ICET-3-15 test procedure:

ICET-3-15 used a debris loading of 15 g NUKON and 10 g Cal–Sil. No TSP was added either to the slurry during the presoak or to the loop during the test. This is a baseline test in a chemically inactive environment for comparison with ICET–3–16.

ICET-3-15 test results:

The bed approach velocity and differential pressure across the screen as a function of time for test ICET-3-15 is shown in Fig. 29.

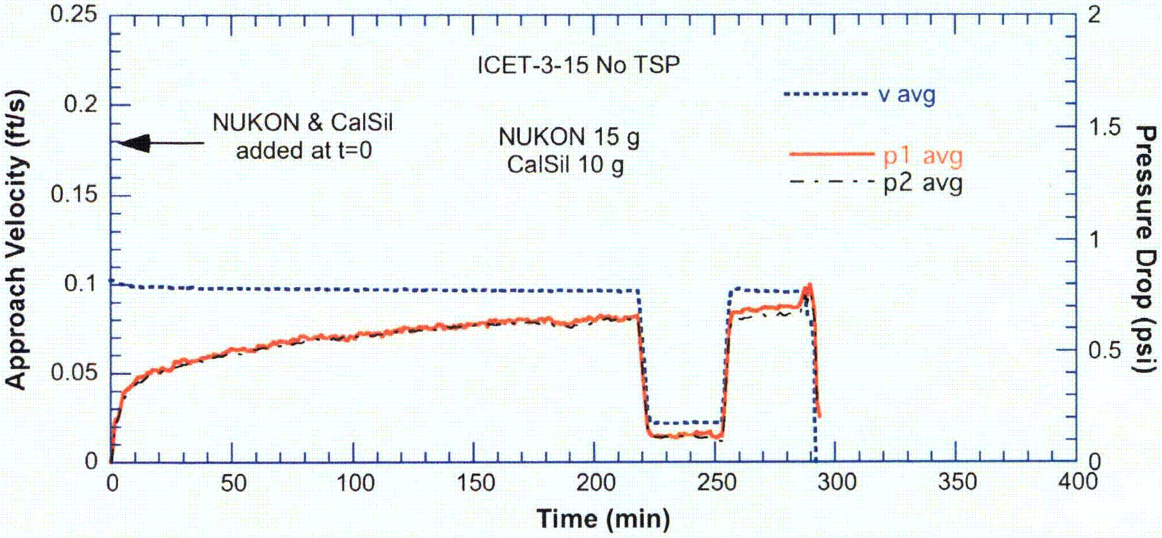

Figure 29. Bed approach velocity and differential pressure across the screen as a function of time for test ICET-3-15.

2.4.15 ICET-3–16-A1 test procedure and results

ICET-3-16-A1 test procedure:

ICET-3-16 also used a debris loading of 15 g NUKON and 10 g Cal–Sil. The debris was presoaked for 30 minutes at 60°C, prior to introduction into the loop. One half of the total TSP addition was added to the debris slurry during the 30 minute presoak period, starting five minutes after the introduction of the debris and then continuing at a nominally uniform rate over the remaining 25 minutes. The remaining half of the TSP was metered directly into the loop over 30 minutes at a nominally uniform rate after the introduction of the debris.

ICET-3-16-A1 test results:

The bed approach velocity and differential pressure across the screen as a function of time for test ICET-3-16 is shown in Fig. 30 along with the corresponding results from ICET–3–15. No effect of the presence of the TSP can be observed.

2.4.16 ICET-17-A1 test procedure and results

ICET-3-17-A1 test procedure:

ICET-3-17–A1 used a debris loading of 15 g NUKON and 15 g Cal–Sil and was a replicate of ICET–3–10. The debris was presoaked for 30 minutes at 60°C, prior to introduction into the loop. One half of the total TSP addition was added to the debris slurry during the 30 minute presoak period, starting five minutes after the introduction of the debris and then continuing at a nominally uniform rate over the remaining 25 minutes. The designation A1 means that the screen with 3/16 in holes was used.

ICET-3-17-A1 test results:

The bed approach velocity and differential pressure across the screen as a function of time for test ICET-3-17–A1 is shown in Fig. 31. This test resulted in a rapid buildup of head loss. After 30 minutes, the flow velocity could not be maintained at 0.1 ft/s and the flow velocity gradually decreased. Comparison with ICET–3–10 shows that the pressure increase is somewhat faster in ICET–3–10 and the pressure drop gets

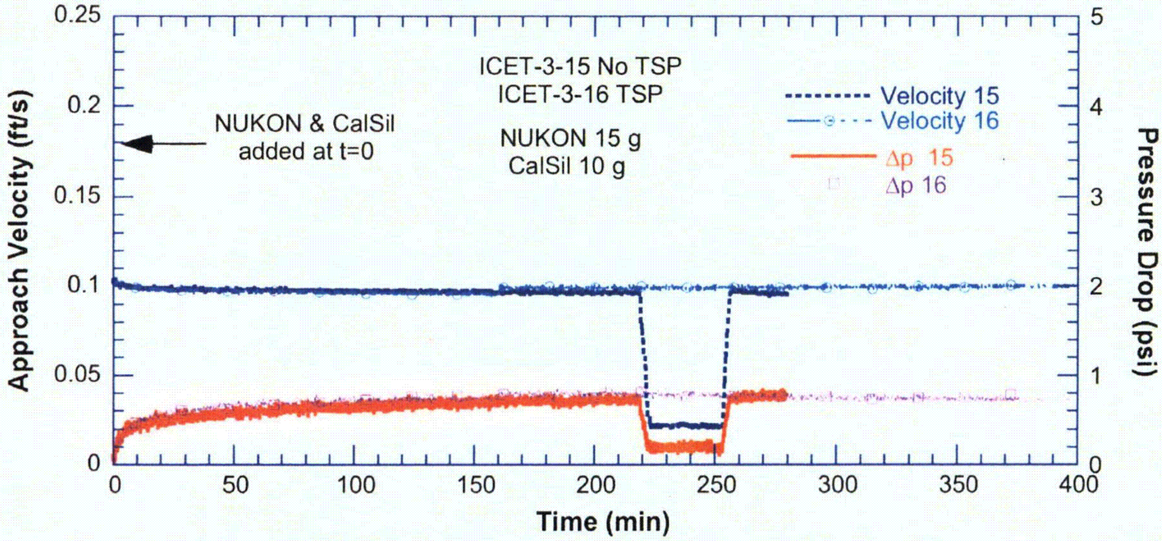

Figure 30. Bed approach velocities and differential pressures across the screen as a function of time for tests ICET-3-15 and 3–16.

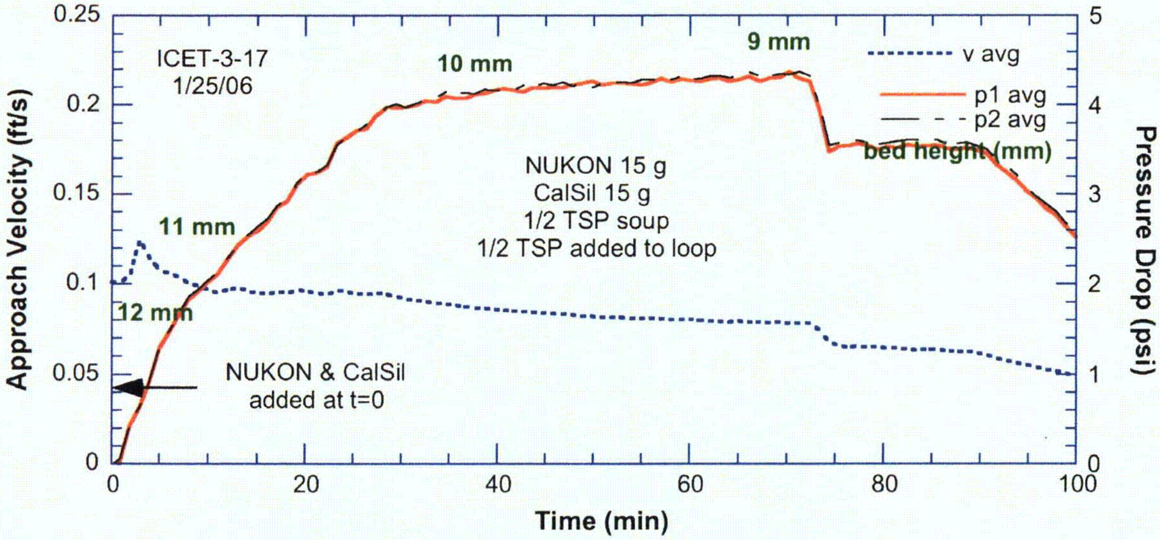

Figure 31. Bed approach velocity and differential pressure across the screen as a function of time for test ICET-3-17–A1.

somewhat higher before the velocity begins to drop. However, the general behavior essentially replicates that of ICET–3–10.

2.4.17 ICET-3–18-A1 test procedure and results

ICET-3-18-A1 test procedure:

ICET-3-18–A1 used a debris loading of 5 g NUKON and 10 g Cal–Sil. This resulted in a thin debris bed about 3–4 mm thick. The debris was presoaked for 30 minutes at 60°C, prior to introduction into the loop. One half of the total TSP addition was added to the debris slurry during the 30 minute presoak period, starting five minutes after the introduction of the debris and then continuing at a nominally uniform rate over

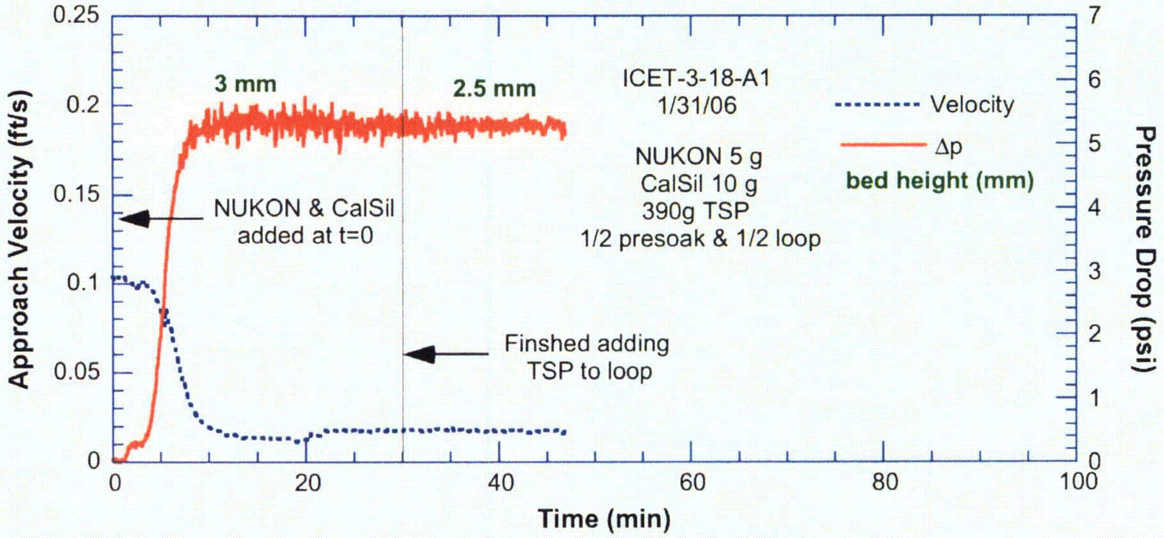

Figure 32. Bed approach velocity and differential pressure across the screen as a function of time for test ICET-3-18–A1.

the remaining 25 minutes. The remaining half of the TSP was metered directly into the loop over 30 minutes at a nominally uniform rate after the introduction of the debris.

ICET-3-18-A1 test results:

The bed approach velocity and differential pressure across the screen as a function of time for test ICET-3-18–A1 is shown in Fig. 32. This test resulted in a rapid buildup of head loss. After 10 minutes, the flow velocity could not be maintained at 0.1 ft/s and the flow velocity gradually decreased. The thinner bed plugged more rapidly than in either ICER–3–10 or ICET–3–17, which had 15 g NUKON and 15 g Cal–Sil and was about 12 mm thick. This test result is consistent with the classic thin–bed head loss behavior observed elsewhere (i.e., a thin fiber bed that becomes saturated with particulate can result in high head loss).

2.4.18 ICET-3–19-A2 test procedure and results

ICET-3-19-A2 test procedure:

ICET-3-19-A2 used a debris loading of 25 g Cal–Sil with no NUKON. This test also used the finer 1/8 in hole screen with the more restricted 40% flow area. The debris was presoaked for 30 minutes at 60°C, prior to introduction into the loop.

ICET-3-19-A2 test results:

The 25 g of Cal–Sil used in this test corresponds to a screen loading of 1.2 kg/m^2, which is probably conservative for most plants after their sump screens are updated. The debris bed that formed on the screen is shown in Figs. 33 and 34. Although a portion of the flow area is blocked by the Cal–Sil, a significant portion of the screen remains open with this loading. The bed approach velocity and differential pressure across the screen as a function of time for test ICET-3-19–A2 is shown in Fig. 35. The pressure drops are very low as expected with a significant open area. The bed approach velocity and differential pressure across the screen are replotted with an expanded scale in Fig. 36. This test is intended to represent a plant condition where a bare screen (i.e., no fiber insulation loading) is loaded with Cal–Sil insulation and calcium phosphate precipitate.

Figure 33. Plan view of debris bed formed by pure Cal–Sil loading in ICET–3–19–A2.

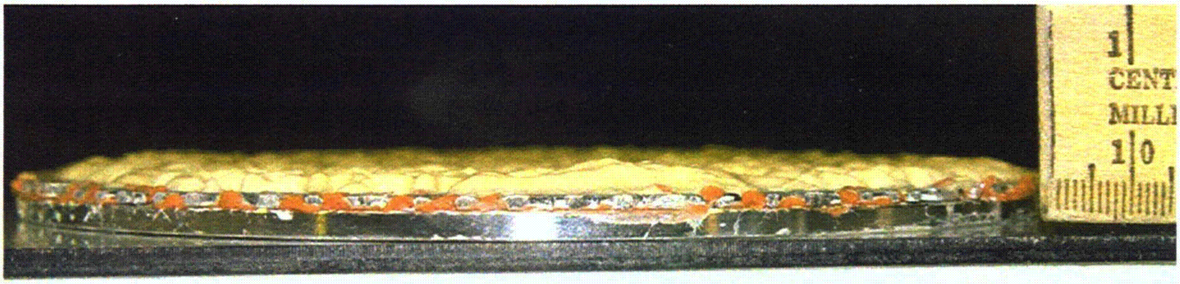

Figure 34. Side view of debris bed formed by pure Cal–Sil loading in ICET–3–19–A2.

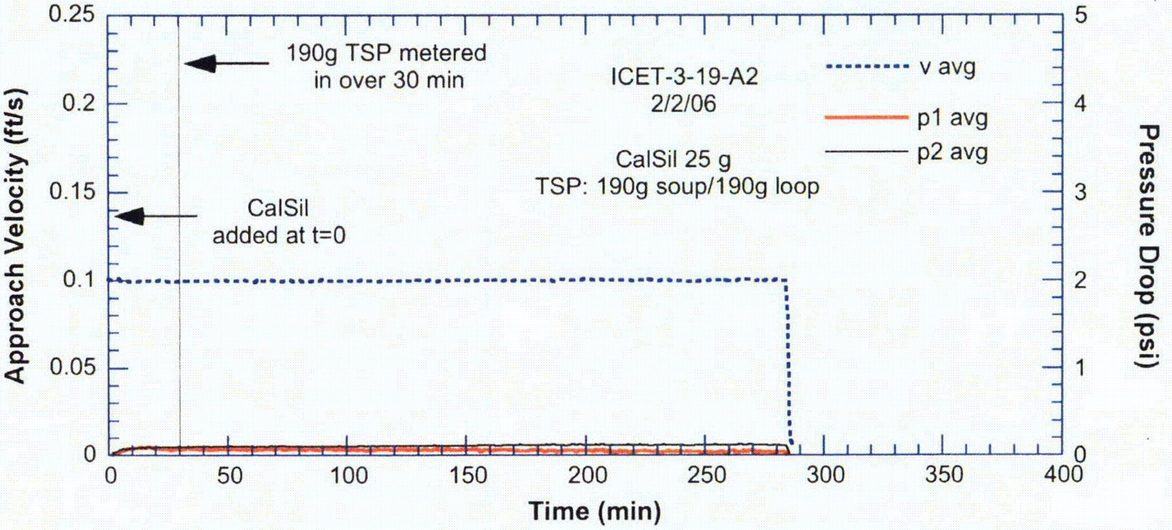

Figure 35. Bed approach velocity and differential pressure across the screen as a function of time for test ICET-3-19–A2.

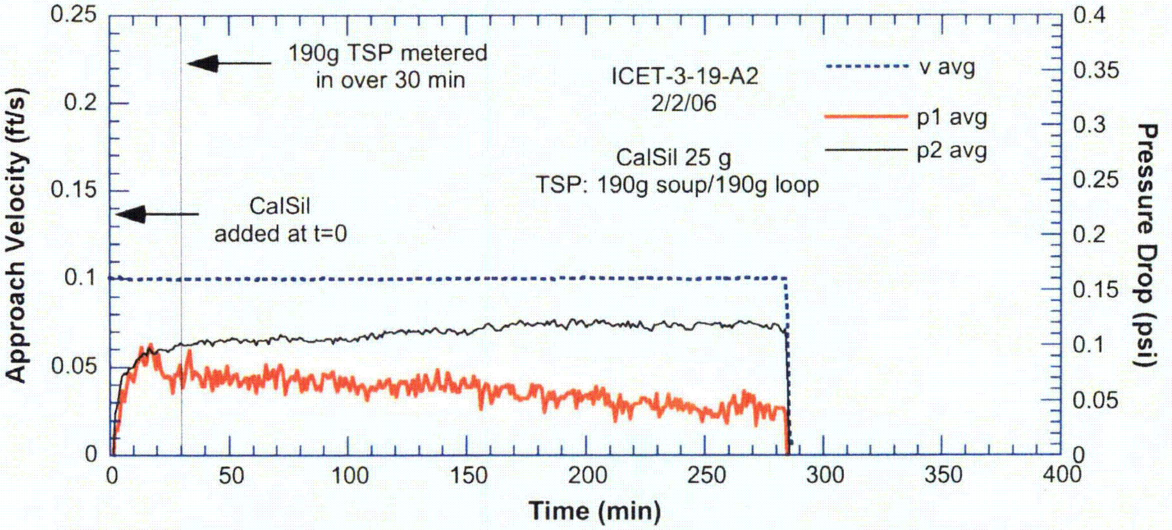

Figure 36. Bed approach velocity and differential pressure across the screen as a function of time for test ICET-3-19–A2.

2.5 Discussion of the ICET–3 series test results

The pressure drops across the bed for tests with physical debris of 15 g NUKON/15 g Cal–Sil and TSP present (ICET-3-6 and ICET-3-10) are compared with the baseline test ICET-3-11, which had 15 g NUKON/15 g Cal–Sil but no TSP, in Figs. 37a and b, respectively. In ICET-3-6, no TSP was added to the presoak in order to limit the possible dissolution of the Cal–Sil. This scenario was intended to give a lower bound for the amount of calcium phosphate precipitate arriving as the debris bed is formed. As expected, the initial pressure drop behavior in ICET-3-6 is very similar to the baseline case ICET-3-11 in which no chemical precipitates are present (Figure 37a). However, a comparison of the maximum pressure drops reached in ICET-3-6 and -11 (Figs. 13 and 21) show that the difference in the pressure drop increases with time. The increase of the pressure drop with time in ICET–3-6 is attributed to the continuing dissolution of Cal–Sil and additional formation of calcium phosphate precipitates.

Test ICET-3-10 was intended to give the "typical" amount of calcium phosphate precipitate arriving as the bed is formed in design basis analyses. As noted previously, at the end of the presoak period, a much larger amount of $CaSiO_3$ will have dissolved, and much larger amount of calcium phosphates precipitates will have formed compared to the ICET-3-6 case. This results in a much more rapid increase in head loss than in ICET-3-6 (Figure 37b), although the pressure drop in ICET-3-6 eventually approaches the steady state value obtained in ICET-3-10. Although this argument qualitatively explains the differences between ICET-3-6 and 10, the "lag" in the pressure drop is greater than the 30 minutes that would be expected due to differences in the amounts of Cal–Sil dissolved during the presoak.

A comparison of the pressure drops in ICET-3-8 and ICET-3-9, shown in Fig. 38, suggests a strongly nonlinear relationship between the amount of the calcium phosphate precipitate and the pressure drop. The first two additions of $CaCl_2$ in ICET-3-9 produced relatively small increases in pressure drop. The third addition resulted in a very rapid increase in pressure drop. The total inventory of dissolved Ca added in ICET-3-9 is equivalent to complete dissolution of 9 g of Cal–Sil. The pressure drop observed in ICET-3-8 after addition of 43.5 ppm of dissolved Ca as $CaCl_2$ is almost as the same as that observed in the ICET-3-2 test (see Reference 3) in which 50 ppm Ca as $CaCl_2$ was added to the loop. However, this comparison may be confounded by the difference in precipitate distribution through the bed. The bed in ICET-3-8 was formed from the simultaneous arrival of fiber and precipitate. In ICET-3-9, the precipitate was deposited on a preformed fibrous bed. Since precipitate can presumably move through and into the bed, the difference in the way the beds were formed may not completely define the actual structure. An additional test would be required to directly compare the effects of either simultaneous or sequential arrival of the chemical precipitate associated with the complete dissolution of 9 g of Cal–Sil.

The pressure drop increases with time occur because more debris is trapped during each pass through the debris bed during recirculation and because of continued Cal–Sil dissolution and formation of additional precipitates. In ICET-3-10, which represents a "typical" amount of Cal–Sil dissolution before the formation of the bed, it takes about 3 recirculations (or approximately 12 minutes) of the test loop fluid to build to the maximum pressure drop. In ICET-3-8, which represents the maximum Cal–Sil dissolution before the formation of the bed, the maximum pressure drop is reached after 1 test loop recirculation. The head losses due to chemical products in both of these tests are dominated by the precipitates that form due to dissolution prior to the initial bed formation, and the pressure drop increases as more of these precipitates are trapped during recirculation. The effect of continued dissolution could not be determined because the pressure drop quickly reached the capability of the loop. However, in ICET-3-6, which represents the minimum Cal–Sil dissolution that would occur before the formation of the bed, it takes about 15 passes test loop recirculations to approach the maximum pressure drop. In this case the pressure increase is probably dominated by the time needed for additional Cal–Sil dissolution.

The degree of dissolution that would occur before the debris reached the sump screen in a prototypical situation would presumably be bounded by the ICET-3-6 and ICET-3-8 limiting cases, and may be most similar to the ICET-3-10 case. Figure 39 shows a comparison of the increase of pressure drop in ICET-3-8 and ICET-3-10. These results suggest that variability in the degree of Cal–Sil dissolution is likely to have a relatively small effect on chemical effects on head loss in this system. Differences in debris transport time would probably have a much large effect on the rate of pressure increase. The actual amount of head loss for a plant specific case is also dependent on many additional factors such as the sump screen debris loading, uniformity of the screen debris loading, propensity for flow bypass (i.e., jetting) through the debris bed, debris bed screen approach velocity, and transport of chemical precipitate not addressed in these tests.

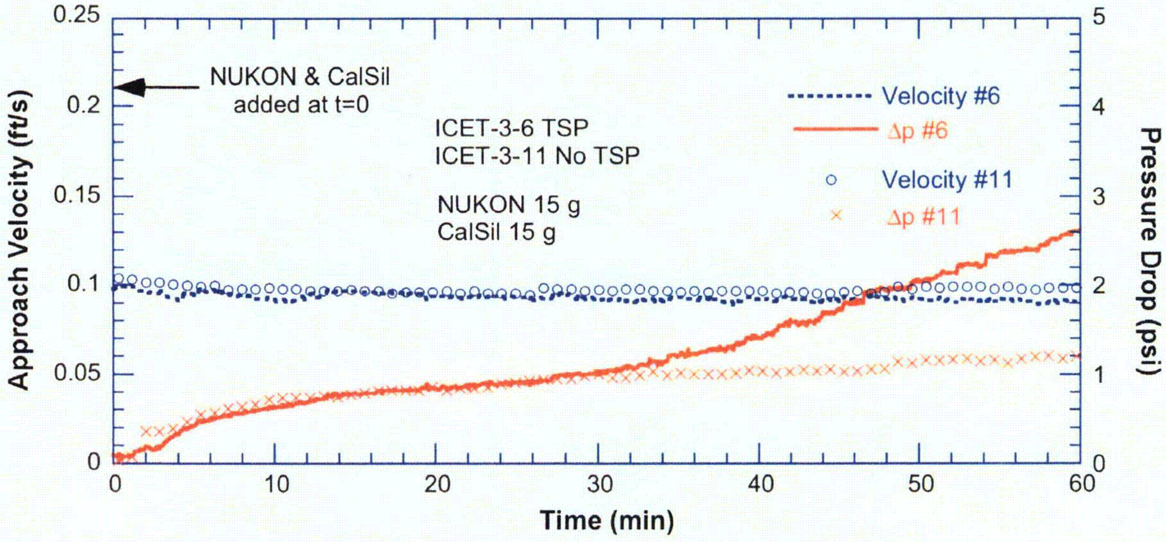

(a)

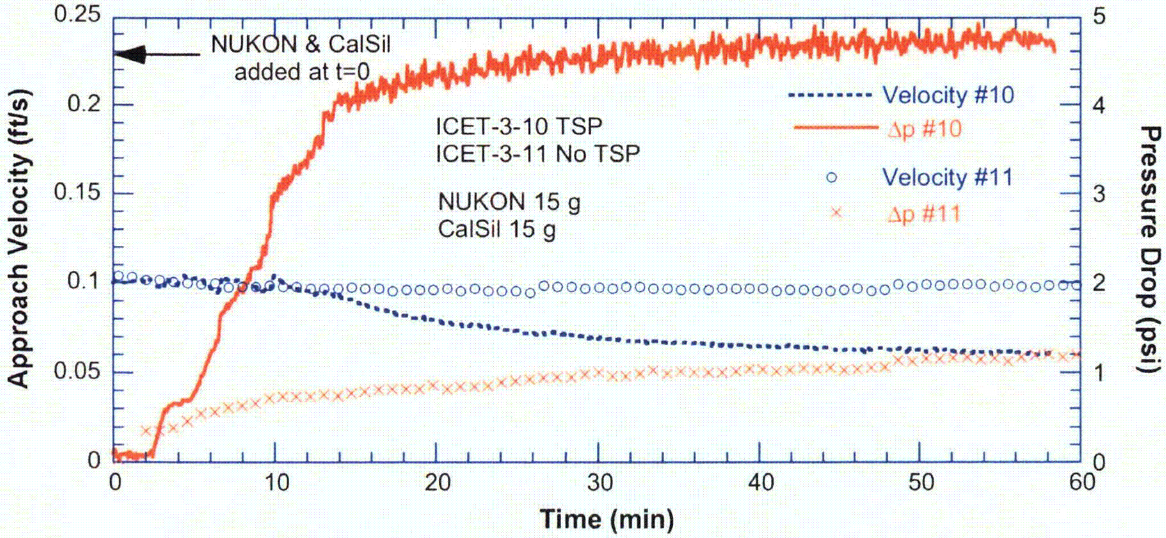

(b)

Figure 37. (a) Bed approach velocities and differential pressures across the screen as a function of time for test ICET-3-6 & 11; (b) Bed approach velocities and differential pressures across the screen as a function of time for test ICET-3-10 & 11.

In the tests with 15 g NUKON/15 g Cal–Sil, the strong effect of the chemical precipitates on pressure drop is readily evident. Such an effect is less evident in the comparison of the tests with 7 g NUKON/25 g Cal–Sil. The pressure drops in ICET-3-4, in which some precipitation of calcium phosphate would occur, and ICET-3-5, in which no precipitation would occur are compared in Fig. 40. Since no TSP was added to the presoak, the Cal–Sil dissolution in ICET-3-4 was limited similarly to ICET-3-6, so that a strong chemical effect would not be expected until there was time for additional dissolution in the loop. However, with this Cal–Sil loading, even without the effect of calcium phosphate precipitates, the head loss increases very rapidly to a high level.

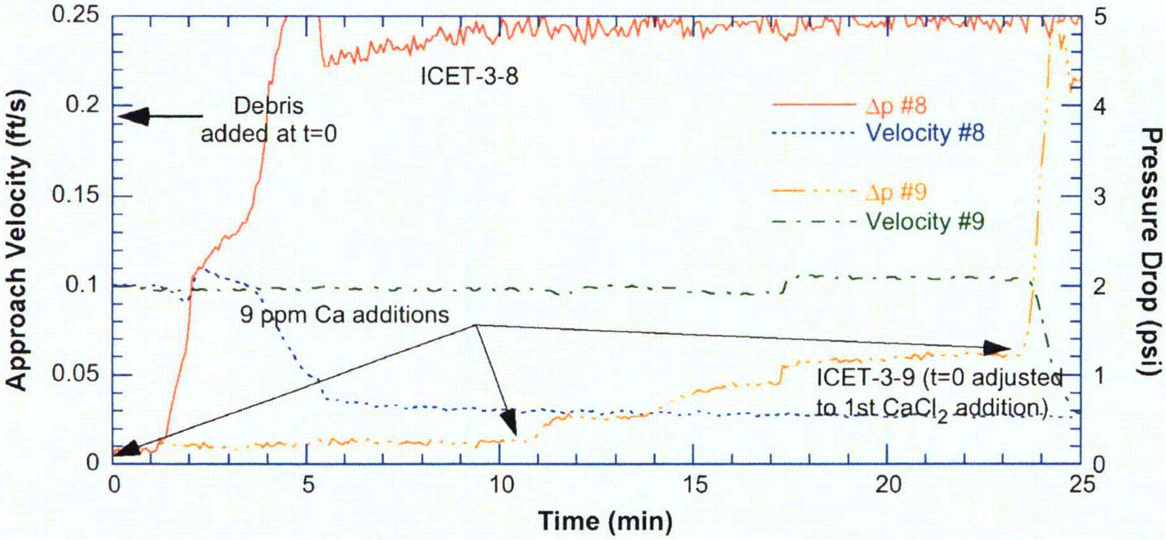

Figure 38. Bed approach velocities and differential pressures across the screen as a function of time for test ICET-3-8 & 9.

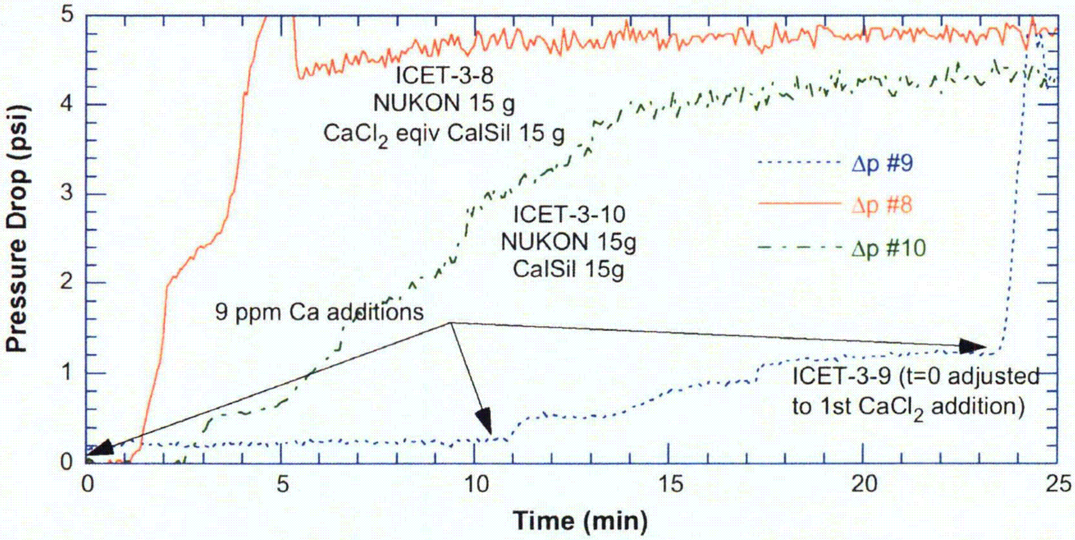

Figure 39. Comparison of the increase of pressure drop in ICET-3-8, which is bounding case for complete dissolution of Cal–Sil prior to formation of the debris bed, and ICET-3-10, which represents the minimum expected dissolution of Cal–Sil prior to bed formation.

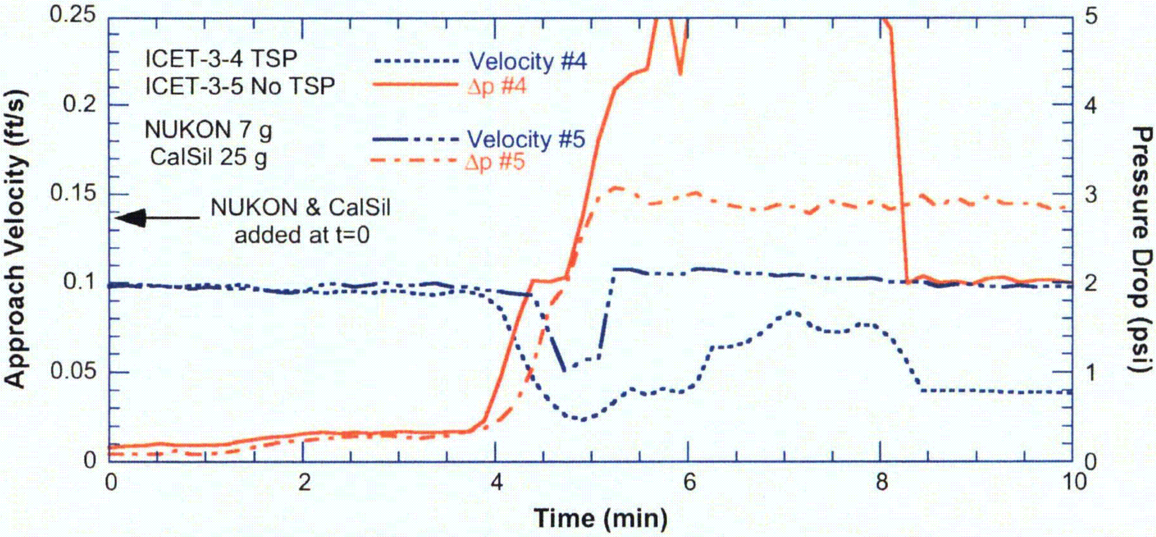

Figure 40. Bed approach velocities and differential pressures across the screen as a function of time for test ICET-3-4 & 5.

Comparison of ICET–3–10, 12, 16, and 18 (Figs. 20, 25, 30, and 32, respectively) shows that the relative contribution of calcium phosphate to head loss depends strongly on the debris loading. These results along with the results for ICET–3–19 (Fig. 35) suggest that there is a highly nonlinear relation between head loss and fiber loading for a given particulate loading as shown schematically in Fig. 41.

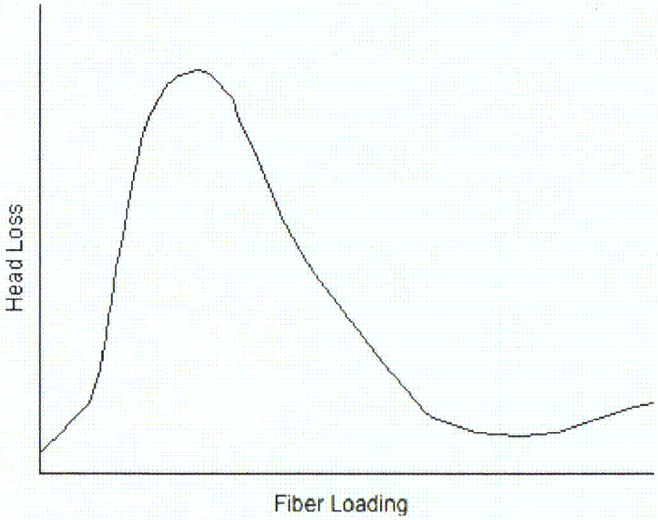

Figure 41.
Schematic dependence of head loss on fiber loading on the screen for a given particulate loading

2.6 Particle sizes of the chemical products in ICET–3

The particle sizes of the chemical products in the ICET–3 experiments have been measured by a laser granulometry technique. This technique uses the diffraction of light passing though a suspension of the particles to measure the size of particles present in the solution. A CILAS Model 1064 granulometer was used for the measurement, and the results are shown in Figs. 42 and 43. The distributions with and without ultrasonic deflocculation are fairly similar suggesting that the median particle size of 4.7 μm that was observed is a reasonable "unit" for the precipitate particles.

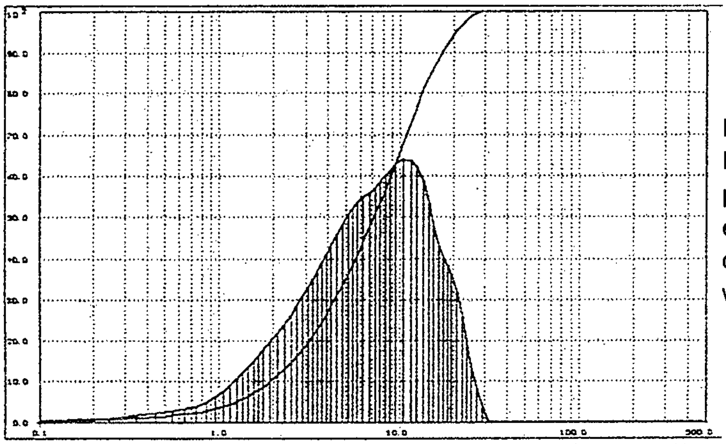

Figure 42.
Particle size histogram for chemical product from ICET-3 simulation experiment analyzed with no ultrasonic deflocculation. The median particle size was 7.1 µm.

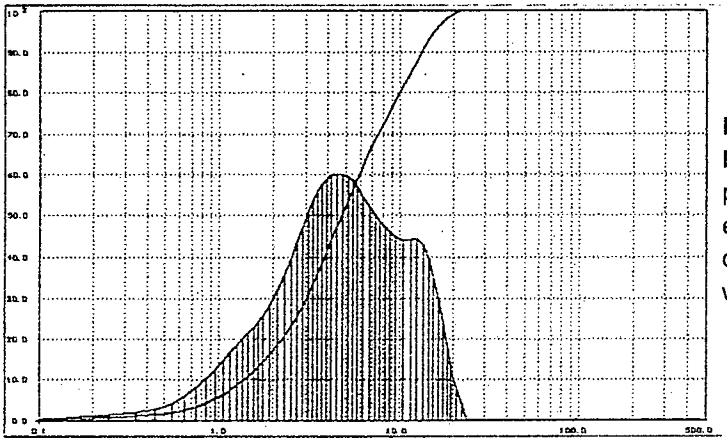

Figure 43.
Particle size histogram for chemical product from ICET-3 simulation experiment analyzed with ultrasonic deflocculation. The median particle size was 4.7 µm.

2.7 Calcium phosphate settling tests

In the head loss loop tests, virtually all the calcium phosphate precipitates that form are transported to the bed. In an actual sump, there is a potential for the precipitates to settle before they reach the sump screen. Settling tests were performed to determine settling rates for calcium phosphate under conditions with no bulk directional flow. Tests were performed in a settling tower with an effective height of 71.5 cm. The tower was filled with a solution containing LiOH (0.7 ppm Li) and boric acid (2800 ppm B) and TSP (3.4 g/l). $CaCl_2$ solution was then added to the tower. The dissolved Ca reacts with the TSP in the solution to form calcium phosphate precipitate. The solution is stirred to get a uniform mixture and then the precipitates are allowed to settle. Two different $CaCl_2$ concentrations were tested. One produced a dissolved Ca inventory equivalent to 300 ppm and the other an inventory equivalent to 75 ppm. The 300 ppm inventory is roughly equivalent to full stoichiometric dissolution of a 1 g/l concentration of Cal–Sil; the 75 ppm inventory is roughly equivalent to full stoichiometric dissolution of a 0.25 g/l concentration of Cal–Sil. In both cases, the solutions are phosphate-rich for a TSP concentration of 3.4 g/l, i.e., the formation of calcium phosphate precipitates is limited by the amount of Ca available. Replicate settling tests were conducted for each concentration.

In the 300 ppm tests, there was more of a tendency for precipitate particles to agglomerate and a visible settling front was observed, as shown in Fig. 44. Grab samples taken before and after the front passed suggest that about half the precipitate was removed as the front passed. The mixture behind the front looked relatively uniform and gradually became less cloudy. In the 75 ppm tests, a front was not visible. The mixture looked relatively uniform throughout most of the tower and gradually became less cloudy. There was a more noticeable mix of upward and downward moving individual particles.

The time histories of the settling front in the 300 ppm dissolved Ca tests were estimated by taking a sequence of pictures of the front at intervals and noting the location of the front relative to a scale mounted on the settling cylinder. As shown in Fig. 45, the front velocity is relatively constant until it approaches the bottom of the settling tower. The average velocity of the front in the 300 ppm tests is 3.8 cm/min. Settling of remaining particulate behind the front occurred much more slowly and the settling velocities are likely more consistent with those measured in the 75 ppm tests.

In the 75 ppm dissolved Ca tests where no front was evident, the settling velocities were estimated by taking three grab samples at intervals from the top of the settling column and noting the relative decrease in the amount of precipitate in the samples with increasing time. The decay in the amount of precipitate in the samples can be modeled as exponential as shown in Fig. 46. The time constant for the decay is approximately 87.5 minutes. This corresponds to a settling velocity of 0.8 cm/min. This is more representative of the settling characteristics of the calcium phosphate precipitates at the concentrations of most interest.

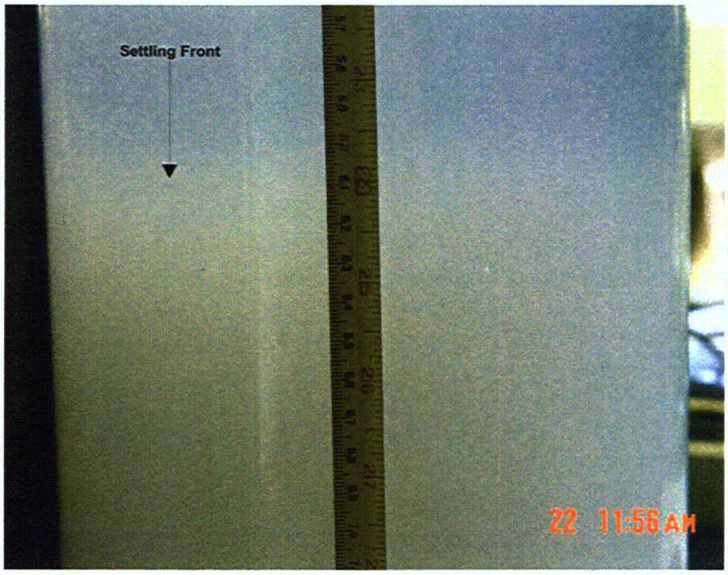

Figure 44.
Settling front in test with 300 ppm Cl

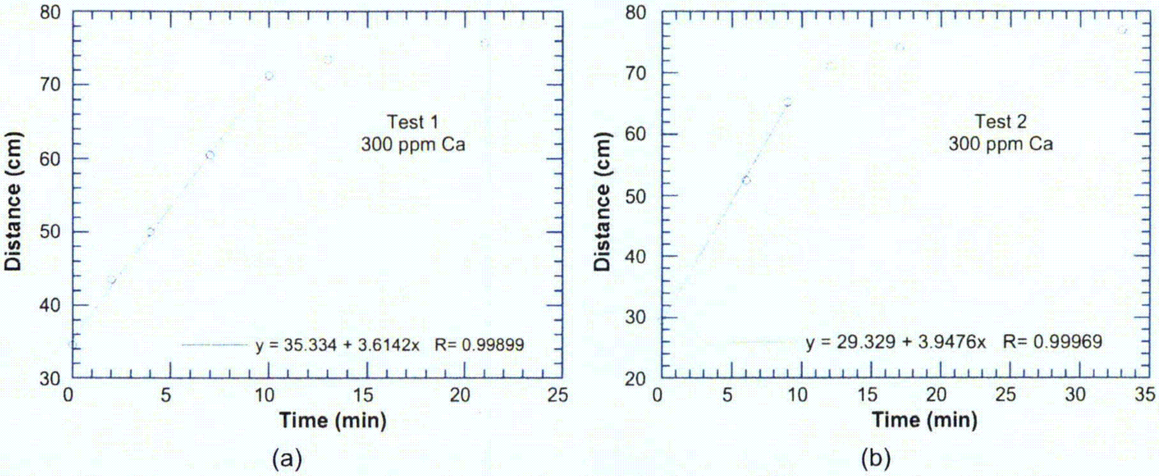

(a) (b)

Figure 45. Time history of the motion of the settling front in the two 300 ppm dissolved Ca settling tests.

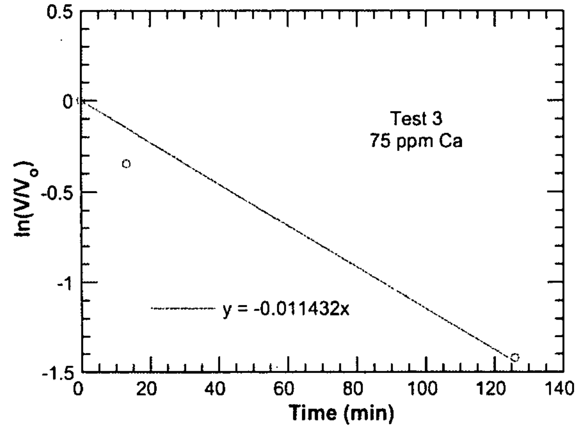

Figure 46.
Assumed exponential decay of volume of suspended precipitate in 75 ppm dissolved Ca test.

2.8 Small–scale dissolution testing

The objective of the small–scale dissolution testing is to identify important environmental variables governing both dissolution of Cal–Sil and the subsequent formation of calcium phosphate precipitates over a range of simulated sump pool conditions. The variables considered in the results reported herein are the effect of the rate of TSP addition to the Cal–Sil solutions for various Cal–Sil concentrations.

Three different histories of TSP addition were studied. These histories are intended to encompass the range of histories of TSP dissolution expected within an actual containment sump:

1. Add TSP before Cal–Sil addition (instantaneous dissolution of TSP).
2. Titrate TSP over 1 hr period into solution after Cal–Sil addition (nominal case).
3. Titrate TSP over 4 hr period into solution after Cal–Sil addition (very slow addition of TSP).

The test temperature was 60°C. The base solution consisted of 2800-ppm-B and 0.7-ppm Li. The TSP concentration was 3.4 g/l which results in a nominal pH value of 7.1 in the buffered solution. The Cal–Sil concentrations for the tests were 0.5 and 1.5 g/l. The 0.5 g/l Cal–Sil concentration is generally representative of current plant design basis concentrations based on a survey of plants that utilize TSP buffering and expect Cal–Sil to be present in the containment sump.[8] The 1.5 g/l concentration is greater than the postulated post-LOCA containment pool concentration for existing plants with both Cal–Sil insulation and TSP buffer. At these concentrations, the formation of calcium phosphate precipitates is expected to be Ca limited, since $Ca_3(PO_4)_2$ [tricalcium phosphate] or $Ca_{10}(PO_4)_6(OH)_2$ [hydroxyapatite] are the two most likely forms for the calcium phosphate precipitates at this pH.[9]

The results from small–scale dissolution tests performed at 60°C to date are summarized in Table 4. Time, in these tables, represents the elapsed time after the Cal–Sil was added to the base solution. However, grab samples were taken only after the TSP additions were completed in each test. The values for Ca, P, Si, and Na in the tables were determined by inductively coupled plasma (ICP) measurements on the grab samples. ICP measures the total amount of elements present in a sample whether they are present as solutes or solid species. However, the samples were filtered prior to ICP analysis and the ICP results are expected to represent only species in solution.

The Na arises as an impurity in the Cal–Sil, probably sodium silicate. It is expected to be extremely soluble and in most of the tests, it appears to dissolve very rapidly. In the test sets denoted as "II" and "III" in Table 4, the Na levels are lower than in any of the other tests. It is not clear why this is the case.

Since the Ca which is released (as the Cal–Sil dissolves) quickly combines with the available dissolved phosphate to form a solid calcium phosphate precipitate, the ICP measurements of Ca in the filtered supernate are not representative of the amount of Ca that has actually dissolved. The measurements of dissolved P have been used to estimate the amount of Ca that has been precipitated. If all the P that was added as TSP remained in solution, the P concentration would be 277 mg/l. The measured P concentrations are always less than this concentration. It is assumed that the missing P has all combined with Ca to form solid calcium phosphate precipitates. There are a variety of calcium phosphate species having different stoichiometries. The least soluble species at the pH values of interest are $Ca_3(PO_4)_2$ [tricalcium phosphate] and $Ca_{10}(PO_4)_6(OH)_2$ [hydroxyapatite].[9] Values of the amount of Ca residing in calcium phosphate precipitate have been calculated for each of these assumed species based on the missing P in solution. This information is summarized in the last two columns of Table 4. The total dissolved Ca can be estimated by adding the measured Ca (column 4 in Table 4) with the Ca from either of the last two columns in Table 4.

The dissolved Ca that has combined to form calcium phosphate can be estimated based on the assumption that the precipitates are primarily hydroxyapatite. These values are shown in Figs. 47a and 47b. In these graphs, the time, once again, is measured from the time that the Cal–Sil is added to the solution. The data legend indicates if the TSP dissolution was instantaneous ("instant"), completed in 1 hour ("nominal"), or completed in 4 hours ("slow"). While there is variability in the data, it appears that the TSP dissolution history has a larger effect at the higher Cal–Sil loading (1.5 g/l) than it does at 0.5 g/l. It appears from the data in Table 2, that it takes substantial time (approximately 4 days) to achieve full dissolution for the 1.5 g/l Cal–Sil concentration while the 0.5 g/l concentration appears to be completed within approximately 1 - 3 days. For both Cal–Sil concentrations, substantial Ca dissolution (> 75 mg/l) has occurred within a few hours regardless of the TSP addition rate.

These data are replotted in normalized form in Fig. 48. In this figure, the total dissolved Ca at each point in time is normalized by the Ca concentration corresponding to complete stoichiometric dissolution of the total amount of Cal–Sil present. The figure shows that for the case of instantaneous TSP dissolution, the fractional amounts of dissolved Ca are significantly different for the two different Cal–Sil loadings. For the more realistic 1 h TSP dissolution history and the bounding 4 h TSP dissolution history, the normalized Ca values are close for the two loadings, i.e., the amount of dissolved Ca just scales with concentration. Even for the case of instantaneous TSP dissolution, the normalized dissolution rate of the 0.5 g/l Cal–Sil loading is similar to that observed for the 1 and 4 h TSP addition rates for the 0.5 and 1.5 g/l loadings. This supports the assumption stated earlier that the Cal–Sil dissolution rate is not too strongly dependent on the Cal–Sil concentration for these low Cal–Sil concentrations. Thus, the screen loading per unit area is the most important scaling parameter for head loss tests with calcium phosphate precipitates.

The data from the small–scale dissolution tests at 90°C are summarized in Table 5. The Na levels are much higher than in the corresponding tests at 60°C, indicating more leaching of the Na from the Cal–Sil. The Ca in solution is lower reflecting the retrograde solubility of $Ca_3(PO_4)_2$. The measured P levels are, however, much higher than those at 60°C indicating that not as much $Ca_3(PO_4)_2$ has formed, which implies that less Ca has leached from the Cal–Sil at the higher temperature.

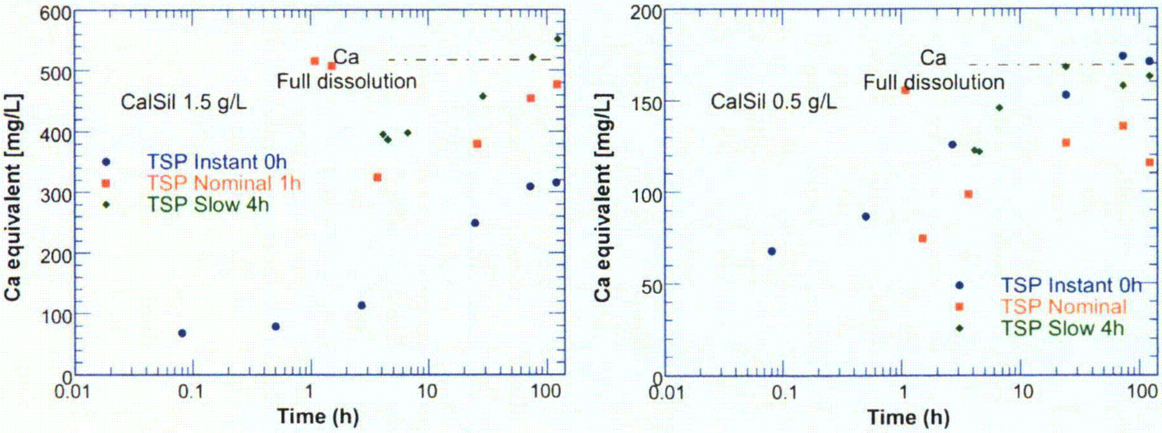

(a) (b)

Figure 47. (a) Dissolution of Cal–Sil at a loading of 1.5 g/l for three different histories of TSP addition; (b) Dissolution of Cal–Sil at a loading of 0.5 g/l for three different histories of TSP addition.

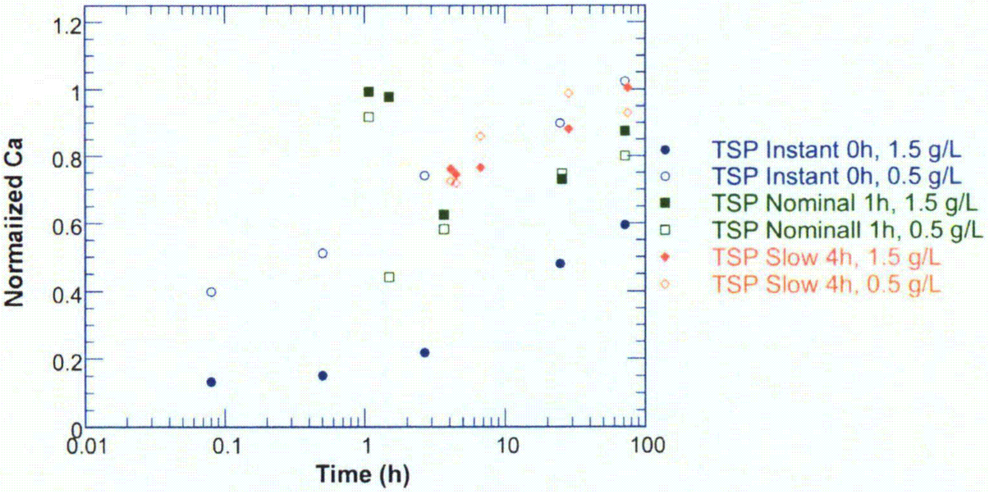

Figure 48. Normalized dissolution data, dissolved Ca/Ca for full dissolution for loadings of 1.5 g/l and 0.5 g/l for three different histories of TSP addition.

Table 4. Summary of results for the small–scale dissolution tests at T= 60°C.

Test series	Time (h)	pH (RT)	Ca (mg/l)	P (mg/l)	Si (mg/l)	Na (mg/l)	Cal–Sil (g/l)	Ca equiv (mg/l) ($Ca_3(PO_4)_2$)	Ca equiv (mg/l) $Ca_{10}(PO_4)6(OH)_2$
I TSP is added before the Cal–Sil is introduced	0.08	7.04	39	263	23	536	1.5	28	31
	0.50	7.17	25	252	24	554	1.5	49	55
	2.67	7.38	16	232	36	549	1.5	88	98
	24.50	7.24	8	165	60	534	1.5	217	242
	71.25	7.33	4	135	67	557	1.5	276	306
	119.00	7.48	3	132	68	567	1.5	281	313
II TSP metered over an hour after the Cal–Sil is added	1.08	6.83	58	65	21	159	1.5	412	458
	1.5	6.79	54	66	22	168	1.5	409	454
	3.67	7.1	11	131	25	357	1.5	283	315
	25.5	7.1	5	103	46	382	1.5	337	375
	72.25	7.15	3	67	62	405	1.5	407	452
	120	7.26	3	57	65	395	1.5	427	474
III TSP metered over a 4 hour period.	4.08	7.12	19	102	26	289	1.5	339	377
	4.5	6.85	14	104	28	295	1.5	336	373
	6.67	6.92	6	95	30	297	1.5	353	392
	28.5	6.99	5	67	42	292	1.5	408	453
	75.25	7.1	3	36	60	327	1.5	467	519
	123	7.25	3	22	65	331	1.5	494	549
IV TSP is added before the Cal–Sil is introduced	0.08	7.13	9	250	7	598	0.5	54	59
	0.50	7.29	9	241	9	585	0.5	70	78
	2.67	7.4	10	223	20	594	0.5	105	117
	24.00	7.37	4	208	36	600	0.5	134	149
	72.00	7.26	3	198	42	579	0.5	154	171
	120.00	7.26	3	199	42	577	0.5	152	168
V TSP metered over an hour after the Cal–Sil is added	1.08	7.2	14	211	9	512	0.5	128	142
	1.5	7.25	14	249	12	618	0.5	55	61
	3.67	7.26	13	237	20	620	0.5	78	87
	25.5	7.32	7	222	37	627	0.5	108	120
	72.25	7.23	4	216	45	631	0.5	118	131
	120	7.2	4	225	47	642	0.5	101	112
VI TSP metered over a 4 hour period.	4.08	7.24	21	230	22	585	0.5	91	102
	4.5	7.24	18	229	24	600	0.5	93	104
	6.67	7.26	7	212	28	582	0.5	126	140
	28.5	7.35	4	201	37	583	0.5	148	164
	75.25	7.24	3	206	44	600	0.5	139	154
	123	7.24	4	203	46	601	0.5	143	159

Table 5. Summary of results for the small–scale dissolution tests at T= 90°C.

Test series	Time (h)	pH (RT)	Ca (mg/l)	P (mg/l)	Si (mg/l)	Na (mg/l)	Cal–Sil (g/l)	Ca equiv (mg/l) ($Ca_3(PO_4)_2$)	Ca equiv (mg/l) $Ca_{10}(PO_4)_6(OH)_2$
I TSP is added before the Cal–Sil is introduced	0.08	7.29	16	272	15	633	1.5	10	11
	0.50	7.35	10	250	28	658	1.5	52	58
	2.67	7.41	3	193	59	671	1.5	163	181
	24.50	7.50	1	143	77	648	1.5	259	288
	71.25	7.51	1	141	77	666	1.5	263	292
	119.00	7.48	2	144	75	686	1.5	257	286
II TSP metered over an hour after the Cal–Sil is added	1.08	7.52	13	206	41	599	1.5	137	153
	1.5	7.48	6	213	55	678	1.5	124	138
	3.67	7.49	3	173	68	651	1.5	201	224
	25.5	7.50	1	149	85	673	1.5	248	275
	72.25	7.42	2	150	85	718	1.5	246	273
	120	7.33	2	171	88	829	1.5	205	228
III TSP metered over a 4 hour period.	4.08	7.38	2	207	62	663	1.5	135	151
	4.5	7.38	3	197	63	647	1.5	155	172
	6.67	7.44	2	172	64	608	1.5	203	226
	28.5	7.45	1	136	76	619	1.5	273	303
	75.25	7.45	1	133	75	625	1.5	279	310
	123	7.49	1	135	70	650	1.5	275	305

More complete descriptions of the dissolution tests and additional experimental results are contained in Appendix B.

3 Head loss tests in ICET–1 and ICET–5 environments

3.1 Background

As noted in Table 1, the ICET–1 environment is a NaOH buffer with NUKON insulation; the ICET–5 environment is a sodium tetraborate buffer with NUKON. Both environments resulted in significant dissolved Al levels: ICET–1 ≈ 375 ppm Al, pH ≈ 9.4; ICET–5 ≈ 50 ppm, pH ≈ 8.4. The dissolved Al concentration in ICET–1 increased linearly over the first 15 days of the test to ≈375 ppm and remained relatively constant for the duration of the test.[2] The dissolved Al concentration is shown in Fig. 49. No precipitates were observed in the ICET test chamber during ICET–1, but cooling of ICET–1 solution produced visible precipitates. Traces of chemical products could be observed at the bottom of sample bottles from early in the test. The volume and rapidity of formation increased as the test continued. Near the end of the 30 day test period, product formed almost as soon as samples were removed from the test chamber.

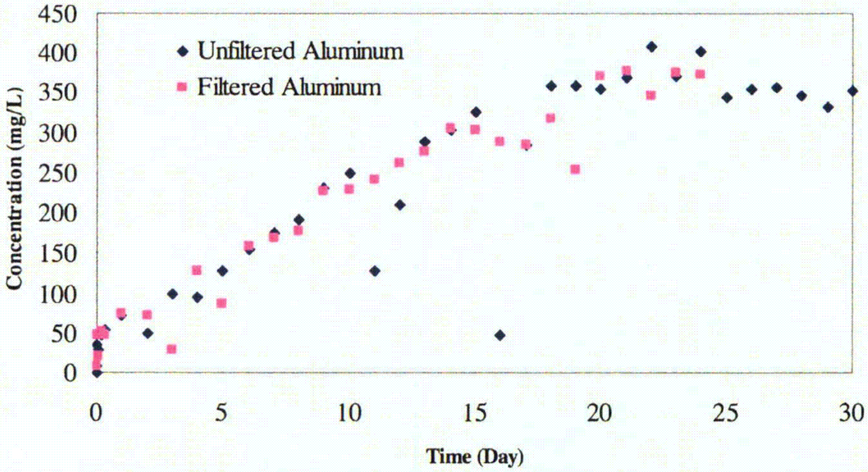

Figure 49. Aluminum concentration trend in ICET–1 daily water samples.[2]

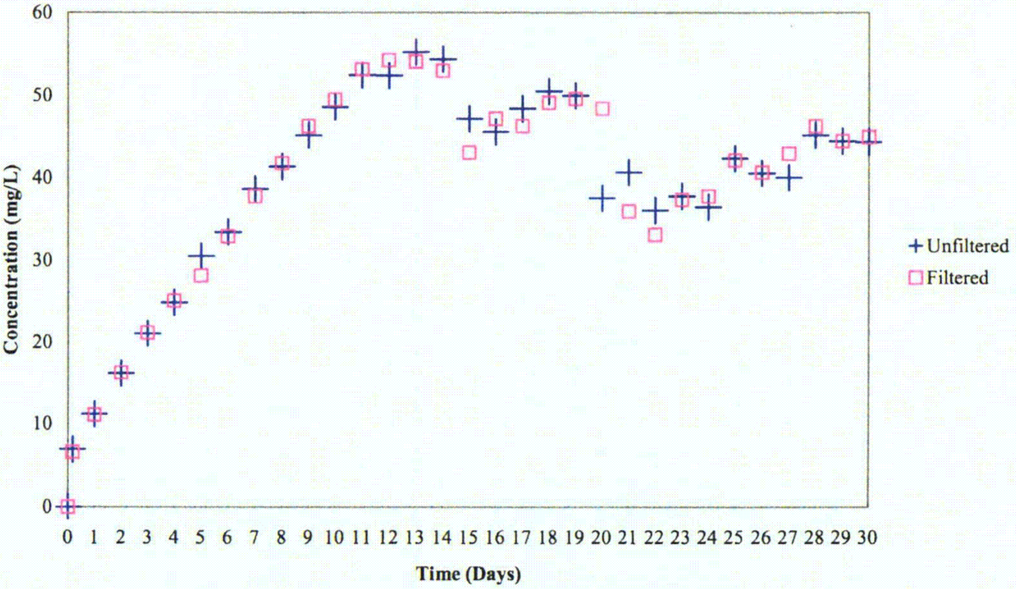

Figure 50. Aluminum concentration trend in ICET–5 daily water samples.[6]

The dissolved Al concentration in ICET–5 also increased linearly for the first portion of the test. The Al concentration peaked at about 55 ppm on days 12 and 13 and then decreased slightly and varied between 35 and 50 ppm for the remainder of the test as shown in Fig 50.[4] Cooling of ICET-5 solution eventually produced small amounts of precipitates. The amount of product was small compared to that observed in ICET–1, and it took much longer times (several days) for the products to become visible.

The low levels of dissolved Al in the ICET–2 and 3 environments[3,4] are not unexpected due to the relatively low pH. Because of the high pH, the ICET–4 environment might be expected to produce comparable dissolved Al levels. It did not, due probably to passivation of the metal surface.[10] Similarly, the leveling off of the dissolved Al concentrations in ICET–1 and 3 is not due to saturation of the Al due to equilibrium between the dissolved Al and a precipitate. Instead a variety of evidence indicates that the behavior is due to passivation of the surface of the aluminum metal.[10]

Thermodynamically–based speciation model predictions[14] made prior to the ICET tests suggested that sodium aluminum silicate might be an important precipitate product. It was not observed in the ICET tests,[2–6] apparently because in the tests in which significant amounts of Al dissolved, dissolution of the NUKON (which would produce silicates) was inhibited. To ensure that this was not an artifact due to the relatively high area of the Al metal in the ICET test series, a series of small–scale dissolution tests were performed on NUKON in different environments, including one with roughly 1/4 the relative surface area of Al metal as in ICET–1. These tests are described in Appendix E. The inhibition of NUKON dissolution observed in ICET–1 was also observed in the case of the lower surface area of Al metal.

3.2 Chemical Surrogates for ICET–1 and ICET–5

3.2.1 Solubility of Aluminum Hydroxides

Aluminum hydroxides, nominally $Al(OH)_3$, are the principal chemical product with potential to cause head loss observed in ICET–1 and 5 environments. The most stable form of $Al(OH)_3$ is the crystalline form gibbsite. Although gibbsite is thermodynamically the most stable form of $Al(OH)_3$, Van Straten et al.[11] showed that in precipitation of aluminum hydroxides from a basic supersaturated solution the first products to form are the less thermodynamically stable forms and then the product transforms through a series of forms to reach the thermodynamically stable form, gibbsite. The progression suggested by Van Straten et al[11] is amorphous, pseudo boehmite, bayerite, and then gibbsite.

For the pH range of interest the primary solubility product is aluminate, $Al(OH)_4^-$ and the equilibrium reaction with the solid phase is given by:

$$Al(OH)_3\text{ (solid)} + H_2O = H^+\text{ (aq)} + Al(OH)_4^-\text{ (aq)}$$

The $Al(OH)_4^-$ concentration at equilibrium is a function of pH:

$$\log Al(OH)_4^- = \log K_{sp} - \log H^+ = \log K_{sp} + pH$$

At 25°C the equilibrium constant $K_{sp} = 8.0 \times 10^{-13}$ (amorphous), $\approx 1 \times 10^{-14}$ (bayerite), and $\approx 1.9 \times 10^{-15}$ (gibbsite).[11] Data on the solubility as a function of temperature are given by Benezeth et al.[13]. Estimates of the equilibrium concentration of Al with amorphous $Al(OH)_3$ as functions of pH and temperature are shown in Fig. 51. The solubilities of the crystalline forms are smaller by a factor of ≈100–500 than that of the amorphous form. These values are for simple solutions and the solubilities could be influenced by borates, organics. There are also uncertainties in thermodynamic values, although the values given by Van Straten et al.[11] are consistent with those reported by Langmuir.[12]

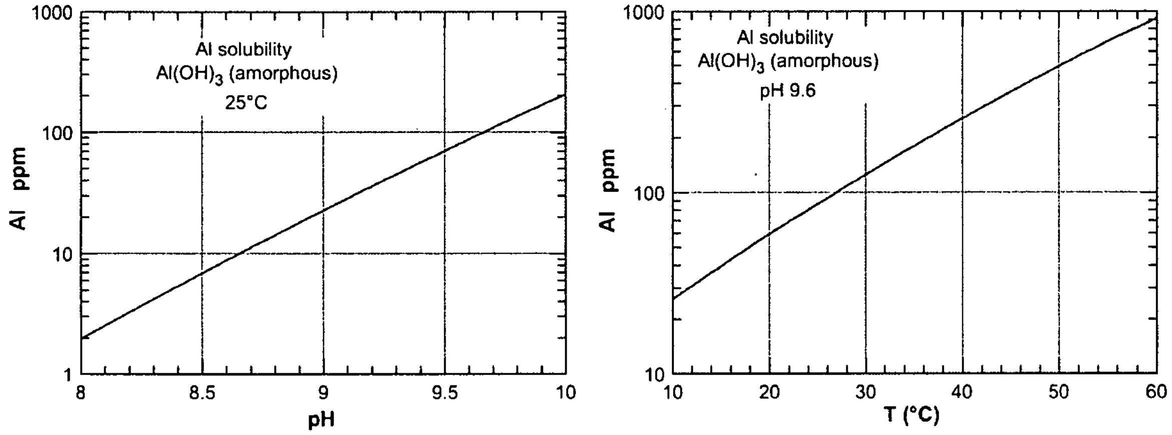

(a) (b)

Figure 51. Equilibrium solubility of amorphous $Al(OH)_3$ as a function of (a) pH at 25°C and (b) temperature at pH =9.6

The predicted solubility limit for amorphous $Al(OH)_3$ at 60°C and pH 9.6 is almost 1000 ppm. The corresponding result for gibbsite is ≈ 2 ppm. For a temperature of 20°C, the equilibrium solubility at pH 9.6 for the amorphous $Al(OH)_3$ is ≈ 60 ppm.

Although there are uncertainties associated with the values of these equilibrium solubilities, these results provide strong evidence that the products in ICET–1 are amorphous rather than crystalline and that the leveling off of the Al concentration after day 15 was due to passivation of the surface of the aluminum plates, not due to reaching a solubility limit for Al.

Klasky et al.[10] provide additional discussion and evidence that the products in ICET–1 are amorphous aluminum hydroxides.

3.2.2 Aluminum nitrate surrogates

Surrogate solutions for ICET–1 environments were developed using aluminum nitrate, $Al(NO_3)_3$-$9H_2O$. Since in ICET–1, the solutions arise from the dissolution of aluminum in a basic solution containing boric acid, the surrogate solutions were prepared by dissolving commercial aluminum nitrate, $Al(NO_3)_3$-$9H_2O$ powder in a base solution containing 2800 ppm B added as boric acid, 0.7 ppm Li as LiOH, and NaOH sufficient to get a pH of 9.6. A detailed description of the benchtop experiments and analyses supporting the development of the surrogates is given in Appendices C and D.

Samples of surrogate solutions containing 100, 200, and 375 ppm Al are shown in Fig. 52. When samples were taken through heating and cooling cycles, the sediments would redissolve at high temperatures. This together with measurements of the Al level in the supernate suggests that solubility behavior is similar to that shown in Fig. 51 and thus the sediments are amorphous or at least act like amorphous $Al(OH)_3$.

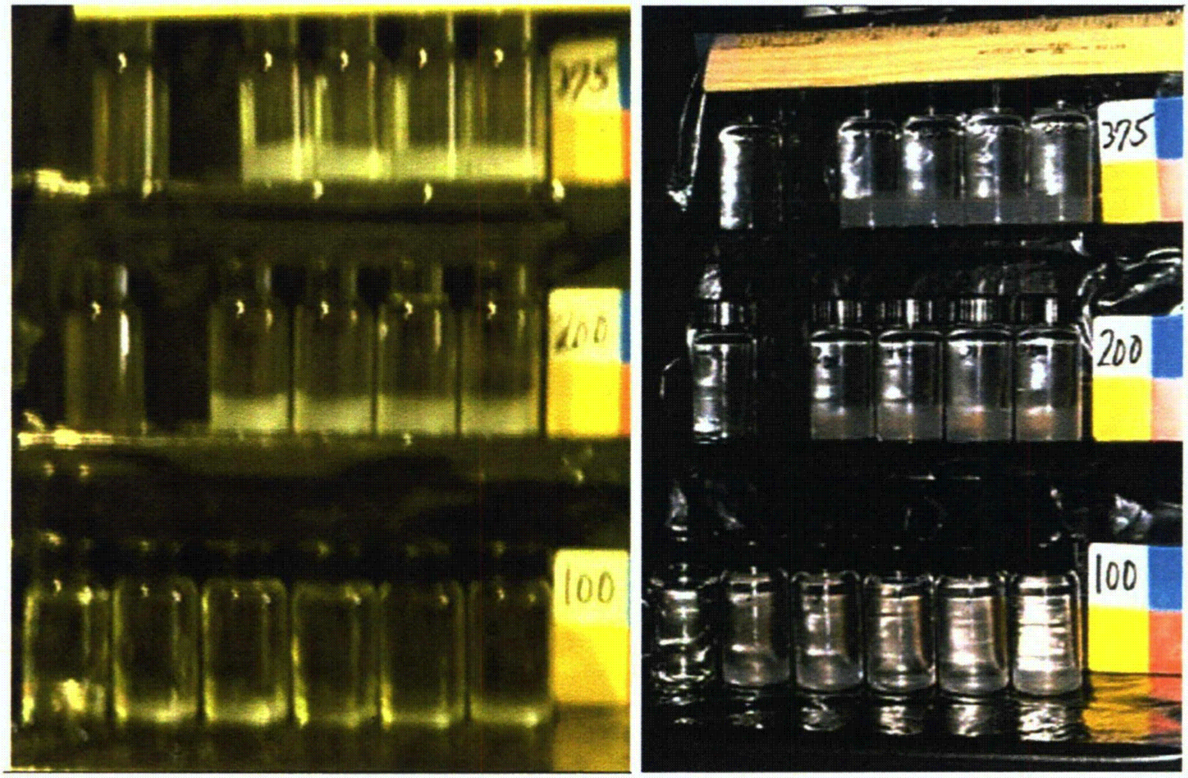

Figure 52. $Al(NO_3)_3$ 100, 200, & 375 ppm surrogates. The photo on left was taken without flash to heighten the contrast between sediment and supernate. The photo on the right characterizes better the semi–translucent nature of the sediment. The bottles on the far left in each photo have no Al additions.

The particle sizes of the chemical products in an ICET–1 experiment were measured by the laser granulometry technique discussed in Section 2.5. The results are shown in Figs. 53 and. 54. The measured particle sizes after ultrasonic deflocculation are much smaller than those measured before deflocculation. This is consistent with the results reported by Klasky et al.[10], which suggest that products are agglomerations of much finer, nano–sized particles. Thus it may be difficult to define a particle size since it may depend on the local stress state and its ability to disturb the agglomerations of smaller particles. No corresponding particle size measurements are available for the actual products from ICET–1. However, the particle size distribution for an aluminum hydroxide surrogate produced at LANL[10] is shown in Fig. 55. Although the results in Fig. 55 are also based on a laser diffractometry technique, it is not clear that the results are directly comparable. The distribution in Fig. 55 is narrower and the median value is probably more like 0.5 µm rather than 1.7 µm. Nevertheless, it appears that the distributions in Figs. 54 and 55 are not too dissimilar.

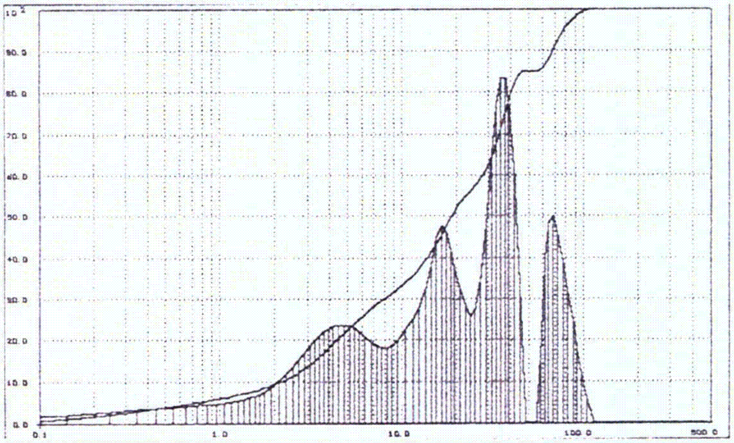

Figure 53.
Particle size histogram for chemical product from an ICET-1 simulation experiment analyzed with no ultrasound deflocculation. The median particle size was 18.6 µm.

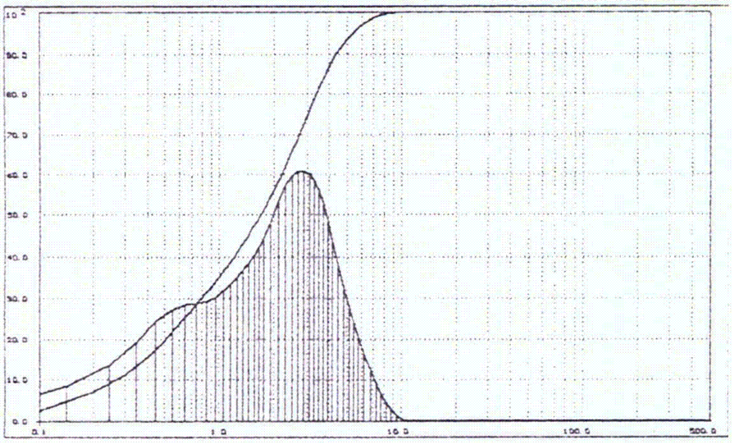

Figure 54.
Particle size histogram for chemical product from an ICET-1 simulation experiment analyzed with ultrasound deflocculation. The median particle size was 1.7 µm.

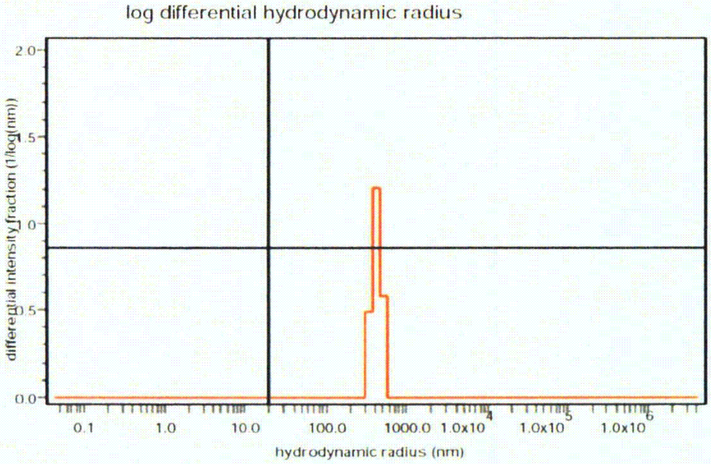

Figure 55.
Particle size distribution for an $Al(OH)_3$ surrogate reported in Ref. (10).

The use of aluminum nitrate to create surrogate solutions has some disadvantages. It introduces a species (nitrate) that is not typically present in the sump environment, and tends to drive the pH down. An alternate approach to developing a surrogate solution was investigated in which sodium aluminate ($NaAlO_2$) was used to create the surrogate solutions. This approach would introduce no new species, would not tend to decrease the pH, and better mimics the actual corrosion process since the formation sodium aluminate ($NaAlO_2$) is probably an intermediate step in the actual dissolution of metallic Al in NaOH solutions.

Benchtop experiments were performed to evaluate the use of sodium aluminate to produce a surrogate. The results are described in Appendix C. The decision was made to use the aluminum nitrate surrogate, because the behavior and appearance of the precipitates in these solutions seemed to better mimic the behavior and appearance of the precipitates in the ICET-1 test.

3. 3 Relationship of ICET–1 environments to plant environments

Although the final level of dissolved Al in ICET–1 was ≈ 350 ppm, actual plant levels of dissolved Al for same environments would "scale" with amount of Al exposed which is plant specific. In addition, the ICET–1 test was run isothermally at a temperature of 60°C (120°F), whereas the actual temperatures will vary considerably over the whole course of the accident. The amount of Al exposed to the environment depends strongly on whether the sprays are on. In most plants, the amount of submerged Al is a small fraction of the total Al in containment.[1] To obtain a better estimate of the range of Al that may be expected in the recirculating water, calculations were performed using more realistic thermal histories for 17 plants for which estimates of the amount of Al in containment were available in Ref. (1).

The time–temperature histories used for the calculations are shown in Fig. 56 and are taken from Ref. (1). As shown in Fig. 49, the dissolved Al concentration in ICET–1 increases linearly over the first 10 days of the test with a rate of ≈ 25 mg/l/day. This corresponds to a corrosion rate of 30.1 mg/m^2/min. For the same pH (9.6) and temperature (60°C), similar corrosion rates were observed in the small–scale tests conducted at CNWRA[14] and at Westinghouse.[15] The corrosion rates of the Al increase with increasing temperature. The data in Ref. (14) give an exponential dependence $e^{0.0195T}$ for temperature in Fahrenheit. The data in Ref. (15) give a somewhat greater temperature dependence, but the results in Ref. (14) were used for the calculations. Because the spray phase has a higher pH, the corrosion rates in the spray were taken as twice those in the submerged phase, based on literature data cited in Ref. (14). When benchmarked against the results of the ICET–1 test, this overestimated the dissolution that occurred in the spray phase. To fit the ICET–1 data, it was necessary to assume that the corrosion rate in the spray phase was 0.6 that in the submerged phase. Nevertheless, a factor of 2 was used for the calculations as being more consistent with our general expectations of the effects of increased pH.

With these assumptions, the time–temperature histories can be digitized and total amount of Al dissolved can be calculated by numerically integrating the corrosion rate over the history to obtain the weight of Al per unit area dissolved from submerged areas over a 30 day period and from areas subjected to sprays over a 4 h period at the initial portion of the accident. These results are summarized in Fig. 56 for the different plant histories and for the isothermal history of ICET–1. For the plant history calculations, no passivation of the Al was assumed to occur. For ICET–1 the corrosion loss per unit area over 30 days would be 878 g/m^2 and half that (439 g/m^2) if passivation is assumed to occur on day 15.

With these results and estimates of the sump volume and the areas of Al that are submerged and that are subjected to wetting by sprays, the concentration of dissolved Al in the sump after 1 day and after 30 days can be estimated. Such estimates are shown in Table 6 for 17 plants that responded to the ICET plant survey.[1] it should be noted that all the plants in the table may not use NaOH buffers and so the results may not actually be applicable to the plant. The results suggest that the dissolved Al concentration in ICET-1 is conservative, and most plants with NaOH buffering would be expected to have dissolved Al concentrations at 30 days below 100 ppm.. Although comparable time–temperature–dissolution history calculations were not performed, the dissolved Al concentration in ICET-5 is probably similarly conservative. Based on the corrosion rates inferred from ICET–5 and the relative amounts of Al in containment compared to ICET–5, most plants with STB buffering would be expected to have dissolved Al concentrations at 30 days below 15 ppm.

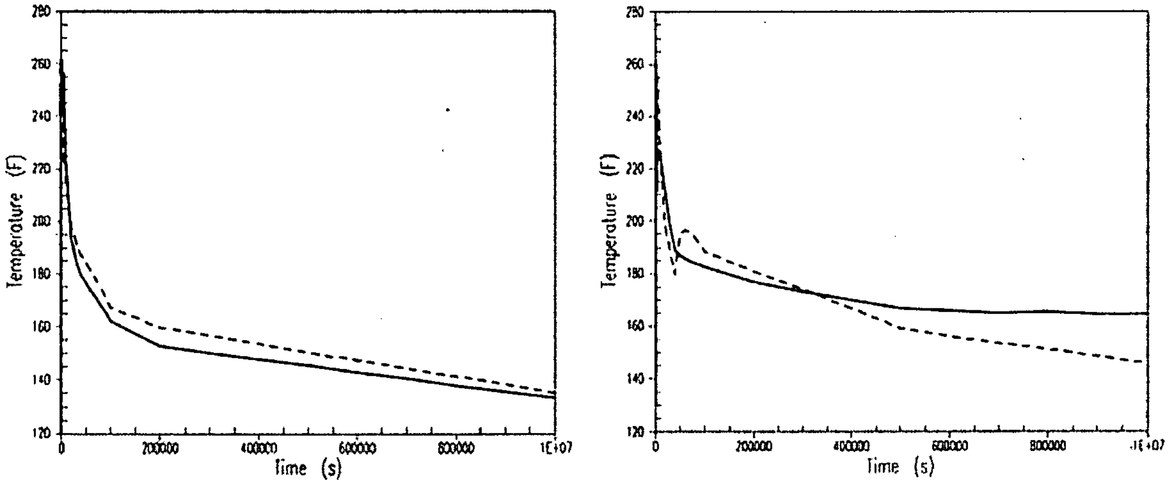

4 loop

3 Loop

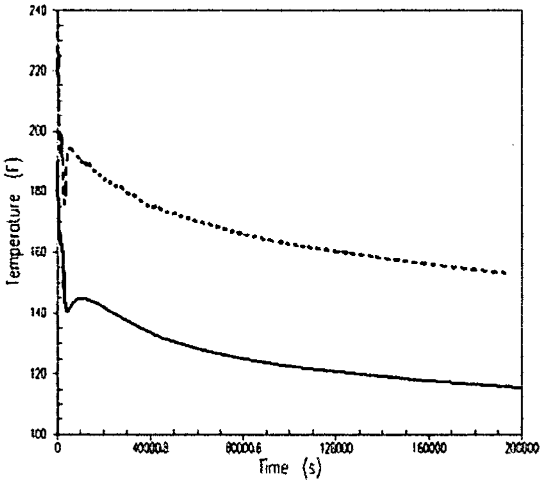

Type	Al 30 days g/m^2	Al spray g/m^2
4 loop	836	30
3 loop	1395	29
Ice	441	3
ICET-1	878(439)	5

Ice Condenser

Figure 56. Estimated sump temperature histories for different types of Westinghouse plants and containments[1]

Table 6. Estimated dissolved Al levels for NaOH buffer based on ICET Plant Survey[1]

Plant	Plant Type	Al / vol. ft^2/ft^3	Al / vol. (Submerged)	Al / vol. (Spray)	1 day total ppm[a,b]	30 day total ppm[c]
T	B&W[d]	0.29	0.003	0.29	65	80
U	CE[d]	0.02	0.000	0.02	5	6
J	3 Loop	0.02	0.02	0.000	2	34
K	3 Loop	0.01	0.01	0.000	1	17
Q	4 Loop	0.05	0.003	0.051	13	20
BB	B&W[d]	0.08	0.001	0.08	18	22
N	2 Loop[d]	0.005	5e-05	0.005	1	1
JJ	4 Loop	0.12	0.001	0.12	27	33
S, KK, LL	B&W[d]	1.91e-05	5e-05	0	0	0
R	CE[d]	3.360	0.840	2.510	678	5026
O,P	2 Loop[d]	0.02	0.002	0.02	5	15
RR	4 Loop	0.04	0.001	0.04	10	13
QQ	3 Loop	0.02	0.000	0.02	4	4
X	4 Loop	0.01	0.001	0.01	3	5
ICET–1		3.5	0.18	3.3	57	375

[a] Sprays active for 4 h

[b] Spray corrosion rates = 2* submerged, except for ICET–1 where the factor is 0.6

[c] No passivation of surfaces except in ICET–1

[d] The time–temperature history for 3–loop plants was used to calculate the results for B&W, CE, and 2–loop plants.

3.4 Individual ICET–1 test procedures and results

3.4.1 ICET-1-3 test procedure and results

ICET-1-3 test procedure

The loop was filled with deionized water and heated to 77°C (170°F) and circulated at 2 ft/s for 15 minutes to remove dissolved air. It was allowed to cool to room temperature overnight. Boric acid in powder form was slowly added to the loop and circulated until it was dissolved. The LiOH was added as a solution. NaOH was added to make the pH 10. These conditions were chosen to match those in ICET–1. The loop was operated at 1 ft/s for 15 minutes to mix the chemicals. After the chemical solution was prepared, the physical debris bed was built by adding a slurry containing 15 g NUKON to the loop with the loop flow at 0.1 ft/s. The bed was about 1/2 in thick. The NUKON bed formed essentially in the first pass of the debris past the test screen.

After the bed had formed and the pressure drop stabilized, the temperature was raised to 71°C (160°F) and the $Al(NO_3)_3$ solution was added. One liter of solution was metered in over a 4–minute period (1 recirculation). The concentration of the solution was chosen so that the concentration in the loop was 375 ppm after all the solution was added. The temperature was reduced to 60°C (140°F). The test plan was to decrease the temperature in stages, and wait for the pressure to equilibrate at each step. However, even before the $Al(NO_3)_3$ solution was added, cracks started to appear in the LEXAN test section. To try to complete the test before the test section failed, the holds were shortened and the pressures recorded at each stage may not represent steady–state conditions at that temperature.

ICET-1-3 test results

Although bench tests had shown that a 375 ppm Al solution at pH 9.6 and 60°C (140°F) could readily be achieved and was below the solubility limit for those conditions, a heavy "snowfall" was observed as the $Al(NO_3)_3$ solution was added to the loop at 71°C (160°F) as shown in Fig. 57.

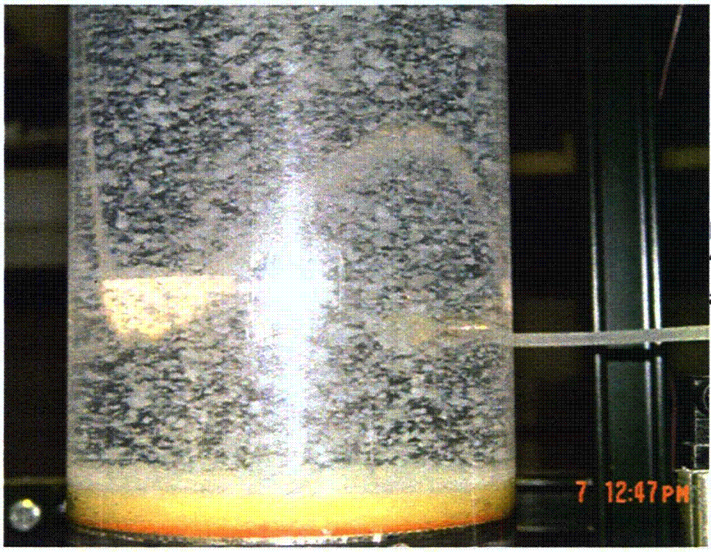

Figure 57.
"Snowfall" as $Al(NO_3)_3$ solution was added to the loop.

The "snow" dissolved in a few minutes (Fig. 58) and there was no visible buildup of precipitate on the bed during most of the test, although the initially clear solution became noticeably cloudier as the temperature decreased. The initiation of cracking in the LEXAN is also evident in Fig. 58. Although the $Al(NO_3)_3$ solution was metered in slowly enough so that the average concentration in a control volume extending over the whole cross–section at the injection point, the local concentration was obviously higher. The locally high concentration and corresponding local decrease in pH caused the solubility limit to be exceeded locally, although as mixing occurred, the precipitates redissolved.

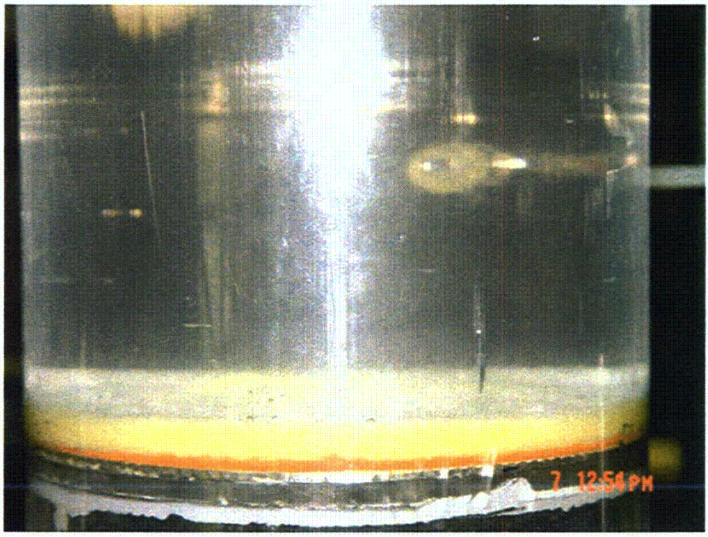

Figure 58.
"Snow" dissolved in a relatively few minutes. The initiation of cracking in the LEXAN is also evident.

The pressure and temperature histories during the test are shown in Fig. 59. An increase in pressure is noted almost immediately after the $Al(NO_3)_3$ is added even at 71°C (160°F). There does seem to be a slight lag in the pressure increase as the temperature is rapidly decreased. The test was halted as temperature dropped to ≈ 90°F, and the 0.1 ft/s velocity could not be maintained. Although the test was compromised by the formation of the nonprototypical "snowfall", it does indicate a strong potential for Al concentrations of this magnitude to greatly increase pressure drops across a bed.

After test was halted, the loop was kept at rest overnight. Due to the cracking, most of the fluid drained from the top half of the loop, and a thick white "jello" layer formed on top of the bed.

The cracking in the LEXAN was not completely unexpected. The susceptibility of LEXAN to degradation in NaOH environments has been noted in the literature, but a polycarbonate window (LEXAN is a GE trade name for their polycarbonate material) had performed without any problems in a similar environment for 30 days in the ICET chamber at UNM. The difference in performance may be due to differences in the particular resins used or in the higher residual stresses that may occur in an extruded tube versus a flat plate. A clear PVC test section was used for all subsequent tests in NaOH environments.

To minimize premature precipitation of $Al(OH)_3$, instead of a single injection point as in the first test in an ICET–1 environment, in all subsequent tests with dissolved Al, a sparger was used to get a more uniform distribution over the cross section of the $Al(NO_3)_3$ solution during injection. The injection rate was also decreased. This reduced, but did not completely eliminate the problem.

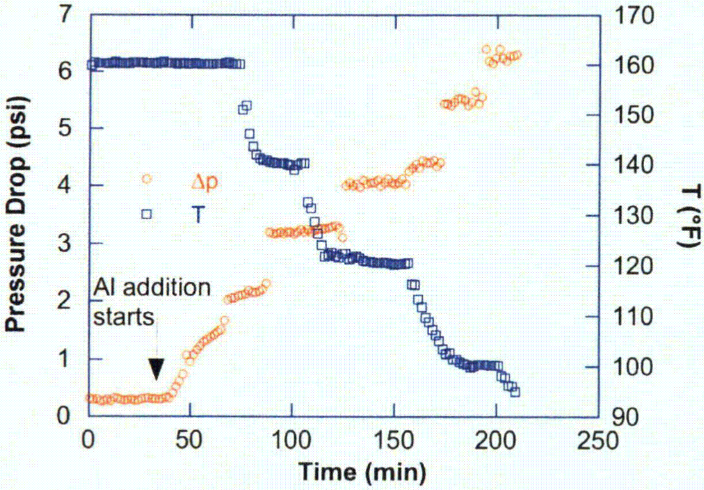

Figure 59.
375 ppm Al additions resulted in large increases in pressure drop

3.4.2 ICET-1-1-B2_100ppm test procedure and results

ICET-1-1-B2_100ppm test procedure

The loop was filled with deionized water and heated to 60°C (140°F) and circulated at 2 ft/s for 15 minutes to remove dissolved air. It was kept at about 27°C (80°F) overnight. Boric acid in powder form was slowly added to the loop and circulated until it was dissolved. The LiOH was added as a solution. NaOH was added to make the pH 10. The loop was operated at 1 ft/s for 15 minutes to mix the chemicals. After the chemical solution was prepared, the physical debris bed was built by adding a slurry containing 15 g NUKON to the loop with the loop flow at 0.1 ft/s. The bed was about 5/8 in thick. The flow velocity was maintained at 0.1 ft/s for the whole test.

After the bed had formed and the pressure drop stabilized, the temperature was raised to 60°C (140°F) and the $Al(NO_3)_3$ solution was added. The concentration of the solution was chosen so that the concentration in the loop was 100 ppm after all the solution was added. The temperature was then decreased to 16°C (60°F) with short holds at 49°C (120°F), and 38°C (100°F). The test was continued at 16°C (60°F) for a hour and then terminated.

ICET-1-1-B2_100ppm test results

The temperature and pressure history during the test is shown in Fig. 60. There is a small decrease in pressure drop as the temperature increases and a small increase in the pressure drop as the temperature decreases that are consistent with the changes in viscosity. No significant increase in pressure drop over that expected for the NUKON bed alone was observed and no precipitation products were observed either during the test or after the loop was allowed to remain still overnight.

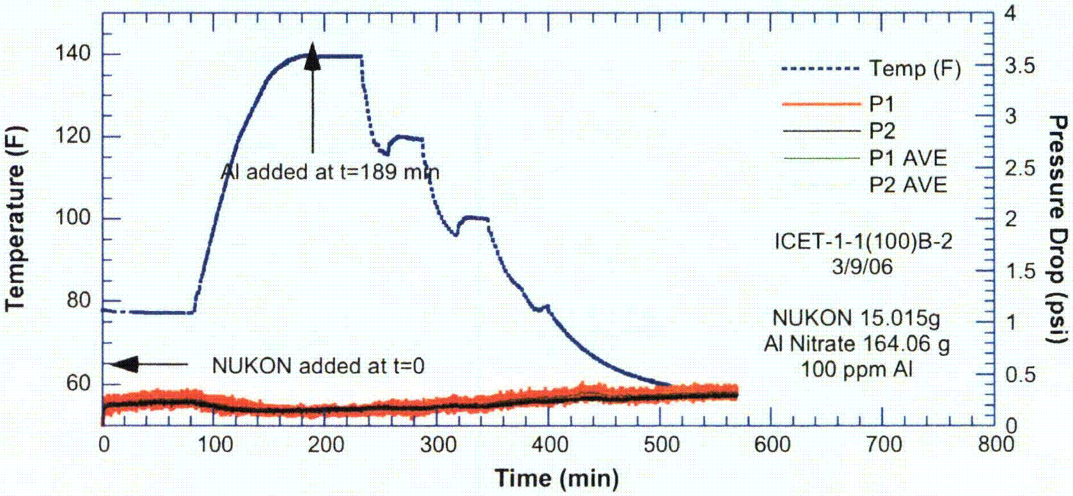

Figure 60. Pressure and temperature history in test ICET-1-1-B2_100ppm

3.4.3 ICET-1-2-B2_200ppm test procedure and results

ICET-1-2-B2_200ppm test procedure

The loop was filled with deionized water and heated to 60°C (140°F) and circulated at 2 ft/s for 15 minutes to remove dissolved air. It was kept at about 27°C (80°F) overnight. Boric acid in powder form was slowly added to the loop and circulated until it was dissolved. The LiOH was added as a solution. NaOH was added to make the pH 10. The loop was operated at 1 ft/s for 15 minutes to mix the chemicals. After the chemical solution was prepared, the physical debris bed was built by adding a slurry containing 11.6 g NUKON to the loop with the loop flow at 0.1 ft/s. The bed was about 1/2 in thick. The flow velocity was maintained at 0.1 ft/s for the whole test.

After the bed had formed and the pressure drop stabilized, the temperature was raised to 60°C (140°F) and the $Al(NO_3)_3$ solution was added. The concentration of the solution was chosen so that the concentration in the loop was 200 ppm after all the solution was added. The temperature was then decreased to 21°C (70°F) with short holds at 49°C (120°F), and 38°C (100°F) and then terminated.

ICET-1-2-B2_200ppm test results

The temperature and pressure history during the test is shown in Fig. 61. There is a small decrease in pressure drop as the temperature increases and a small increase in the pressure drop as the temperature decreases that are consistent with the changes in viscosity. No significant increase in pressure drop over that expected for the NUKON bed alone was observed and no precipitation products were observed either during the test or after the loop was allowed to remain still overnight.

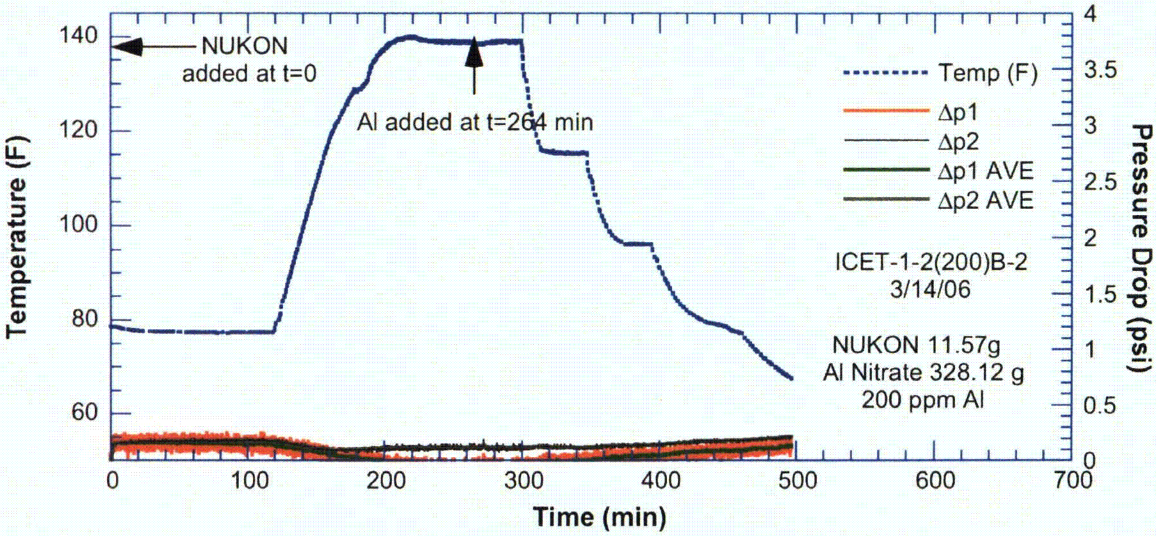

Figure 61. Pressure and temperature history in test ICET-1-2-B2_200ppm

3.4.4 ICET-1-3-B2_375ppm test procedure and results

ICET-1-3-B2_375ppm test procedure

The loop was filled with deionized water and heated to 60°C (140°F) and circulated at 2 ft/s for 15 minutes to remove dissolved air. It was kept at about 27°C (80°F) overnight. Boric acid in powder form was slowly added to the loop and circulated until it was dissolved. LiOH was added as a solution. NaOH was added to make the pH 10. The loop was operated at 1 ft/s for 15 minutes to mix the chemicals. After the chemical solution was prepared, the physical debris bed was built by adding a slurry containing 11.6 g NUKON to the loop with the loop flow at 0.1 ft/s. The bed was about 1/2 in thick. The flow velocity was maintained at 0.1 ft/s for the entire test.

After the bed had formed and the pressure drop stabilized, the temperature was raised to 60°C (140°F) and the $Al(NO_3)_3$ solution was added. At this higher concentration the initial "snowfall" was more significant and appears to have caused a small, very short duration, increase in the pressure drop. The concentration of the solution was chosen so that the concentration in the loop was 375 ppm after all the solution was added. The temperature was then decreased to 38°C (100°F) with a short hold at 49°C (120°F). The temperature was then held at 38°C (100°F) for the duration of the test.

ICET-1-3-B2_375ppm test results

The temperature and pressure history during the test is shown in Fig. 62. There is a small decrease in pressure drop as the temperature increases and a small increase in the pressure drop as the temperature decreases that are consistent with the changes in viscosity. There is, as noted previously, a small, very short duration, increase in the pressure drop just as the Al solution is added. No significant increase in pressure drop over that expected for the NUKON bed alone was observed until the temperature was decreased to 38°C (100°F) and held there. However, at that point the pressure drop began to increase and rapidly rose until the test had to be terminated because the pump could no longer maintain the flow. This increase in pressure drop occurred with no visible build–up of precipitation products during the test, although a 20–in. high layer of "jello" was observed on top of the bed after the loop was allowed to remain still overnight.

In the previous test with 375 ppm of dissolved Al, ICET–1–3, an increase in pressure drop was observed almost instantly after the Al was introduced even at 71°C (160°F). The reasons for the differences in behavior are not clear. J. Apps[*] has suggested that one possibility is that the system needs certain critical embryos to be present before nucleation can proceed, and that the activation energy for formation of these embryos is so high that the system persists metastably without their formation unless a critical supersaturation is reached. Although the heavy "snowfall" observed in the previous test appeared to have quickly redissolved, it might have provided such critical embryos. However, Apps also noted that it is difficult to imagine that the system would be so clean that no preexisting nuclei were present that could not have induced nucleation without the presence of embryos. To eliminate heterogeneous nuclei would have required draconian preparation procedures.

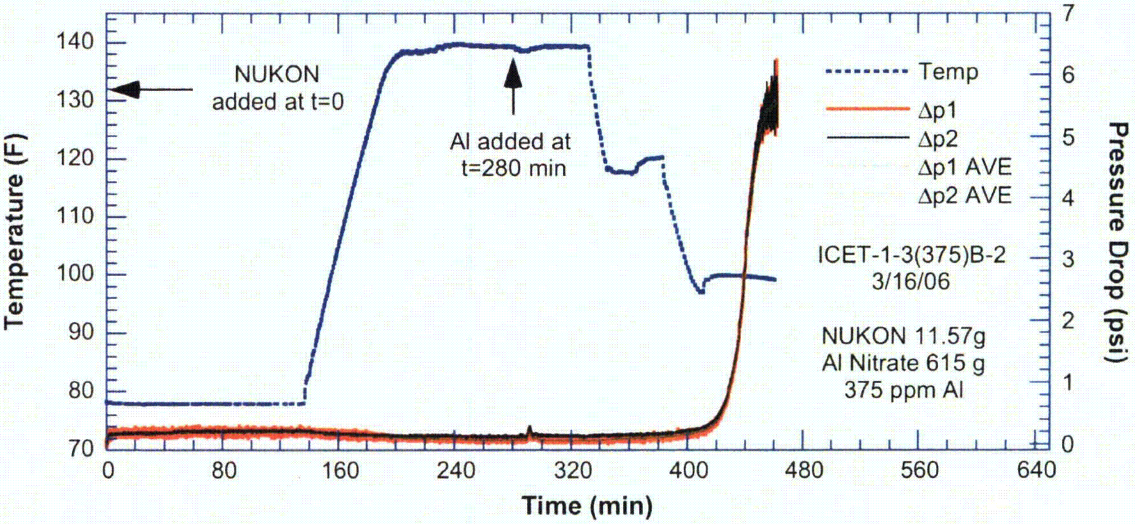

Figure 62. Pressure and temperature history in test ICET-1-3-B2_375ppm

3.4.5 ICET-1-1-B2_100ppm repeat test procedure and results

Because the kinetics of precipitation, especially in systems like aluminum hydroxides where the initiation precipitation product can be an amorphous colloid, are complex and difficult to control, it was decided that longer term tests needed to be run. Sufficient experience with the test loop had been gained that is was deemed acceptable to run it overnight and over weekends unattended. This was the first long–duration test.

ICET-1-1-B2_100ppm repeat test procedure

The loop was filled with deionized water and heated to 60°C (140°F) and circulated at 2 ft/s for 15 minutes to remove dissolved air. It was kept at about 27°C (80°F) overnight. Boric acid in powder form was slowly added to the loop and circulated until it was dissolved. The LiOH was added as a solution. NaOH was added to make the pH 10. The loop was operated at 1 ft/s for 15 minutes to mix the chemicals. After the chemical solution was prepared, the physical debris bed was built by adding a slurry containing 11.6 g NUKON to the loop with the loop flow at 0.1 ft/s. The bed was about 1/2 in thick. The flow velocity was maintained at 0.1 ft/s for the whole test.

---

[*] Personal communication, John Apps, Lawrence Berkeley Laboratory, to W. J. Shack, Tuesday, April 11, 2006.

After the bed had formed and the pressure drop stabilized, the temperature was raised to 60°C (140°F) and the $Al(NO_3)_3$ solution was added. The concentration of the solution was chosen so that the concentration in the loop was 100 ppm after all the solution was added. The temperature was then decreased to 27°C (80°F). For the first two days, the system run with no cooling water overnight so the pump heat increased the temperature to ≈32°C (90° F) overnight, then the system was cooled back to 27°C (80°F). Over the weekend the pump was turned off and the system remained at 27°C (80°F). The system was run under these conditions for about 8 days. Then nitric acid was added to the loop to decrease the pH from 9.6 to 9.4. The system was then run for another 6 days until the test was terminated.

ICET-1-1-B2_100ppm repeat test results

The temperature and pressure history during the test is shown in Fig. 63. The velocity and pressure history is shown in Fig. 64. There are small variations in pressure with the diurnal cycles. Part of the change is due to changes in viscosity as temperature changes; another part is probably an artifact of the temperature compensation of the pressure transducers. Over the weekend when the pump was off (≈2000–6000 minutes) the pressure drop vanished. No significant increase in pressure drop over that expected for the NUKON bed alone was observed until the addition of the nitric acid and the associated decrease in pH. The pressure variations associated with the diurnal temperature changes are much larger after the pH change. It appears that once formation of the chemical had been initiated, it was highly reversible with changes in temperature. No precipitation products were observed either during the test or after the loop was allowed to remain still overnight after the test was terminated.

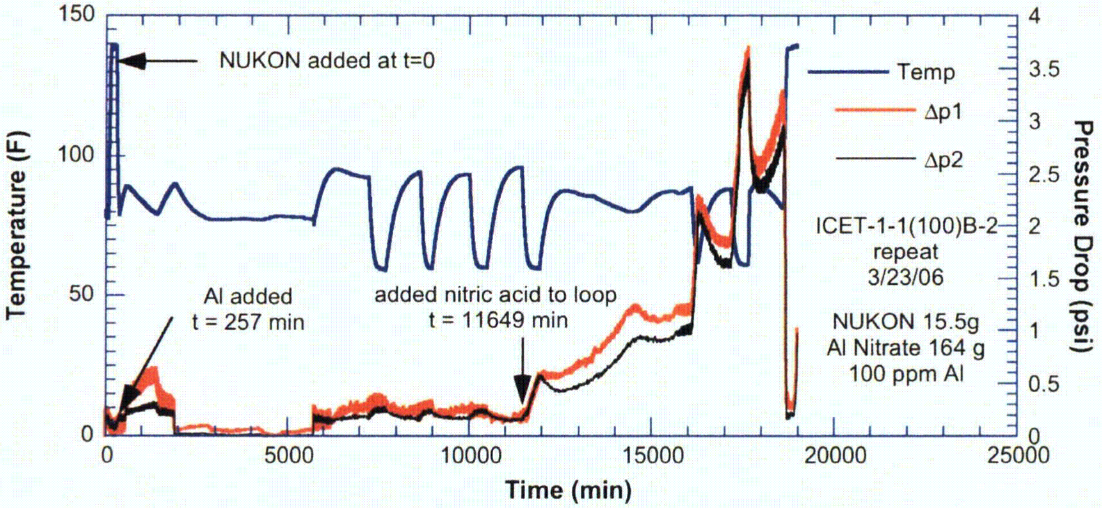

Figure 63. Pressure and temperature history in test ICET-1-1-B2_100ppm repeat

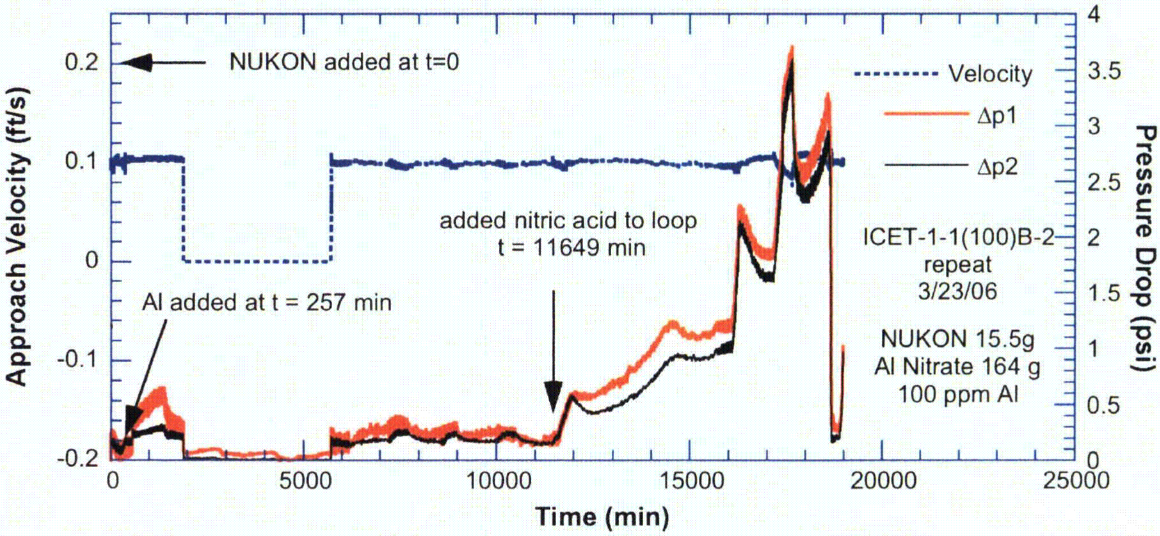

Figure 64. Pressure and velocity history in test ICET-1-1-B2_100ppm repeat

3.4.6 ICET-1-1-B2_100ppm repeat2 test procedure and results

The ICET-1-1-B2_100ppm repeat test had shown that large pressure drops were possible in a system with 100 ppm, although the pH had to be decreased to induce an effect. The test was repeated to determine whether in a longer–term test, it was possible to get a large head loss without the pH change.

ICET-1-1-B2_100ppm repeat2 test procedure

The loop was filled with deionized water and heated to 60°C (140°F) and circulated at 2 ft/s for 15 minutes to remove dissolved air. It was kept at about 27°C (80°F) overnight. Boric acid in powder form was slowly added to the loop and circulated until it was dissolved. The LiOH was added as a solution. NaOH was added to make the pH 9.5. The loop was operated at 1 ft/s for 15 minutes to mix the chemicals. After the chemical solution was prepared, the physical debris bed was built by adding a slurry containing 11.6 g NUKON to the loop with the loop flow at 0.1 ft/s. The bed was about 1/2 in thick. The flow velocity was maintained at 0.1 ft/s for the whole test.

After the bed had formed and the pressure drop stabilized, the temperature was raised to 60°C (140°F) and the $Al(NO_3)_3$ solution was added. The concentration of the solution was chosen so that the concentration in the loop was 100 ppm after all the solution was added. The system was held at 60°C (140°F) overnight The temperature was then decreased to 21°C (70°F). About 2 g of alumina nanoparticles (15 nm) were added to provide potential nuclei for precipitation. If fully dissolved, they would increase the dissolved Al level by ≈ 8 ppm. Over the weekend the system was run with no cooling water overnight so the pump heat increased the temperature to ≈32°C (90° F). When the cooling water was turned back on, the temperature decreased to about 18°C (65°F). The system was held at that temperature

ICET-1-1-B2_100ppm repeat2 test results

The temperature and pressure history during the test is shown in Fig. 65. These is a rapid increase in pressure drop starting at ≈ 7500 min (5 days), there seems to a much slower but steadier rise stating at about 3500 min (≈ 1day after the nanoparticles were added). The large pressure drops again occurred with no visible precipitation products on the bed or cloudiness in the solution were observed either during the test or after the loop was allowed to remain still overnight after the test was terminated.

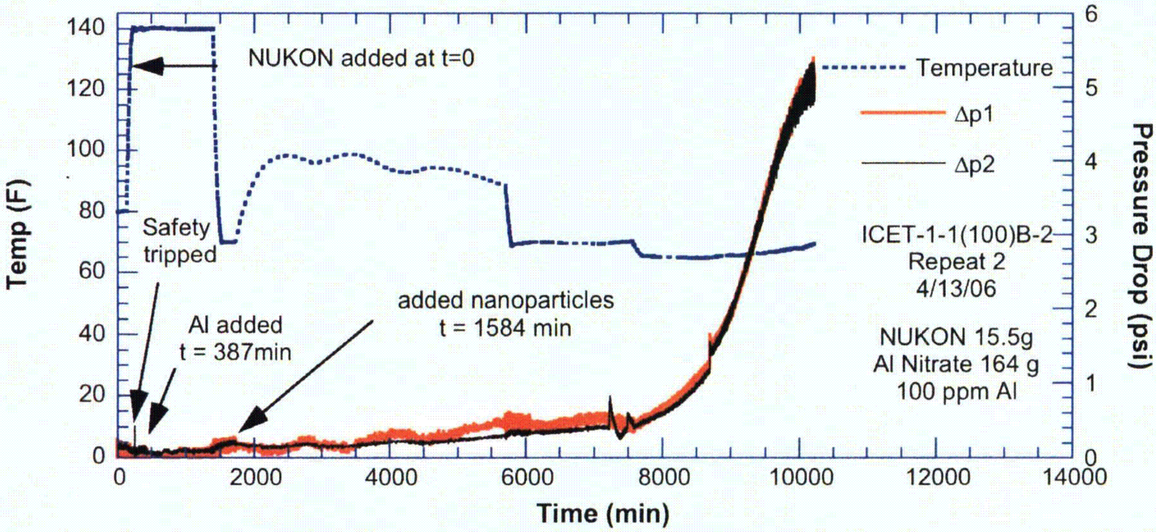

Figure 65. Pressure and velocity history in test ICET-1-1-B2_100ppm repeat2

3.5 Individual test procedures and results for tests with sodium tetraborate buffering (ICET–5 environments)

3.5.1 ICET-5-1-B2_042606 test procedure and results

ICET-5-1-B2_042606 test procedure

The loop was filled with deionized water and heated to 60°C (140°F) and circulated at 2 ft/s for 15 minutes to remove dissolved air. It was kept at about 27°C (80°F) overnight. Boric acid in powder form was slowly added to the loop and circulated until it was dissolved. The LiOH was added as a solution. Sodium tetraborate was added to get a pH of 8.3. The loop was operated at 1 ft/s for 15 minutes to mix the chemicals. After the chemical solution was prepared, the physical debris bed was built by adding a slurry containing 11.6 g NUKON to the loop with the loop flow at 0.1 ft/s. The bed was about 1/2 in thick. The flow velocity was maintained at 0.1 ft/s for the whole test.

After the bed had formed and the pressure drop stabilized, the temperature was raised to 60°C (140°F) and the $Al(NO_3)_3$ solution was added. The concentration of the solution was chosen so that the concentration in the loop was 50 ppm after all the solution was added. The temperature was then decreased to $\approx$ 21°C (70°F) and held there for $\approx$ 6 days. No significant increase in pressure drop was observed. Hydrochloric acid was used to reduce the pH 0.2 units. No change in pressure drop was observed as the test was run for another day. Two g of 30 nm alumina particles were then added and the test was continued for another 5 days. At that time additional $Al(NO_3)_3$ was added so that the total Al concentration was increased to 100 ppm. The pressure drop began to quickly rise and the test was terminated when the pump could no longer maintain flow.

ICET-5-1-B2_042606 test results

The temperature and pressure history during the test is shown in Fig. 66. Despite a decrease in pH and the addition of nanoparticles, no significant increase in pressure drop in was observed $\approx$ 11 days of testing. Only after the Al level was raised to 100 ppm did the pressure drop increase significantly. The large pressure drops again occurred with no visible precipitation products on the bed or cloudiness in the solution were observed either during the test or after the loop was allowed to remain still overnight after the test was terminated.

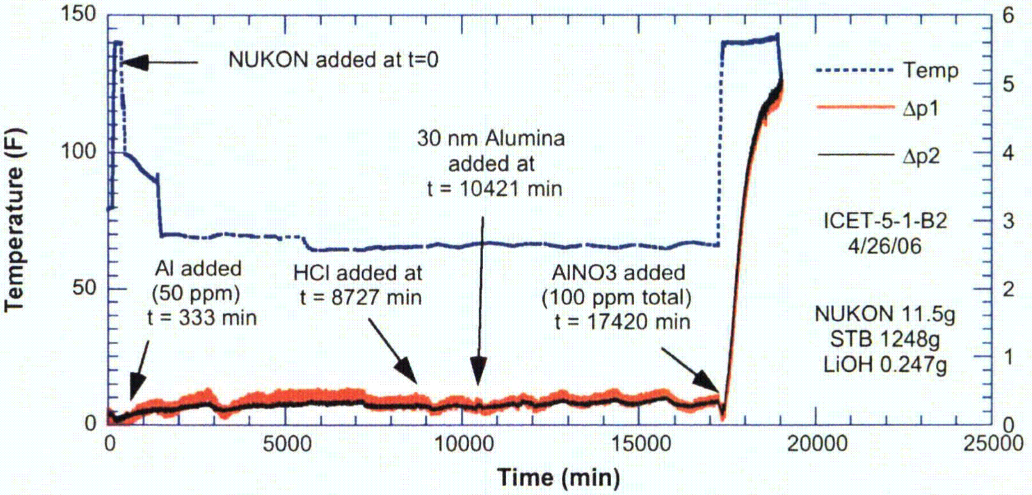

Figure 66. Pressure and velocity history in test ICET-5-1-B2_042606

3.5.1 ICET-3-STB1-A2 test procedure and results

ICET-3-STB1-A2 test procedure

This test was run with the LEXAN test section. The loop was filled with deionized water and heated to 60°C (140°F) and circulated at 2 ft/s for 15 minutes to remove dissolved air. It was kept at about 27°C (80°F) overnight. Boric acid in powder form was slowly added to the loop and circulated until it was dissolved. The LiOH was added as a solution. The loop was operated at 1 ft/s for 15 minutes to mix the chemicals. The loop was heated to 60°C (140°F). A slurry containing 15 g NUKON and 15 g of Cal–Sil was prepared and maintained at 60°C (140°F) for 30 min prior to adding to the loop. During the 30 min, 1/2 of the sodium tetraborate was titrated into slurry at a approximately constant rate. The slurry was then added to the loop with the loop flow at 0.1 ft/s. The bed was about 1/2 in thick. The remainder of the sodium tetraborate was titrated in over a 30 min period. The flow velocity was maintained at 0.1 ft/s for the whole test.

After the bed had formed and the pressure drop stabilized, the temperature was raised to 60°C (140°F) and the $Al(NO_3)_3$ solution was added. The concentration of the solution was chosen so that the concentration in the loop was 50 ppm after all the solution was added. The temperature was then decreased to $\approx$ 21°C (70°F) and held there for $\approx$ 6 days. No significant increase in pressure drop was observed. Hydrochloric acid was used to reduce the pH 0.2 units. No change in pressure drop was observed as the test was run for another day. Two (2) g of 30 nm alumina (Al_2O_3) particles were then added and the test was continued for another 5 days. At that time additional $Al(NO_3)_3$ was added so that the total Al concentration was increased to 100 ppm. The pressure drop began to quickly rise and the test was terminated when the pump could no longer maintain flow.

ICET-3-STB1-A2 test results

The temperature and pressure history during the test is shown in Fig. 67. The initial pressure drop is somewhat higher than seen in tests with similar NUKON/Cal–Sil loadings and no additional chemical effects. The pressure drop decreases with time to levels more typical of pure NUKON loading. This is consistent with dissolution of the Cal–Sil from the bed. At least at the Cal–Sil loadings in this test (0.12 g/l), no chemical products appear to form that could lead to significant additional head losses over those expected from the corresponding debris in a chemically inert environment.

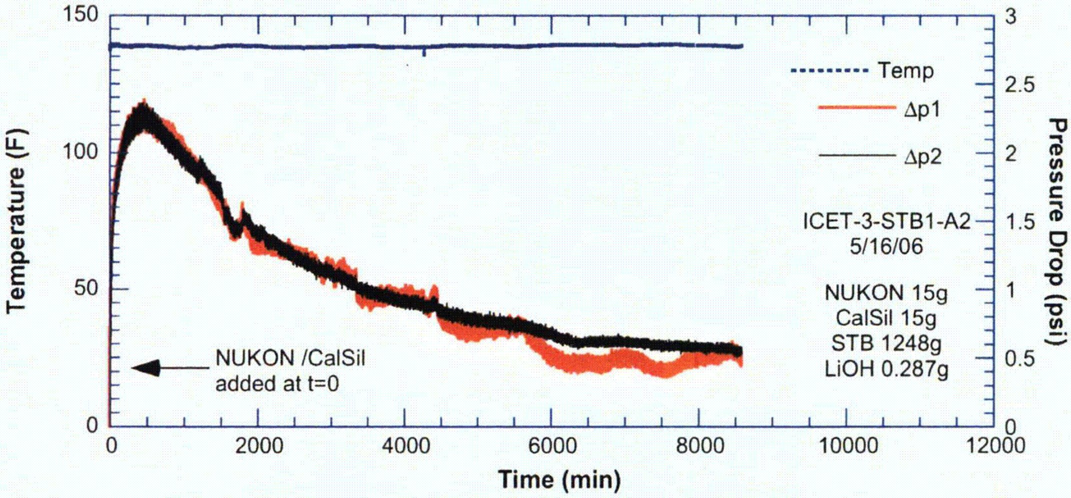

Figure 67. Pressure and velocity history in test ICET-5-1-B2_042606

3.6 Discussion of the ICET–1 and ICET–5 loop test results

Pressure drops much larger than would be expected from corresponding debris beds in an inert environment have been observed in environments with NaOH buffer for dissolved Al levels of 375 and 100 ppm. These high pressure drops can occur with no visible precipitates. The increases in pressure drops are much larger than those expected due to the small changes in bulk fluid properties like viscosity for these solutions which are shown in Fig. 68.

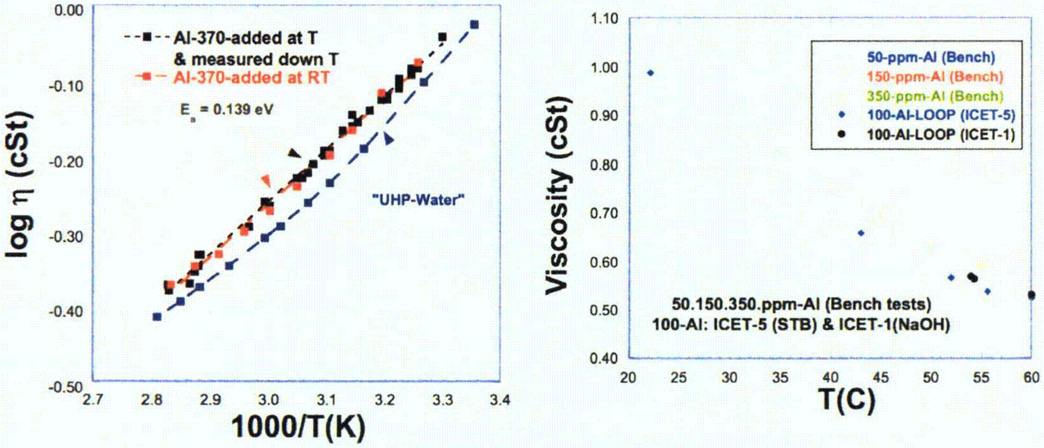

Figure 68. Viscosities for ultra high purity (UHP) water and solutions with 50–375 ppm dissolved Al concentrations.

In Table 7 are shown the results of ICP measurements of supernate solutions from samples taken periodically during a head loss test. When allowed to remain at room temperature for some time, all the samples formed emulsions that settled to the bottom of the sample containers. All the solutions were made by aluminum nitrate additions to an initially alkaline solution. The samples in Table 7 are from the clear supernate solutions above the emulsions. This does not, however, preclude the possibility that some fine precipitates remain. The measurements may somewhat overestimate the solubility of amorphous $Al(OH)_3$ at room temperature at nominally pH 9.6 in sump solutions. The variability in the results is probably due primarily to small variations in pH. Literature estimates of the solubility at room temperature[11,12] such as those shown in Fig. 51 give values of 37–59 ppm for pH values 9.4–9.6, which are reasonably consistent with the results in Table 7.

Table 7. ICP-chemical analysis on the supernate solutions from samples taken from loop tests with 100, 200, and 375 ppm Al.

Samples	Dissolved Al [mg/l]	Si	Ca	B	Na	Al in Emulsion[a]
1-375	-	1.23	2.54	2570.00	4420.30	-
3-375	49.88	0.84	1.31	2380.00	4254.00	325.12
4-375	59.28	0.84	2.39	2390.00	4274.90	315.72
5-375	55.12	0.84	1.01	2370.00	4240.20	319.87
6-375	46.03	0.84	0.82	2310.00	4145.60	328.97
1-200	-	1.57	8.31	2460.00	3831.80	-
2-200	38.42	1.13	3.49	2450.00	3901.10	161.58
4-200	32.00	0.84	2.83	2090.00	3360.90	168.00
5-200	37.49	0.84	2.72	2400.00	3837.70	162.51
6-200	31.14	0.84	2.79	2480.00	3949.00	168.87
1-100	-	4.22	2.47	2470.00	3582.50	-
2-100	50.46	1.30	4.12	2370.00	3471.40	49.544
3-100	37.84	1.29	3.06	2390.00	3468.30	62.163
5-100	62.99	1.44	3.91	2460.00	3559.00	37.013
6-100	44.28	1.14	3.67	2410.00	3509.40	55.720

[a] Estimate based on the total Al in the base solution and the measured value in the supernate.

Thus for the 100 ppm solution, about half of the Al is estimated to remain in solution and half forms a precipitation product. The actual loading on the screen depends not only on this concentration, but also on the loop volume and screen size. For the ANL loop the volume is 119 liters, and the screen area with the PVC section is 0.016 m^2. Assuming that 50 ppm of the Al has been precipitated out as a product, this means that there is about 1 kg/m^2 of chemical product impinging on the sump screen. With a NUKON loading of 0.7 kg/m^2, this is sufficient to produce the very high pressure drops observed in ICET-1-1-B2_100ppm repeat and ICET-1-1-B2_100ppm repeat2.

These estimates assume that the product is $Al(OH)_3$. The real amount of product is probably larger since water is undoubtedly incorporated into the structure. However, whatever the real product is, this approach can be used to scale the loading on the screen in the test to the loading in situations with a different screen area/ volume ratio.

Subsequent tests with a surrogate precipitate produced externally following the procedure outlined in Reference (15) and then added to the loop suggest that even much lower loadings of precipitation product (< 0.1 kg/m^2) are sufficient to produce high head losses in debris beds with a NUKON loading of 0.7 kg/m^2.

To form a product, the dissolved Al concentration (which is controlled by the amount of Al in containment) must exceed the solubility limit. The literature data suggest that for a temperature of 4°C (40°F) and a pH of 9.2, this is ≈ 30 ppm in Al/NaOH solutions. This might be considered a practical lower bound on Al concentrations that can form precipitates and would increase with the pH and temperature of the sump. At 60°C(140°F) and a pH of 9.2, the amorphous solubility is ≈370 ppm. However, because of the complexity of the sump environment, it the applicability of the literature data to this situation has not been established. In Ref. (15) it is recommended that all the dissolved Al be assumed to form a precipitation product.

In short–term laboratory testing with surrogate solutions, the kinetics of the formation of chemical products can lead to substantial test–to–test variability. The rapidity with which precipitation products formed towards the end of the 30 day test period in the ICET–1 test[2] suggests that kinetics will be less limiting in an actual plant situation.

Sodium tetraborate buffers seem more benign than NaOH or TSP. A submerged Al area and sump volume that results in a 375 ppm dissolved Al concentration in a NaOH environment, results in a 50 ppm dissolved Al concentration with a sodium tetraborate buffer. The 375 ppm concentration resulted in high head loss in 0-2 h with a NaOH buffer; the corresponding 50 ppm concentration produced no significant head loss observed in ≈ 11 days with a STB buffer. Interaction with NUKON/Cal–Sil debris mixtures produced much lower head losses than observed in corresponding tests with TSP, although tests were not performed over the full range of Cal–Sil loadings that might be of interest.

4 Benchmark tests

4.1 Background

Baseline tests with minimal chemical effects were performed for comparison with tests in which chemical effects might be expected to occur. However, to facilitate comparison with ongoing related work at Pacific Northwest National Laboratory (PNNL) additional benchmark tests were run at relatively low temperatures with no chemical additions to minimize potential chemical effects. The PNNL tests are described in Ref. 16. The objective of the tests was to benchmark the test loops against each other by comparing head loss measurements as a function of screen approach velocity, debris bed dimensions, and post-test debris mass measurements.

4.2 Procedures and test matrix

The target NUKON and Cal–Sil loadings for each of the tests are shown in Table 8. A repeat test was performed for each of the loading conditions in Table 8. In order to minimize any differences in results due to differences in test procedures, this series of tests was performed under detailed test protocols that were coordinated with the researchers at PNNL in order to obtain a measure of laboratory to laboratory variability due to uncontrolled or unknown variables. Detailed test protocols were developed by C. W. Enderlin and B. E. Wells of PNNL and are described in Appendix F. They include details on the preparation of the NUKON and Cal–Sil in order to get a consistent "fineness" of the debris. The two types of debris were thoroughly mixed before adding to the loop and no presoak period was used. The debris slurry is to be introduced into the test loop with the screen approach velocity at 0.1 ft/s. During debris bed formation the screen approach velocity is to be maintained between 0.09 and 0.1 ft/s. The fluid temperature during bed formation and for the duration of the test is to be maintained at 25° ± 5°C (77° ± 9°F). In order to assure that measurements were made under steady–state conditions, the absolute change in head loss was to be less than 2% over a 10 minute measurement period. The criteria had to be assessed and satisfied three times. The minimum time between assessments was one minute.

The tests were performed with the LEXAN cross–section and the flow screen with 40% flow area and 1/8 in. holes with 3/16 in. staggered centers. After the initial formation of the bed, a prescribed velocity sequence was followed in each test. The sequence is shown in Table 9. The test times at each point in the test sequence were not prescribed, but were determined based on whether the pressure at that point met the criteria for a steady–state value.

Table 8. Benchmark test cases for ANL and PNNL test loops

Test No.	Nukon Mass Loading lb/ft^2 (kg/m^2)	Cal–Sil Mass Loading lb/ft^2 (kg/m^2)	Total Mass Loading lb/ft^2 (kg/m^2)	Cal–Sil to Nukon Mass Ratio
BM-1	0.044 (0.217)	0.0 (0.0)	0.044 (0.217)	0.0
BM-2	0.148 (0.724)	0.0 (0.0)	0.148 (0.724)	0.0
BM-3	0.148 (0.724)	0.030 (0.145)	0.178 (0.869)	0.2

Table 9. Velocity sequence for the ANL and PNNL test loop benchmark cases

Test point	Velocity (ft/s)	Test sequence
Initial condition	0.10	Bed Formation
1	0.10	Ramp down 1
2	0.05	Ramp down 1
3	0.02	Ramp down 1
4	0.05	Ramp up 1
5	0.10	Ramp up 1
6	0.05	Ramp down 2
7	0.02	Ramp down 2
8	0.10	Ramp up 2
9	0.15	Ramp up 2
10	0.20	Ramp up 2
11	0.15	Ramp down 3
12	0.10	Ramp down 3
13	0.15	Ramp up 3
14	0.20	Ramp up 3
15	0.10	Ramp down 4
16	0.05	Ramp down 4
17	0.02	Ramp down 4
18	0.10	Ramp up 4

*Up and down indicate a velocity increase or decrease, respectively

4.3 Results of the benchmark tests

The pressure and velocity in the benchmark tests as a function of time during the test are shown in Figs. 69–74. In these tests some drift is occurring in the p1 transducer, which measures the pressure difference between two points, one 2.5 inches above the screen and the other 2.5 inches below the screen. The p2 transducer, which measures the pressure difference between points 12.0 inches above and below the screen, was used in all tests for the reported values of the pressure drop.

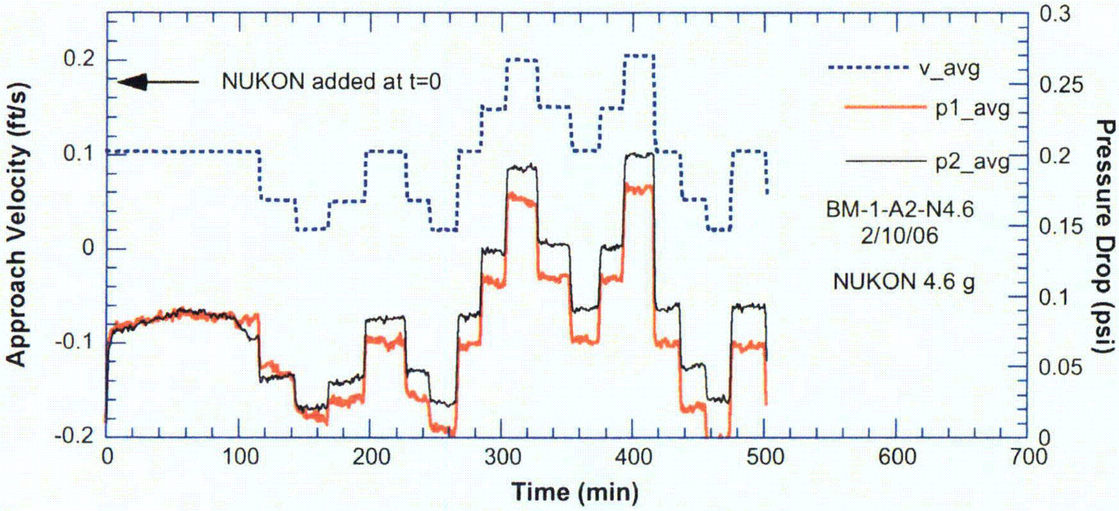

Figure 69. Pressure and velocity history in test BM–1–A2–N4.6

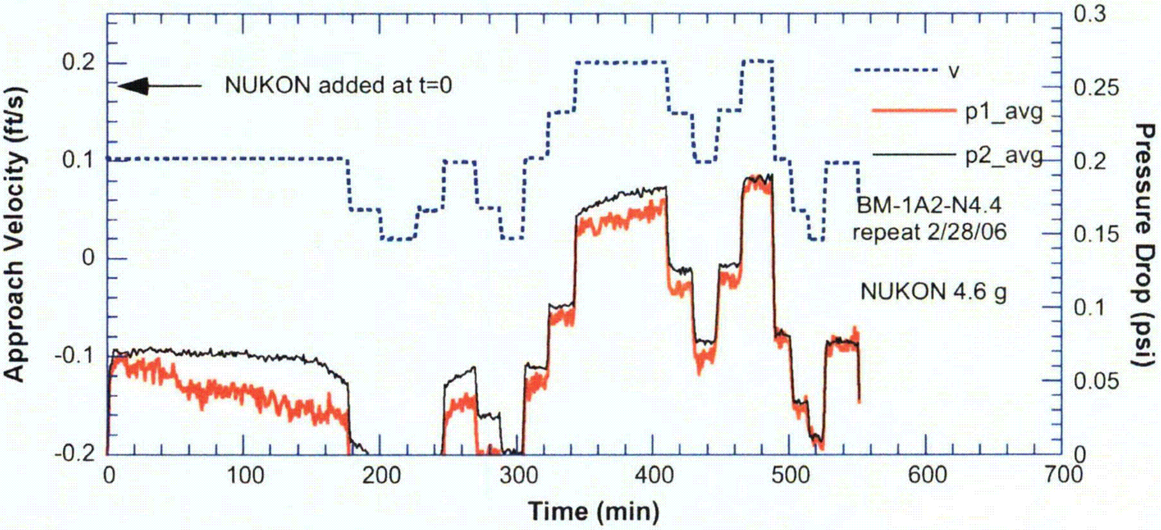

Figure 70. Pressure and velocity history in test BM–1–A2–N4.6 repeat 2/28/06

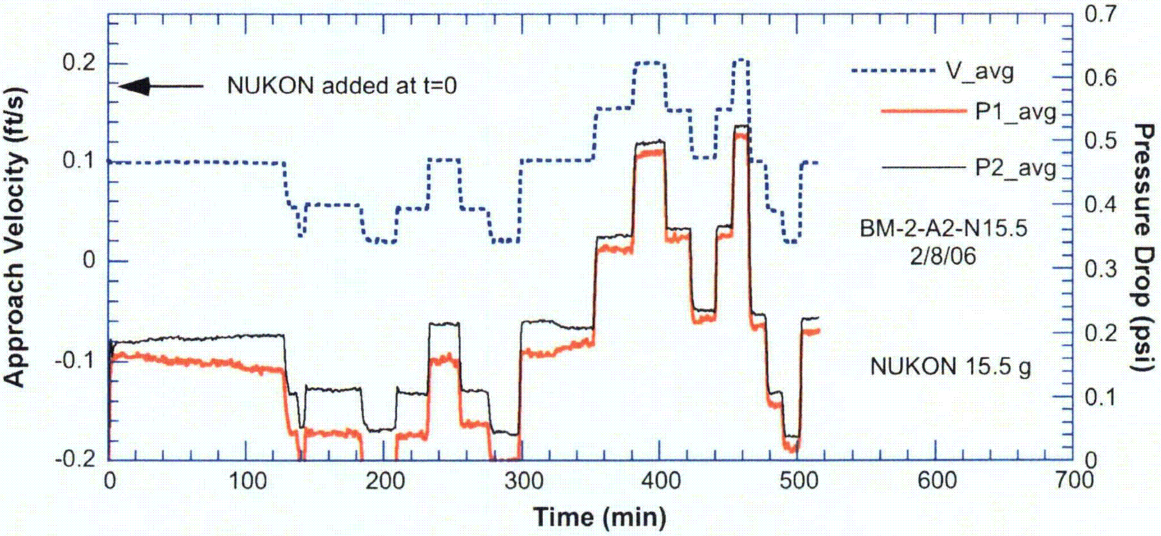

Figure 71. Pressure and velocity history in test BM–2–A2–N15.5

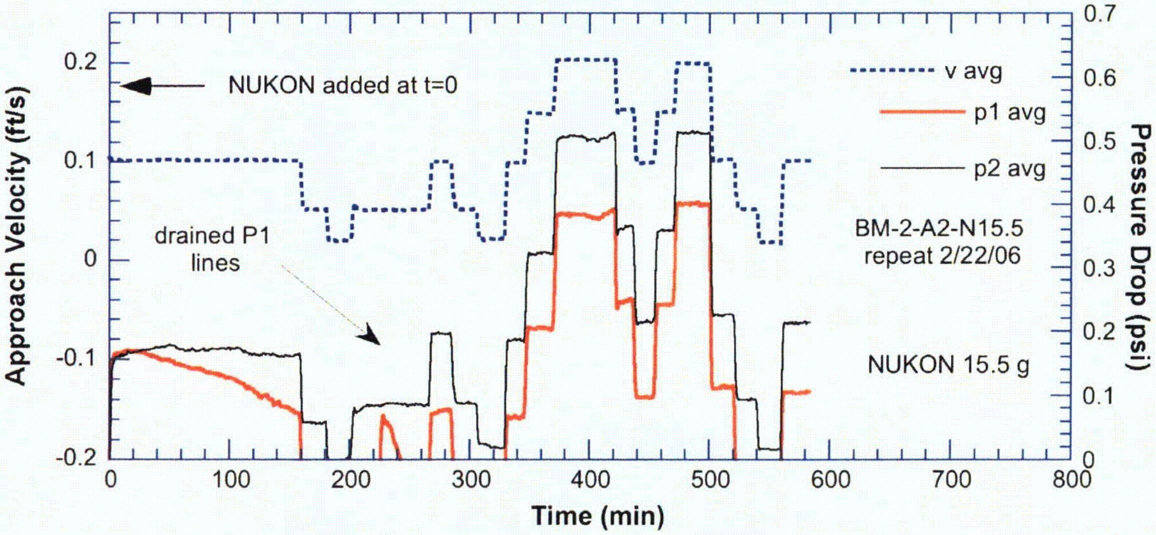

Figure 72. Pressure and velocity history in test BM–2–A2–N15.5 repeat

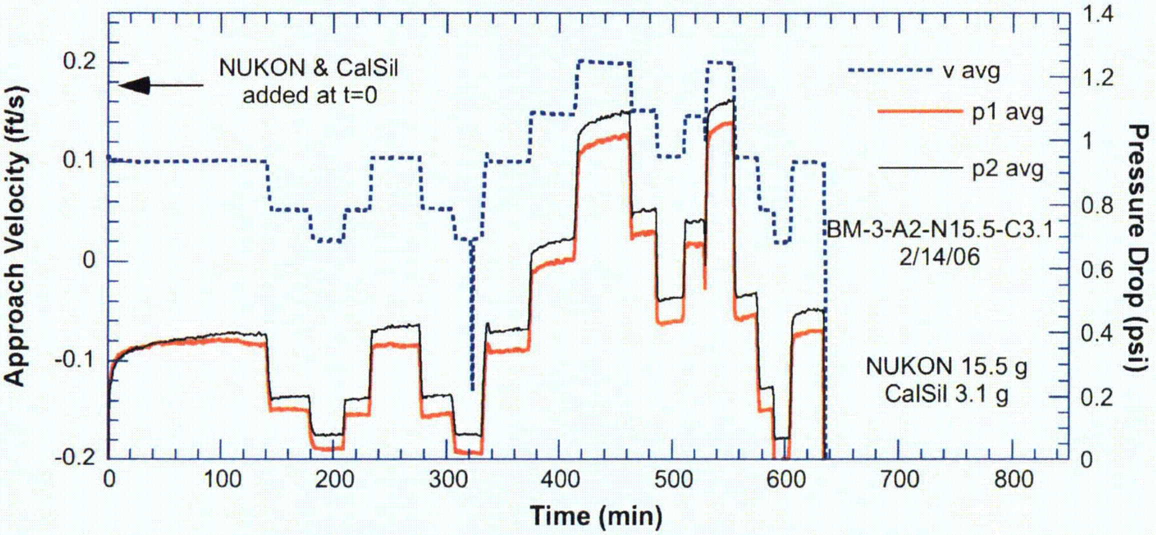

Figure 73. Pressure and velocity history in test BM–3–A2–N15.5–C3.1

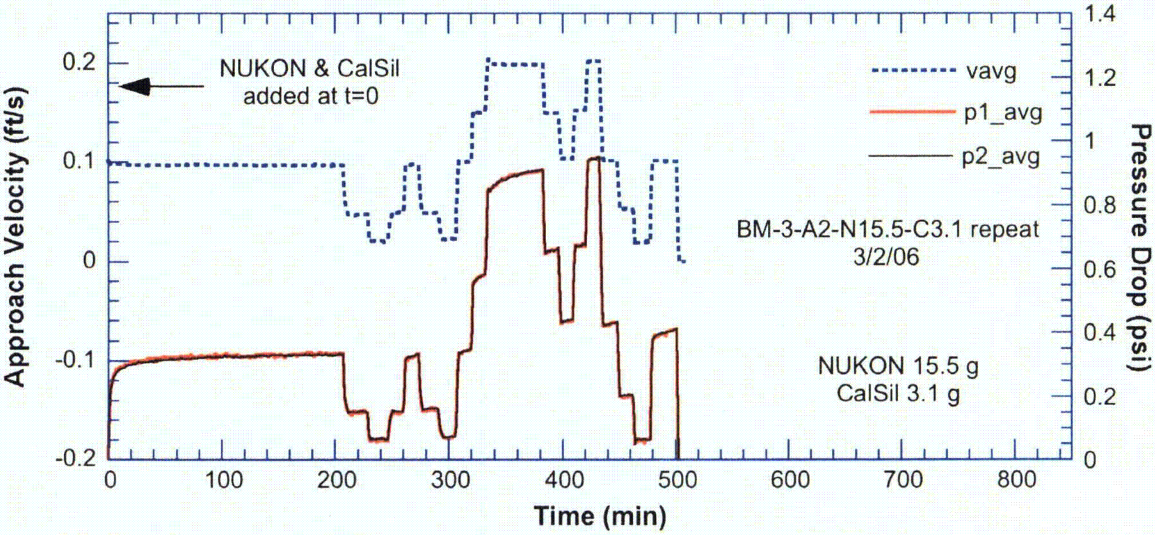

Figure 74. Pressure and velocity history in test BM–3–A2–N15.5–C3.1 repeat

The results of the benchmark tests are summarized in terms of the relation between pressure and flow velocity in Fig. 75–77. The relation is close to linear over the velocity range in the tests. Some hysteresis is observed, i.e., the pressure at a given velocity (e.g., 0.1 ft/s) is not unique. It depends on the previous flow history. This can also be seen in Table 10, which gives the approximate bed thickness at the final step in the flow history. The beds compress as the velocities and pressure drops increase. Some of this change in thickness is elastic and a bed that is compressed at a higher velocity tends to expand as the velocity is subsequently decreased. But some of the thickness change is irrecoverable, and all the beds are more compressed at the end of the test sequence, although the final velocity is the same as the initial velocity. Table 11 compares the amount of debris added with the final weight of the dried bed. For tests BM–1 and BM–2 the recovered fraction is higher for the thicker bed. This may reflect the greater filtering capability of the bed and its ability to remove smaller fines that could pass through a thinner bed. The recovered fraction is lower for BM–3 than for BM–2. This may reflect the fineness of some of the particulate generated by the Cal–Sil. The high effective surface area of the Cal–Sil may also lead to dissolution even at the low temperature of these tests. Although the primary component of Cal–Sil is $CaSiO_3$, it could contain ≈5% Na_2SiO_3, which is relatively soluble and would be expected to dissolve.

Figures 75a and b, 76a and b, and 77a and b show the repeatability of the tests. The variability in the slopes between the replicate tests is about ±10%; the uncertainty in the slope for an individual test is about ±5%. Figures 75c, 76c, and 77c show PNNL results for their parallel BM–1, 2, and 3 tests. The agreement with ANL results is good for BM–3. Their results are within the scatter for the two ANL BM–3 tests. However, there are significant differences between the ANL and PNNL results for BM–1 and 2. The increase in pressure drop per unit increase in velocity determined in the PNNL tests is about twice that determined in the ANL, which is much larger than would be expected just from test to test variability.

The reasons for these differences are not clear. The processing of the NUKON fiber is done similarly at the two laboratories, but the equipment used is different and thus different blending times may be used. PNNL developed a test based on the amount of water retained by the shredded fiber blanket that was intended to assure the processing results were consistent even though different equipment and processing times were used. The processing at PNNL and ANL resulted in processed fiber that retained similar amounts of water. However, it may be for the relatively thin beds in BM–1 and BM–2, that this was not sufficient to ensure similar flow resistances. In the BM–3 test the presence of the particulate from Cal–Sil may overwhelm any differences due to the processing of the fiber, and the differences in the pressures drops between the ANL results and the PNNL results are on the order of the test–to–test variability at ANL.

There may also be variations due to the differences in the sensitivities of the pressure measurement instruments in the two flow loops. The transducers in the ANL loop are rated at 1.5% error at full scale, 150 psi. The PNNL measurements were made with transducers rated at ≈ 1 or 5 psi. Thus their uncertainty would be expected to be smaller for these tests. However, independent checks show that the transducers used in the ANL tests are in fact more accurate than implied by their rating and that the differences between the ANL and PNNL are much larger than can be explained by transducer error. This is consistent with the results of the BM–3 tests where the pressure drops are still small, but the agreement between the two labs is within the test–to–test variability. Thus it seems more likely that differences between the ANL and PNNL results in the BM–1 and 2 tests reflect genuine differences in flow resistance from beds developed from fibers with different processing histories. A more definitive assessment would require additional testing using the ANL procedure for preparing the fibers and pressure transducers better matched to actual pressure drops.

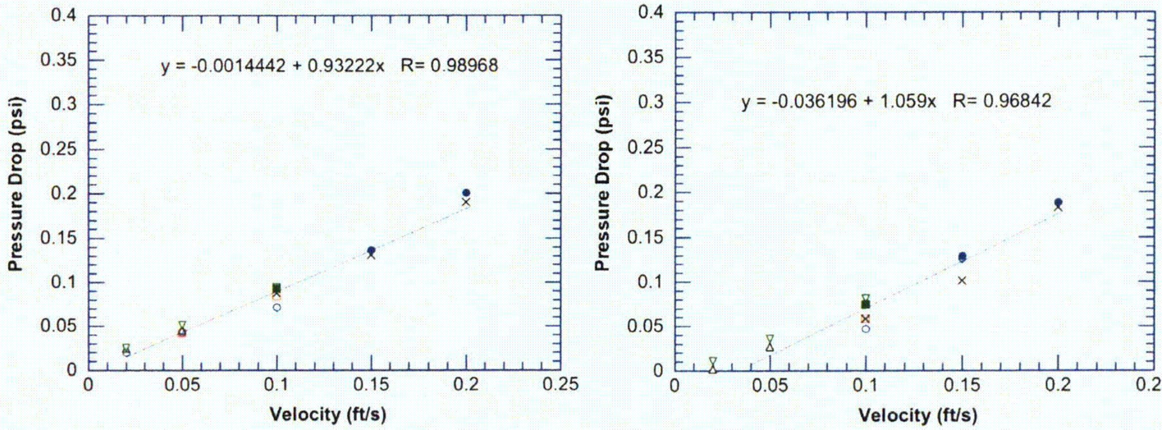

(a) ANL BM–1

(b) ANL BM–1 replicate

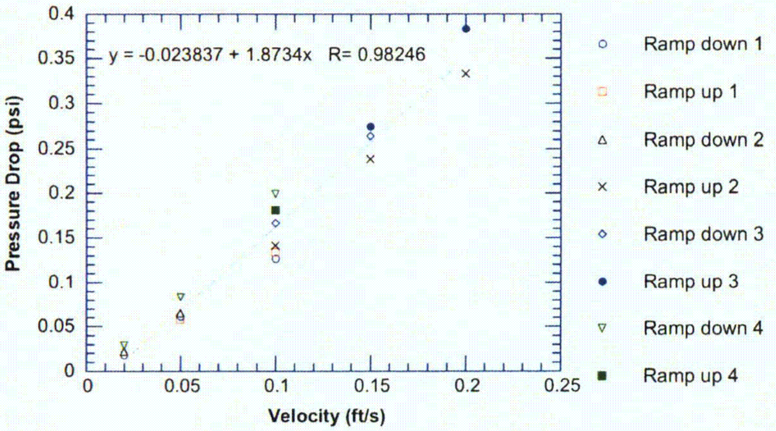

(c) PNNL BM–1

Figure 75. Pressure drop as a function of flow velocity (a) ANL BM–1, (b) replicate test ANL BM–1, and (c) PNNL BM–1

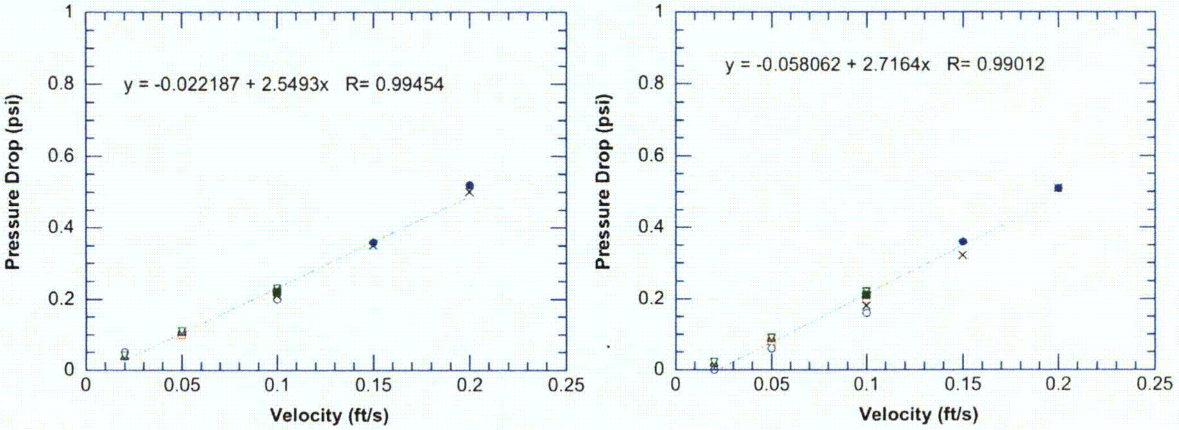

(a) ANL BM–2 (b) ANL BM–2 replicate

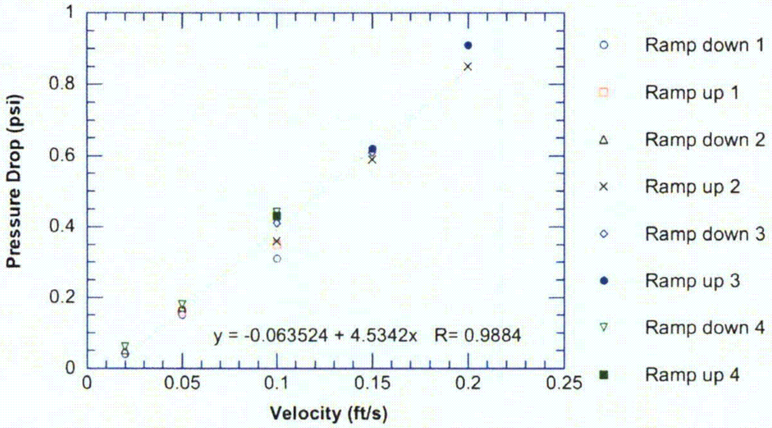

(c) PNNL BM–2

Figure 76. Pressure drop as a function of flow velocity (a) ANL BM–2, (b) replicate test ANL BM–2, and (c) PNNL BM–2

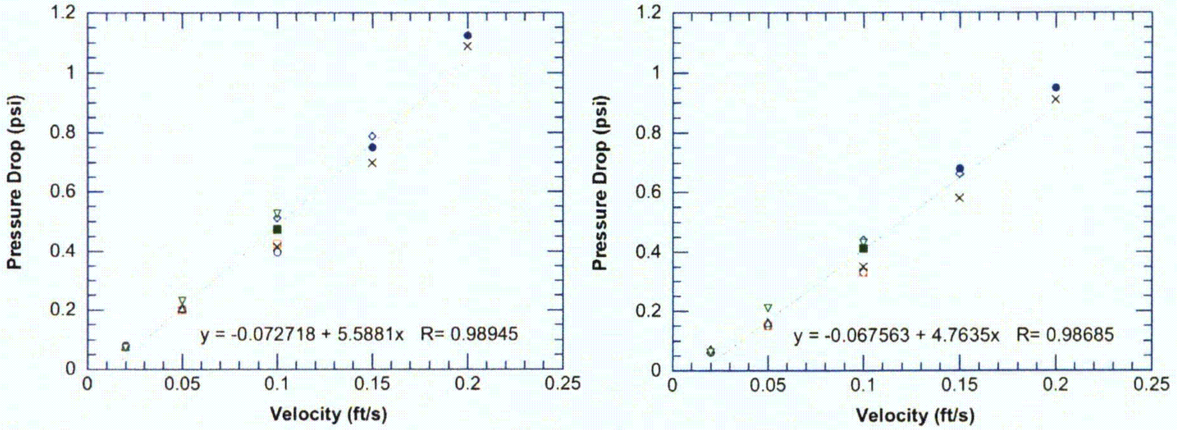

(a) ANL BM–3

(b) ANL BM–3 replicate

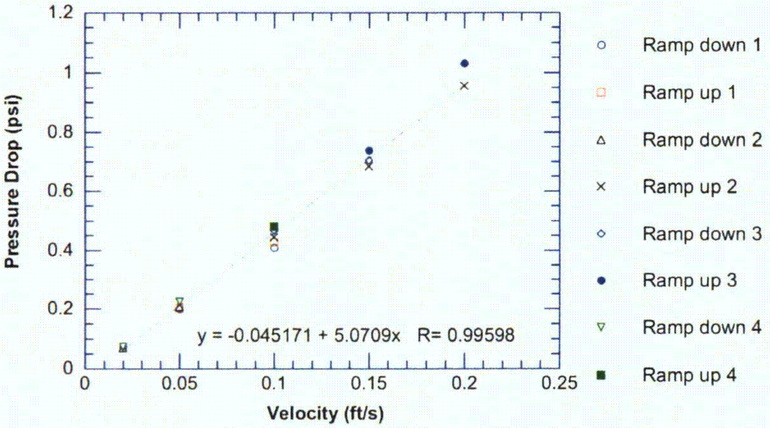

(c) PNNL BM–3

Figure 77. Pressure drop as a function of flow velocity (a) ANL BM–3, (b) replicate test ANL BM–3, and (c) PNNL BM–3

Table 10. Bed heights in benchmark test

Test point	Velocity (ft/s)	Bed Height (mm) BM–1	BM–1 repeat	BM–2	BM–2 repeat	BM-3	BM-3 repeat
1	0.10	4.0	5.5	12.0	12.0	12.0	12.0
2	0.05	5.0	5.5	13.0	12.5	12.0	12.0
3	0.02	5.5	6.5	13.5	13.5	12.5	13.0
4	0.05	5.0	6.0	13.5	12.5	12.0	12.0
5	0.10	4.5	5.5	11.5	12.5	9.0	11.5
6	0.05	5.0	5.5	12.0	12.0	12.0	11.5
7	0.02	5.0	6.0	13.0	13.0	12.0	11.5
8	0.10	4.5	5.0	11.0	11.5	10.0	10.5
9	0.15	4.0	5.0	10.5	9.0	12.0	10.0
10	0.20	4.0	4.5	9.0	9.5	8.0	9.5
11	0.15	4.0	4.5	9.0	9.5	9.5	9.5
12	0.10	3.5	4.5	9.0	9.5	10.0	10.0
13	0.15	3.5	4.5	9.0	9.5	9.5	9.5
14	0.20	3.5	4.5	9.0	9.5	8.5	9.5
15	0.10	4.0	4.5	9.5	9.5	10.0	9.5
16	0.05	4.0	5.0	10.0	10.0	10.0	10.0
17	0.02	4.0	5.0	11.0	11.5	10.0	10.0
18	0.10	3.5	4.5	9.5	10.5	9.0	10.0

Table 11. Initial debris load and final weight of the bed

Test run	Initial weight NUKON, Cal–Sil (g)	Weight, dried bed (g)	Fraction captured
BM-1	4.6	3.76	0.83
BM–1 replicate	4.6	3.80	0.83
BM-2	15.5	14.89	0.96
BM–2 replicate	15.5	14.58	0.94
BM-3	15.5, 3.1	15.63	0.84
BM-3-Repeat	15.5, 3.1	15.13	0.81

5 Summary

A test loop that can be used to measure head losses due to chemical effects has been constructed. The piping in most of the loop is CPVC; the clear test section containing the test screen was either LEXAN or clear PVC. The heater and cooler sections are stainless steel. Temperatures around the loop during operation are typically ±0.6°C (1°F). Loop velocities can be controlled over the range from 0.02 to 2 ft/s. Physical debris and chemicals are introduced to the loop through a charging port at the top of the loop. The loop has a horizontal screen. This orientation is not intended to reflect a plant situation in which the screen orientation may be primarily vertical, but rather to permit the development of uniform beds with well–defined characteristics. The head loss behavior for such beds would characterize the local head loss behavior of more complex, nonuniform beds that might form on more complex screen geometries.

A series of tests were performed to evaluate the potential for head loss due to chemical effects in a TSP-buffered environment with NUKON and Cal–Sil insulation. The tests were designed to explore conditions corresponding to a range of debris amounts, containment sump residence times, and TSP dissolution times. The NUKON and Cal–Sil mass loading per unit screen area utilized in these tests are reasonably representative of those plants that currently have, or will have after sump modifications, relatively low debris mass loading (i.e., less than 2 kg/m^2).

The tests show that head losses associated with pure physical debris beds of NUKON and Cal–Sil are typically much smaller than those that occur across debris beds in which some of the Cal–Sil has been replaced with a corresponding amount of calcium phosphate precipitates. This increase in head loss was observed both when significant dissolution of the Cal–Sil occurred prior to the formation of the bed, and when the dissolution and formation of the precipitate occurred subsequent to the build–up of Cal–Sil in the bed.

The relative importance of chemical effects depends strongly on the debris loading at the screen. For a screen loading corresponding to 0.71 kg/m^2 of Cal–Sil and an ≈ 12 mm thick NUKON bed (0.71 kg/m^2), the pressure drop across the physical debris bed in benchmark testing in chemically inactive environments is approximately 1.4 psi at an approach velocity of 0.1 ft/s. With TSP, and thus calcium phosphate precipitates present, the same debris loading caused the pressure drop across the bed to be greater than 5 psi for the same approach velocity. For a thin NUKON bed (≈ 3 mm), very large pressure drops were observed for the lowest tested Cal–Sil loading, 0.47 kg/m^2. However, with thicker ≈ 12 mm NUKON beds, little chemical effect could be observed for Cal–Sil loadings ≤ 0.47 kg/m^2. These results show that the relation between head loss and fiber loading for a given particulate loading is highly nonlinear and not monotonic.

Beds in which no NUKON was present were also examined. In this case, a significant portion of the screen remains open for the highest screen loading of Cal–Sil tested, 1.2 kg/m^2. The pressure drops are very low with this open area.

Dissolution tests showed that virtually complete leaching of calcium from the Cal–Sil could take one to four days or more depending on the TSP dissolution rate and the Cal–Sil concentration. Dissolution of low Cal–Sil concentrations (≤ 1.5 g/l) is retarded by instantaneous TSP dissolution. However, the Cal–Sil dissolution rate (for the concentrations studied) is not strongly dependent on the TSP dissolution rate for more realistic TSP dissolution rates. Even with instantaneous dissolution of the TSP, the equivalent dissolved Ca exceeded 75 mg/l in a few hours for Cal–Sil concentrations as low as 0.5 g/l. Such an equivalent dissolved Ca concentration was shown to produce pressure drops on the order of 5 psi at an approach velocity of 0.1 ft/s across a 0.71 kg/cm^2 NUKON debris bed.

Settling tests were performed to determine settling rates for calcium phosphate under conditions with no bulk directional flow. At higher dissolved calcium concentrations (300 ppm), the precipitates can agglomerate. The agglomerated precipitates settle more quickly, but approximately one half of the total precipitate settles more slowly than the agglomerated precipitate. At a lower dissolved calcium concentration

(75 ppm), which is expected to be more representative of plant conditions, the estimated settling velocity is 0.8 cm/min.

Significant chemical effects are also observed in environments with significant dissolved aluminum and NaOH buffers which correspond to the ICET–1 test. Pressure drops much larger than would be expected from corresponding debris beds in an inert environment have been observed in environments with NaOH buffer for dissolved Al levels of 375 and 100 ppm. These high pressure drops can occur with no visible precipitates. They occur although there are very small changes in bulk fluid properties like viscosity for these solutions.

Tests were also performed to simulate environments in which sodium tetraborate is used to buffer pH. Sodium tetraborate buffers seem more benign than NaOH or TSP. A submerged Al area and sump volume that results in a 375 ppm dissolved Al concentration in a NaOH environment, results in a 50 ppm dissolved Al concentration with a sodium tetraborate buffer. A submerged Al area sump volume that resulted in high head loss in 0-2 h in NaOH buffer, no significant head loss observed in ≈ 11 days with STB buffer. Interaction with NUKON/Cal–Sil debris mixtures produced much lower head losses than observed in corresponding tests with TSP, although tests were not performed over the full range of Cal–Sil that might be of interest.

Small–scale dissolution tests were performed on NUKON in different environments, including one with roughly 1/4 the relative surface area of Al metal as was present in ICET–1. The inhibition of NUKON dissolution observed in ICET–1 was also observed in the case of the lower surface area of Al metal.

To facilitate comparison with ongoing related work at Pacific Northwest National Laboratory (PNNL) additional benchmark tests were run at relatively low temperatures with no chemical additions to minimize potential chemical effects. The objective of the tests was to benchmark the test loops against each other by comparing head loss measurements as a function of screen approach velocity, debris bed dimensions, and post-test debris mass measurements. Three test series were run. Two had NUKON only debris beds with thicknesses of ≈ 4 and 12 mm, respectively. The third had a NUKON/Cal–Sil bed ≈ 12 mm thick. The results of the tests showed good reproducibility of test results in the ANL flow loop. There was also good agreement between the ANL and PNNL tests with the NUKON/Cal–Sil beds. However, for the tests with NUKON only beds, the flow resistance determined in the tests at PNNL was about twice that observed in the corresponding tests at ANL.

The reasons for these differences are not clear. It is most likely due to differences in the processing of the NUKON fiber. This processing is done similarly at the two laboratories, but the equipment used is different and thus different blending times may be used. PNNL developed a test based on the amount of water retained by the shredded fiber blanket that was intended to assure the processing results were consistent even though different equipment and processing times were used. The processing at PNNL and ANL did results in processed fiber that retained similar amounts of water. However, it may be for relatively thin NUKON beds, this was not sufficient to ensure similar flow resistances. In the test with the NUKON/Cal–Sil bed, the presence of the particulate from Cal–Sil may overwhelm any differences due to the processing of the fiber, and thus good agreement is obtained between the results developed at the two laboratories.

References

1. T. S. Andreychek, Test Plan: Characterization of Chemical and Corrosion Effects Potentially Occurring Inside a PWR Containment Following a LOCA (ADAMS ML052100426)
2. J. Dallman, B. Letellier, J. Garcia, J. Madrid, W. Roesch, D. Chen, K. Howe, L. Archuleta, and F. Sciacca, F. *Integrated Chemical Effects Test Project: Test # 1 Data Report*, NUREG/CR-6914, Volume 2, U.S. Nuclear Regulatory Commission, Washington, D.C., 2006.
3. J. Dallman, B. Letellier, J. Garcia, M. Klasky, W. Roesch, J. Madrid K. Howe, and D. Chen, *Integrated Chemical Effects Test Project: Test # 2 Data Report,* NUREG/CR-6914, Volume 3, U.S. Nuclear Regulatory Commission, Washington, D.C., 2006.
4. J. Dallman, B. Letellier, J. Garcia, J. Madrid, W. Roesch, D. Chen, K. Howe, L. Archuleta, and F. Sciacca, *Integrated Chemical Effects Test Project: Test # 3 Data Report,* NUREG/CR-6914, Volume 4, U.S. Nuclear Regulatory Commission, Washington, D.C., 2006.
5. J. Dallman, B. Letellier, J. Garcia, J. Madrid, W. Roesch, D. Chen, K. Howe, L. Archuleta, and F. Sciacca, *Integrated Chemical Effects Test Project: Test # 4 Data Report,* NUREG/CR-6914, Volume 5, U.S. Nuclear Regulatory Commission, Washington, D.C., 2006
6. J. Dallman, B. Letellier, J. Garcia, J. Madrid, W. Roesch, D. Chen, K. Howe, L. Archuleta, and F. Sciacca, *Integrated Chemical Effects Test Project: Test # 5 Data Report,* NUREG/CR-6914, Volume 6, U.S. Nuclear Regulatory Commission, Washington, D.C., 2006.
7. ANL Quick Look Report Tests 1 & 2, September 16, 2005 (ADAMS ML052590238)
8. MEMORANDUM on "Summary of Meeting on September 30, 2005, to Discuss GSI-191 Chemical Effects Head Loss Information," dated November 2, 2005, ADAMS Accession Number ML053060359, http://www.nrc.gov/reactors/operating/ops-experience/pwr-sump-performance/public-mtgs/2005/index.html
9. Solubility of Calcium Phosphates, http://www.azom.com/details.asp?ArticleID=2140.
10. M. Klasky, J. Zhang, M. Ding, , B. Letellier, D. Chen, and K. Howe, *Aluminum Chemistry in Prototypical Post-LOCA PWR Containment Environment,* NUREG/CR-6915, U.S. Nuclear Regulatory Commission, Washington, D.C., 2006
11. H. A. van Straten, B. T. W. Holtkamp, and P. L. de Bruyn, "Precipitation from Supersatured Aluminate Solutions", *Journal of Colloid and Interface Science* V. 98, No 2, April 1984, pp 342–362
12. D. Langmuir, *Aqueous Environmental Geochemistry,* Prentice Hall, New York, 1996
13. P. Benezeth, D.A. Palmer and D.J. Wesolowski (2001) Aqueous high-temperature solubility studies. II. The solubility of boehmite at 0.03m ionic strength as a function of temperature and pH as determined by in situ measurements, *Geochimica et Cosmochimica Acta,* v. 65, pp. 2097-2111.
14. J. McMurry, V. Jain, X. He, D. Pickett, R. Pabalan, and Y. M. Pan, *GSI-191 PWR Sump Screen Blockage Chemical Effects Tests-Thermodynamic Simulations,* NUREG/CR-6912, U.S. Nuclear Regulatory Commission, Washington, D.C., 2006.
15. A. E. Lane, T. S. Andreychek, W. A. Byers, R. J. Jacko, E. J. Lahoda, and R. D. Reid, *Evaluation of Post-Accident Chemical Effects in Containment Sump Fluids to Support GSI-191,* WCAP-16530-NP, Revision 0, 2006.

16. C. W. Enderlin, B.E.Wells, M. White, F. Nigl, A. Guzman, D. R. Rector, T. J. Peters, and E. S. Mast, *Experimental Measurements of Pressure Drop Across Debris Beds on PWR Sump Screens in Support of Generic Safety Issue 191*, NUREG/CR-6917, U.S. Nuclear Regulatory Commission, Washington D.C., 2006.

For more information on the ICET program see: http://www.nrc.gov/reactors/operating/ops-experience/pwr-sump-performance/tech-references.html